

31.2

DOE/ET/21050-1/3

**COMBINED CYCLE SOLAR CENTRAL RECEIVER HYBRID POWER  
SYSTEM STUDY**

Final Technical Report, Volume III, Appendices

November 1979

Work Performed Under Contract No. ET-78-C-03-2051

Bechtel National, Inc.  
San Francisco, California



**U.S. Department of Energy**



**Solar Energy**

0104 VOL I

## DISCLAIMER

"This book was prepared as an account of work sponsored by an agency of the United States Government. Neither the United States Government nor any agency thereof, nor any of their employees, makes any warranty, express or implied, or assumes any legal liability or responsibility for the accuracy, completeness, or usefulness of any information, apparatus, product, or process disclosed, or represents that its use would not infringe privately owned rights. Reference herein to any specific commercial product, process, or service by trade name, trademark, manufacturer, or otherwise, does not necessarily constitute or imply its endorsement, recommendation, or favoring by the United States Government or any agency thereof. The views and opinions of authors expressed herein do not necessarily state or reflect those of the United States Government or any agency thereof."

This report has been reproduced directly from the best available copy.

Available from the National Technical Information Service, U. S. Department of Commerce, Springfield, Virginia 22161.

Price: Paper Copy \$12.00  
Microfiche \$3.50

**VOLUME III**  
**APPENDICES**

**COMBINED CYCLE SOLAR CENTRAL RECEIVER  
HYBRID POWER SYSTEM STUDY**

**Final Technical Report**

**prepared by**  
**Bechtel National, Inc.**  
**San Francisco, CA**

**Subcontractors: Foster Wheeler Development Corporation**  
**Northrup, Inc.**  
**Westinghouse Electric Corporation,**  
**Combustion Turbine Systems Division**

**Utility Advisor: Public Service Company of New Mexico**

**for the**  
**United States Department of Energy**  
**San Francisco Operations Office**

**November, 1979**

**Contract No.:**  
**DE-AC03-78ET21050**  
**Bechtel Job No. 13007**

## CONTENTS

<u>Appendix</u>	<u>Page</u>
A Preconceptual Design Data	A-1
B Market Potential Analysis Methodology	B-1
C Parametric Analysis Methodology	C-1
D EPGS Systems Descriptions	D-1
E Commercial-Scale Solar Hybrid Power System Assessment	E-1
F Conceptual Design Data Lists	F-1

**APPENDIX A**

**PRECONCEPTUAL DESIGN DATA**

## CONTENTS

<u>Section</u>		<u>Page</u>
A.1	General Data	A-3
A.2	Collector Subsystem	A-4
A.3	Receiver Subsystem	A-6
A.4	Solar/Nonsolar Interface	A-10
A.5	Electric Power Generation Subsystem	A-11
A.6	Master Control Subsystem	A-13
A.7	Balance of Plant Subsystem	A-16

This appendix presents the available technical data on the Strawman and Advanced Strawman concepts compiled at the beginning of the study project to provide a common point of departure for parametric analyses, market potential studies, and a preconceptual cost estimate.

#### A.1 GENERAL DATA

Nominal Net Power (MWe)	100
Baseline Fossil Fuel	No. 2 fuel oil
Solar and Meteorological Data Site	Barstow, California
Technical Requirements	Technical Requirement Definition, Issue "C" dated 11/6/78
Operating Modes	Hybrid, fossil only

## A.2 COLLECTOR SUBSYSTEM

Direct Normal Insolation ( $W/m^2$ )	950 (at design point)	
Reflective area per heliostat ( $m^2$ )	38.6	
Efficiency (%)*		
Peak, design point	65.7	
Avg. for Barstow Conditions	59.2	
Collector Field Data	STRAWMAN	ADV. STRAWMAN
Maximum Net Electrical Output - Solar (MWe)	52.7	68.1
Power to Receiver (MWt)	139.2	173.8
Number of Heliostats	5682	7095
Reflective area per heliostat ( $m^2$ )	38.6	38.6
Field Arrangement	See attached layout for intermediate field with 6500 heliostats (Figure A-1)	
Layout Grid	Rectangular	
Area of Collector Field (Acres)	270	340
Land Utilization (%)	20	20
Reference Tower Height (m)	175	196
Focusing Control	Central source/target position computer, local focusing control	
Signal Transmission	Hard wired	
Drive System Voltage (V ac)	120/240	

\*Definition: 
$$\frac{\text{energy to aperture} \times 100}{\text{energy incident to heliostats}}$$



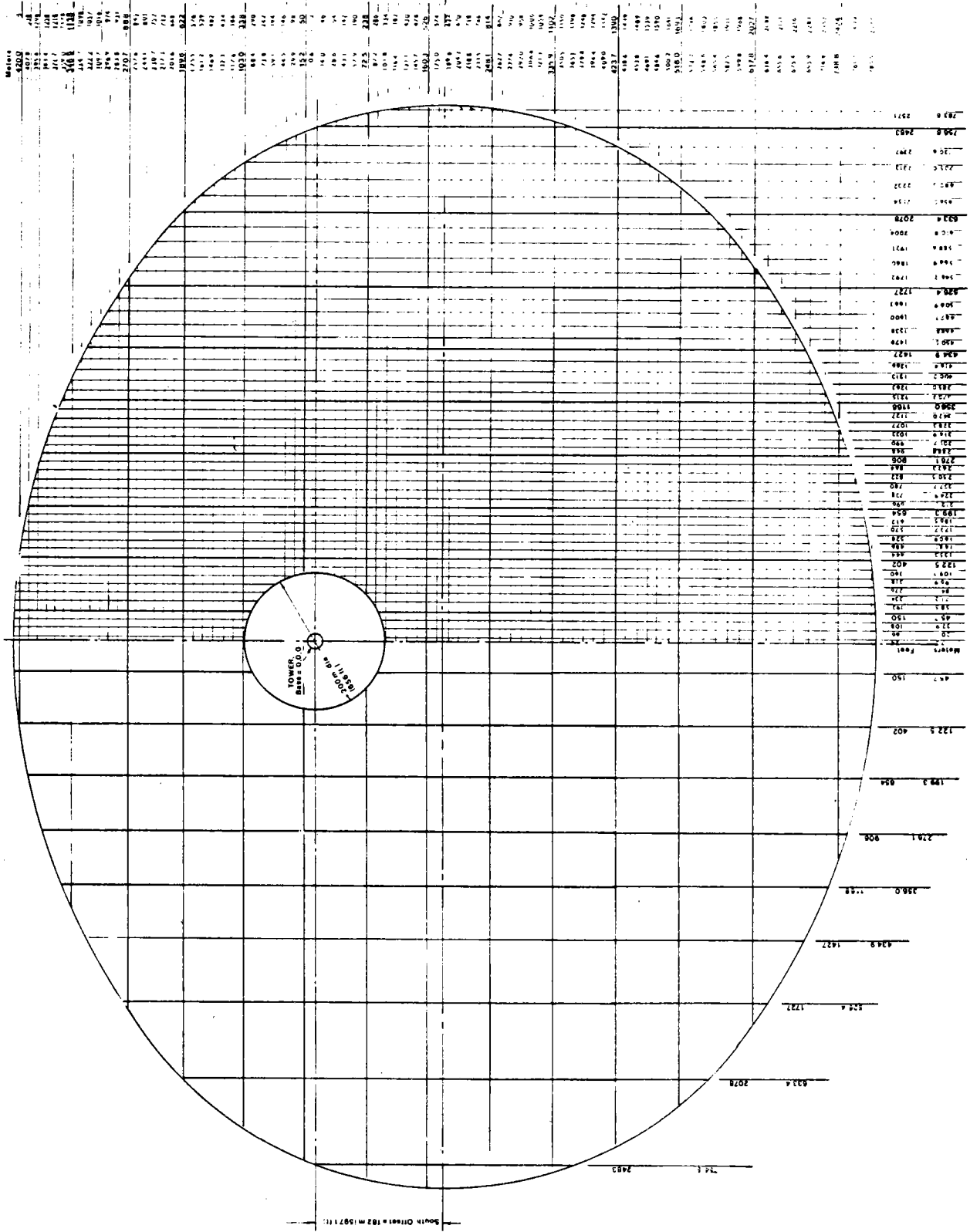


Figure A-1 COLLECTOR FIELD "D"

### A.3 RECEIVER SUBSYSTEM

	STRAWMAN	ADV. STRAWMAN
Receiver Type	multicavity	multicavity
Absorber Type	heat pipe	ceramic tube
Total Energy Input to Absorber (MWt)	139	174
Efficiency (%)*	89	84
Peak Heat Flux (MWt/m <sup>2</sup> )	1.12	
Flux Distribution	see Figures A-2 and A-3	
Cooling Medium	air	air
Inlet Pressure (kPa)	1095	1092
Receiver Pressure Drop (kPa)	28	69
Inlet Temperature (C)	378	378
Outlet Temperature (C)	816	1093
Peak Wall Temperature (C)	870	1315
Receiver Energy Distribution (%):		
North Facing	34	34
South Facing	22	22
East Facing	22	22
West Facing	22	22
Height of Aperture Above Ground (m)	175	196
Aperture Area (m <sup>2</sup> )		
North Facing	38.5	
Others	28.3	

\*Definition: 
$$\frac{\text{energy absorbed in coolant} \times 100}{\text{energy incident at the aperture}}$$

	STRAWMAN	ADV. STRAWMAN
Number of Absorber Panels:		
North Facing	11	N/A
Others	9	N/A
Absorber Panel Setback (m):		
North Facing	7	N/A
Others	5.7	N/A
Absorber Panel Dimensions (m): (height X width)		
North Facing	12 X 1	N/A
No. of Heat Pipes per Panel		N/A
Air Velocity in Receiver (m/sec):		
Inlet	8.9	
Outlet	13.5	
Panel Flow Balancing	Dampers	
Heat Loss (% of incident energy)	10-12	14-18
Materials:		
Pipes, ducts	Inconel	
Panel walls	"	N/A
Heat Pipe Sheeting	"	N/A
Heat Pipe Fins	"	N/A
Heat Pipe Working Fluid	Sodium & Potassium	N/A
Tower Structure	Reinforced concrete	

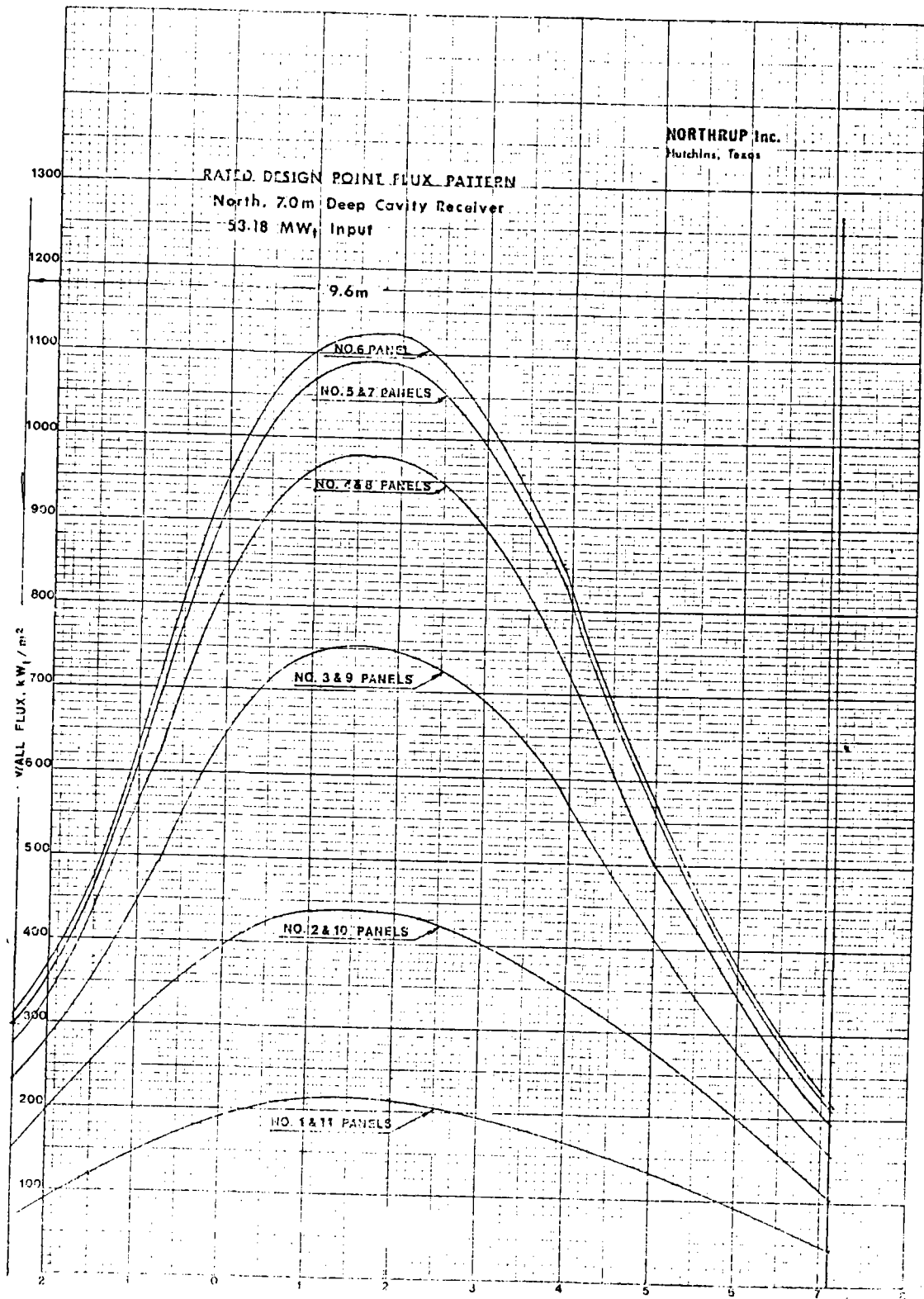


Figure A-2 RATED DESIGN POINT FLUX PATTERN, NORTH

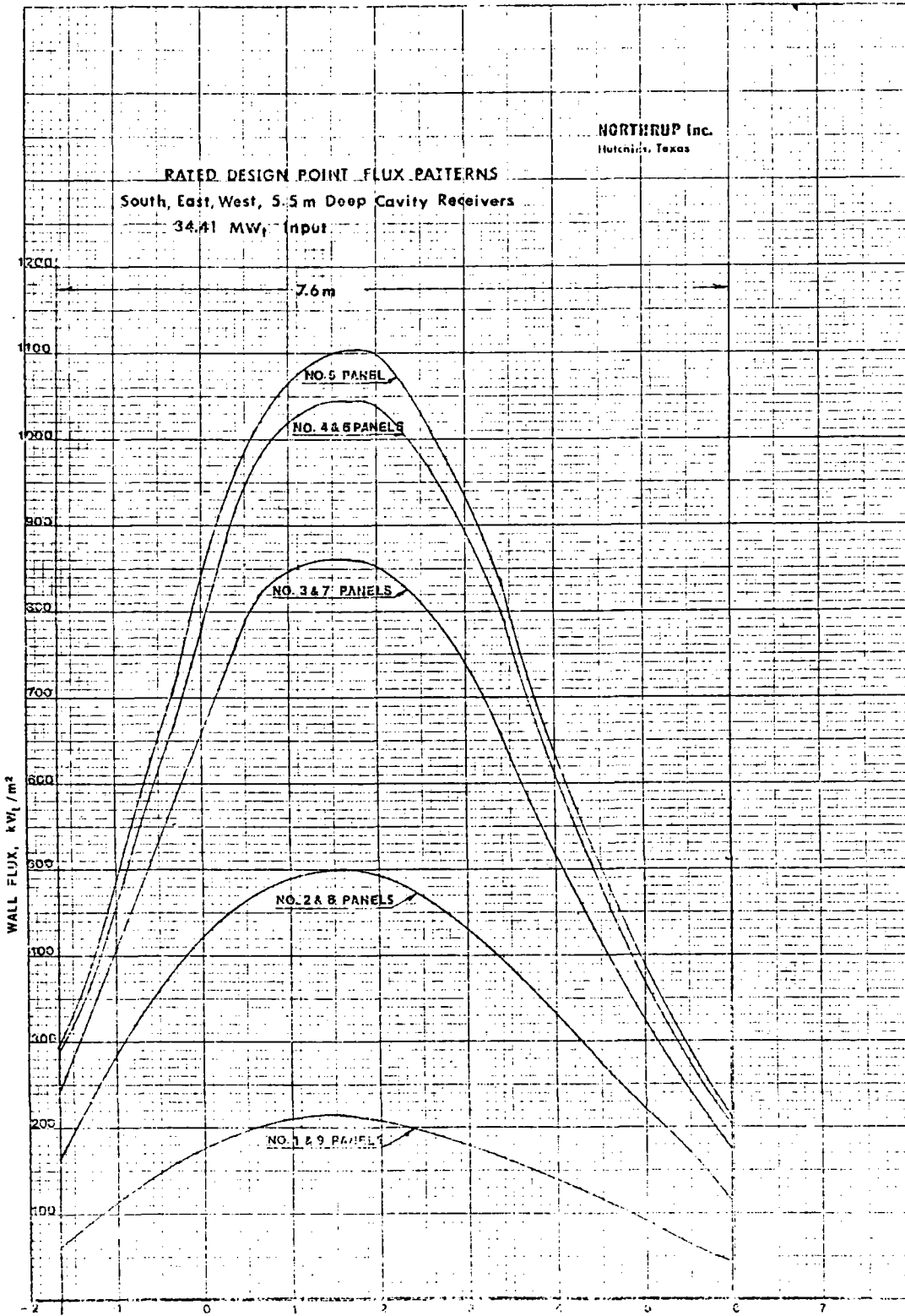


Figure A-3 RATED DESIGN POINT FLUX PATTERNS, SOUTH, EAST, AND WEST

#### A.4 SOLAR/NONSOLAR INTERFACE

	STRAWMAN	ADV. STRAWMAN
Solar Coupling Concept	In series, receiver bypassed for nighttime mode	
Solar Fraction of Design Point	.563	.719
Riser Pipe Configuration:		
Pipe Diameter (m)	1.52	1.22
Wall Thickness (cm)	1.3	1.3
Construction Method	welded	welded
Insulation Thickness (cm) (external)	12.7	12.7
Straight Length (m)	390	440
No. of 90° long radius Elbows	30	35
Pipe Material	carbon steel	carbon steel
Pressure Rating (kPa)	1480	1480
Air Velocity (m/sec)	26.5	27.4
Pressure Drop (kPa)	13.8	17.2
Downcomer Pipe Configuration:		
Pipe Diameter (m)	1.83	1.83
Wall Thickness (cm)	1.6	1.6
Construction Method	welded	welded
Insulation Thickness (cm) (internal)	18	23
Straight Length (m)	330	350
No. of 90° long radius Elbows	15	20
Pipe Material	carbon steel	carbon steel
Liner Material	inconel	tantalum
Pressure Rating (kPa)	1480	1480
Air Velocity (m/sec)	48	49
Pressure Drop (kPa)	13.8	17.2

## A.5 ELECTRIC POWER GENERATION SUBSYSTEM

### Power Cycle Characteristics:

Type	Open Brayton, heat recovery steam generator with deaerator, steam Rankine bottoming, water cooled condenser	
Total Power Generation (MWe)	103	103
Auxiliary Load (MWe)	3	3

### Design Point Conditions:

Air Flow (kg/sec)	274	190
Inlet Air Temperature (C)	28	28
Inlet Air Pressure (kPa)	94	94
Compression Ratio	12:1	12:1
Gas Turbine Inlet Temp. (C)	1093	1316
Gas Turbine Inlet Pressure (kPa)	1000	955
Gas Turbine Outlet Temp. (C)	539	688
Gas Turbine Outlet Press. (kPa)	96.5	96.5
HRSG Outlet Air Temp. (C)	201	149
Net Power - Gas Turbine (MWe)		
Hybrid Mode	68.4	64.7
Fossil Mode (Long Term)	73.7	72.7
Fossil Mode (Short Term)	71.5	68.9
Steam Flow (kg/sec)	32	35.8
Steam Turbine Inlet Temp. (C)	510	510
Steam Turbine Inlet Pressure (kPa)	10,100	10,100
Condenser Pressure (kPa)	8.5	8.5
Pinch Point Temperature (C)	17	49

	STRAWMAN	ADV. STRAWMAN
Net Power - Steam Turbine (MWe):		
Hybrid Mode	31.6	35.3
Fossil Mode (Long Term)	32.4	36.8
Fossil Mode (Short Term)	33.1	38.0
Generator Voltage (kV)	13.8	13.8
Condenser Cooling Load (kJ/sec)	60	68
Wet Bulb Temperature (C)	23	23
Approach Temperature (F)	5.6	5.6
Temperature Range (C)	11	11
Circ. Water Flow Rate (m <sup>3</sup> /sec)	1.44	1.64
Circ. Water Pump Head (m)	18.3	24.4
Circ. Water Pump Power (kW)	300	550
Pipe Diameter (m)	0.76	0.76
Cooling Tower Type	Mech. Draft	Mech. Draft



## A.6 MASTER CONTROL SUBSYSTEM

Type	Analog EPGS and digital solar control
Control Block Diagram	See Figure A-4
Control Schematic	See Figure A-5
Combined Cycle Control	Westinghouse Model 7300 (analog control)
Solar Control System	Hewlett-Packard components
Digital Data Logger	Westinghouse Model W2500

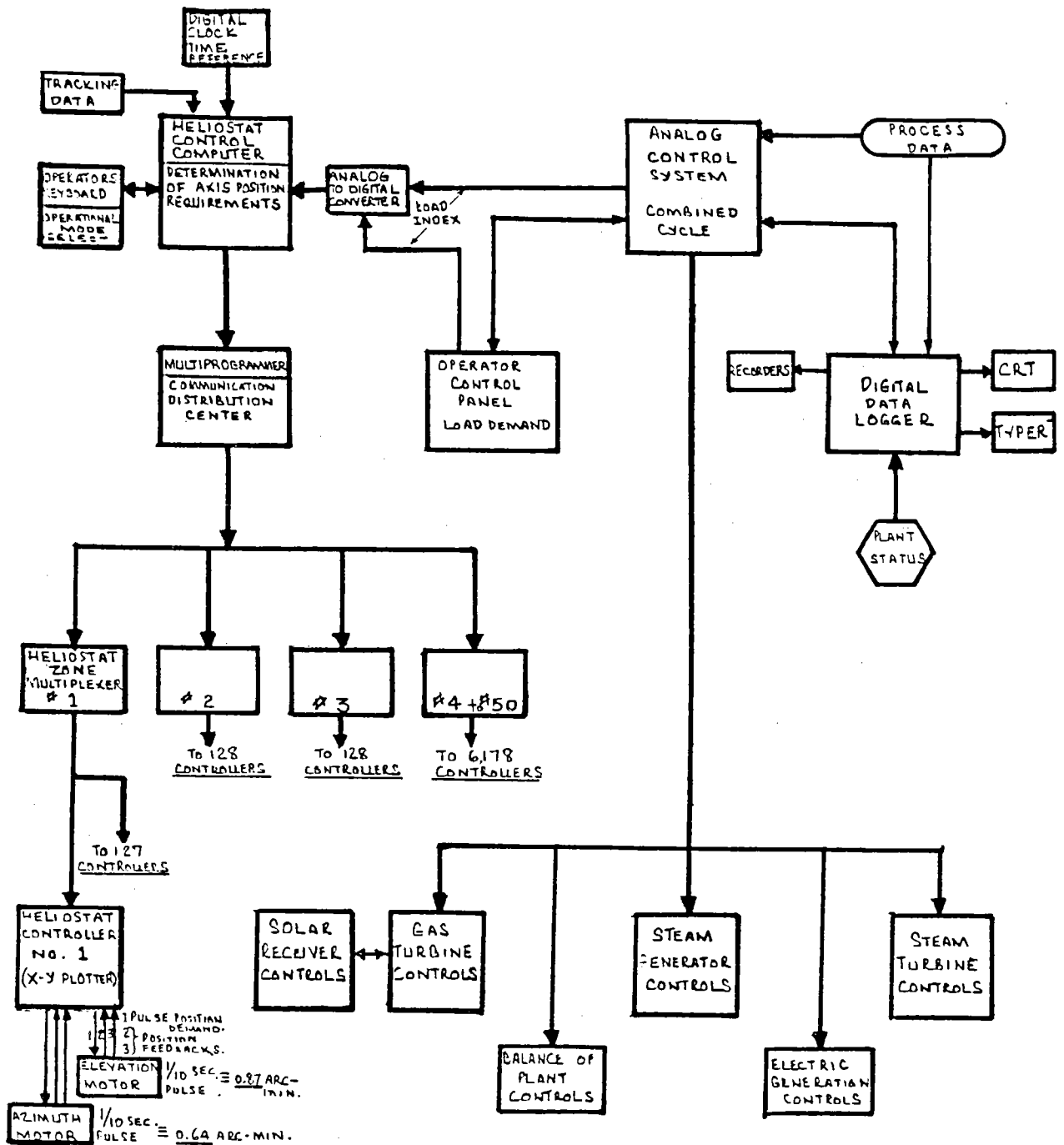


Figure A-4 CONTROL BLOCK DIAGRAM

A-15

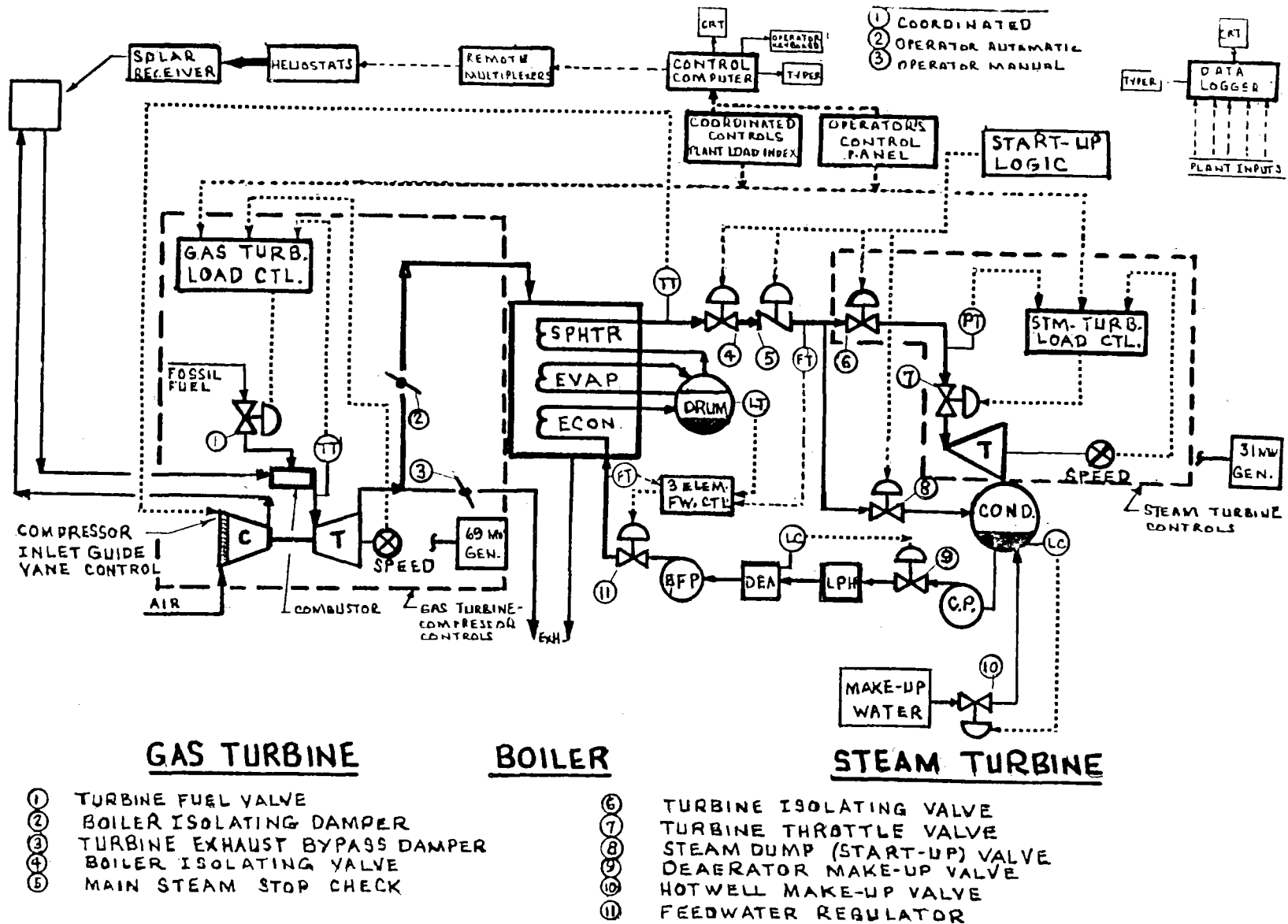


Figure A-5 CONTROL SCHEMATIC

## A.7 BALANCE OF PLANT SUBSYSTEM

### Control and Administration Bldg.:

No. of Floors	2
Total Floor Area (m <sup>2</sup> )	800
Type of Structure	Metal frame, insulated siding and roof
Utilities	Lighting, HVAC, potable water sanitary sewer

### Maintenance and Warehouse Bldg.:

Shop Floor Area (m <sup>2</sup> )	300
Warehouse Floor Area (m <sup>2</sup> )	450
Type of Structure	Conventional metal warehouse structure
Utilities	Lighting, ventilation, potable water, sanitary sewer, compressed air, local office air conditioning

### Switchyard, Transmission Lines

Transformers and switchgear to connect to 115 kV utility grid and supply site power. Underground transmission to site boundary. Overhead transmission to utility line 1.5 km from site boundary.

### Water Supply (m<sup>3</sup>/sec):

	<u>Strawman</u>	<u>Advanced Strawman</u>
Cooling Water Makeup	.038	.044
Potable Water	.005	.005
Fire Protection	.01	.01

### Water Source

Wells

### Potable Water Treatment

Filtration, chlorination

### Cooling Water Treatment

Periodic algicide addition

Fire Protection/Safety Provisions:

Automatic Sprinkler System	Administration building, maintenance/warehouse bldg.
Preaction Sprinkler System	Control building, cable spreading space switchyard
Fire hydrants	120
Manual (ABC) Extinguishers	200
Sodium Catch Pans with METALEX	in receiver
First Aid Equipment	

Mirror Cleaning Provisions:

Washing Trucks	2
----------------	---

Roadways

APPENDIX B

MARKET POTENTIAL ANALYSIS METHODOLOGY

## CONTENTS

<u>Section</u>		<u>Page</u>
B.1	Plant Economic and Performance Data	B-3
B.2	Levelized Busbar Cost Calculations	B-11
B.3	Sensitivity Analysis	B-14
B.4	Incremental Load Duration Curve	B-23
B.5	Regional Electricity Demand Forecasts	B-24
B.6	Forecasted Coal/Nuclear Fraction of Capacity Additions	B-25
B.7	Cost Input Data to Computer Program, ALLOCATE	B-26

B.1 PLANT ECONOMIC AND PERFORMANCE DATA

B.1.1 Baseline Solar Hybrid Cost/Performance Data

The major cost categories of the solar hybrid capital cost estimates presented in Volume II, Section 2 include:

- Direct Field Construction Cost: Major mechanical and electrical equipment, structures, bulk materials, construction labor and subcontract items.
- Indirect Field Cost: Temporary construction facilities, miscellaneous construction services, construction equipment and supplies, field office, testing, taxes, permits and insurance. Based on past Bechtel experience these costs are estimated at 75% of direct construction labor cost.
- Engineering Services: Engineering costs, home office costs and fee. Based on past experience, these costs are estimated at 12% of the total field costs of non-solar systems and 10% of the total field cost of solar systems (which are largely subcontracted).
- Contingency: Allowance for uncertainty within the conceptual designs in the quantity, pricing or productivity that is within the control of the constructor and within the scope of the project as defined. For the conceptual level of the hybrid estimates, 15% of the sum of total field costs and engineering services is allowed.
- Allowance for Funds During Construction (AFDC): The bulk of AFDC is interest costs. Per DOE/SAN guidelines, AFDC is estimated at 15% of the sum of direct construction cost, engineering services and contingency.

B.1.2 Regional Variation of Cost/Performance Data

Four regions were selected for the regional market assessment:



- Middle Atlantic Region: Pennsylvania, New York and New Jersey.
- South Central Region: Texas, Oklahoma, Arkansas and Louisiana.
- South Mountain Region: Nevada, Utah, Colorado, Arizona and New Mexico.
- Pacific Southern Region: California.

Table B-1 shows regionally adjusted hybrid system capital and operating and maintenance costs. The adjustments reflect regional labor and material price differences.

Table B-2 lists regional variations in important performance characteristics relative to Barstow.

TABLE B-2  
NORMALIZED REGIONAL PERFORMANCE VARIATIONS

<u>Region</u>	<u>Average Annual Solar Fraction</u>	<u>Breakpoint Capacity Factor</u>	<u>Solar System Size</u>
Barstow (base)	1.00	1.0000	1.0000
Middle Atlantic	0.51	1.0025	1.0173
South Central	0.73	0.9991	0.9928
South Mountain	1.01	1.0004	1.0024
Pacific Southern	0.91	1.0007	1.0048

For the regions studied, only average annual solar fraction exhibits appreciable variation, as shown in Table B-3, and was the only factor adjusted regionally for the economic comparisons.

TABLE B-1  
REGIONAL CAPITAL AND OPERATING COSTS

REGION	CAPITAL COST, (\$/kW)				FIXED O&M COST, (\$/kW-YR)				VARIABLE O&M COST, (Mills/kWh)			
	1978		1990		1978		1990		1978		1990	
	MS	AS	MS	AS	MS	AS	MS	AS	MS	AS	MS	AS
Middle Atlantic	1431	1623	4491	5094	8.73	11.54	21.98	29.06	0.99	1.16	2.49	2.92
South Central	1236	1402	3879	4400	7.54	9.97	18.99	25.11	0.85	1.01	2.14	2.54
South Mountain	1279	1451	4014	4554	7.80	10.32	19.64	25.99	0.88	1.04	2.22	2.62
Pacific Southern	1279	1451	4014	4554	7.80	10.23	19.64	25.99	0.88	1.04	2.22	2.62

MS = Modified Strawman

AS = Advanced Strawman

TABLE B-3

## AVERAGE ANNUAL SOLAR FRACTION BY REGION

<u>Region</u>	<u>Average Annual Solar Fraction (%)</u>	
	<u>Modified Strawman</u>	<u>Advanced Strawman</u>
Barstow	31.2	40.8
Middle Atlantic	15.9	20.8
South Central	22.8	29.8
South Mountain	31.5	41.2
Pacific Southern	28.4	37.1

B.1.3 Conventional Technology Cost/Performance Data

Cost/performance data for the four conventional technologies considered in regional comparisons were adapted from the EPRI Technical Assessment Guide and are shown in Tables B-4, B-5, and B-6. Capital costs are for single unit plants and include:

- Total field construction cost
- Contingency
- Startup
- Allowance for funds during construction
- Engineering services
- Average standing inventory

Operating and maintenance costs are first year averages for an assumed capacity factor. Although they are expected to vary with capacity factor, the variation is small and should not distort the economic comparisons. Regional variations include labor and material price differences, and where appropriate, design

TABLE B-4

CONVENTIONAL TECHNOLOGIES PERFORMANCE/COST DATA  
 MIDDLE ATLANTIC REGION  
 (SOURCE: EPRI TECHNICAL ASSESSMENT GUIDE)

COMPETING TECHNOLOGY	PLANT CHARACTERISTICS			CAPITAL COST, (\$/kW)		FIXED O&M COST, (\$/kW-YR)		VARIABLE O&M COST, (Mills/kWhr)	
	CAPACITY, MWe	LIFE, Yrs.	HT RATE, Btu/kWh	1978	1990	1978	1990	1978	1990
COMBUSTION TURBINE	75	30	14000	145	455	0.55	1.38	2.26	5.69
COMBINED CYCLE	250	30	8700	330	1036	1.32	3.32	1.40	3.53
COAL.*	1000	30	10100	765	2401	2.67	6.73	3.16	7.96
LIGHT WATER REACTOR	1000	30	10400	875	2746	3.01	7.58	0.76	1.91

\* With flue gas desulfurization.

TABLE B-5

CONVENTIONAL TECHNOLOGIES PERFORMANCE/COST DATA  
 SOUTH CENTRAL REGION  
 (SOURCE: EPRI TECHNICAL ASSESSMENT GUIDE)

COMPETING TECHNOLOGY	PLANT CHARACTERISTICS			CAPITAL COST, (\$/kW)		FIXED O&M COST, (\$/kW-YR)		VARIABLE O&M COST (Mills/kWhr)	
	CAPACITY, MWe	LIFE, Yrs.	HT RATE, Btu/kWh	1978	1990	1978	1990	1978	1990
	COMBUSTION TURBINE	75	30	14000	152	477	0.48	1.21	1.95
COMBINED CYCLE	250	30	8700	285	894	1.14	2.87	1.21	3.05
COAL*	1000	30	10700	735	2307	2.31	5.82	2.26	5.69
LIGHT WATER REACTOR	1000	30	10400	775	2432	2.66	6.70	0.67	1.69

\* With flue gas desulfurization.

TABLE B-6

CONVENTIONAL TECHNOLOGIES PERFORMANCE/COST DATA  
 WEST REGION (SOUTH MOUNTAIN & PACIFIC SOUTHERN)  
 (SOURCE: EPRI TECHNICAL ASSESSMENT GUIDE)

COMPETING TECHNOLOGY	PLANT CHARACTERISTICS			CAPITAL COST (\$/kW)		FIXED O&M COST (\$/kW-YR)		VARIABLE O&M COST (Mills/kWhr)	
	CAPACITY, MWe	LIFE, Yrs.	HT RATE, Btu/kWh	1978	1990	1978	1990	1978	1990
COMBUSTION TURBINE	75	30	14000	157	493	0.49	1.23	2.02	5.09
COMBINED CYCLE	250	30	8700	295	926	1.18	2.97	1.25	3.15
COAL*	1000	30	10400	745	2338	2.58	6.50	1.64	4.13
LIGHT WATER REACTOR	1000	30	10400	825	2589	2.84	7.15	0.72	1.81

\* With flue gas desulfurization.

differences. To ensure consistent comparisons, the regional estimates of solar hybrid power plants were adjusted on the same basis. Finally, the EPRI Western region (the Pacific and Mountain Census Regions) cost/performance data were assumed applicable in both the South Pacific and South Mountain insolation regions.

## B.2 LEVELIZED BUSBAR COST CALCULATIONS

### B.2.1 Conventional Technology Levelized Costs

Levelized costs are assumed to include four major components:

- Levelized fixed capital charges
- Levelized fixed operating and maintenance costs
- Levelized variable operating and maintenance cost
- Levelized fuel costs

The sum of the first two components is levelized fixed costs (F); the sum of the second two is levelized variable cost (V). F and V are computed according to:

$$F = \left[ \frac{CCB \cdot FCR}{MWE} \right] + \left[ FOM \cdot LF_{O\&M} \right]$$

$$V = \left[ \frac{VOM}{10^3} \cdot LF_{O\&M} \right] + \left[ FC \cdot \frac{HR}{10^6} \cdot LF_{Fuel} \right]$$

where:

- CCB = Capital cost basis (\$1000)
- FCR = Fixed charge rate
- MWE = Capacity (MWe)
- FOM = First year fixed operating and maintenance cost (mills/kWh)
- VOM = First Year Variable Operating and Maintenance Cost (mills/kWh)
- FC = First year fuel cost (\$/MBtu)
- HR = Average heat rate (Btu/kWh)



$LF_{O\&M}$  = Levelizing factor for operating and maintenance cost

$LF_{Fuel}$  = Levelizing factor for fuel cost

The levelizing factors are calculated according to:

$$LF = \left[ \frac{1+g}{r-g} \right] \left[ 1 - \left( \frac{1+g}{1+r} \right)^n \right] \left[ \frac{r}{1 - \left( \frac{r}{1+r} \right)^{-n}} \right] \quad \text{if } r \neq g$$
$$= n \left[ \frac{r}{1 - \left( \frac{r}{1+r} \right)^{-n}} \right] \quad \text{if } r = g$$

where:

$g$  = Nominal escalation rate for fuel or operating and maintenance costs

$r$  = Discount rate

$n$  = Plant economic life

### B.2.2 Solar Hybrid Levelized Costs

Hybrid system levelized costs are computed identically except that separate variable costs are computed for both hybrid and fossil operation. The levelized variable cost,  $V_1$ , corresponding to hybrid operation is:

$$V_1 = \left[ \frac{VOM}{10^3} \cdot LF_{O\&M} \right] + \left[ FC \left( \frac{DAHR}{10^6} \right) \left( 1 - \frac{SF}{100} \right) \left( LF_{Fuel} \right) \right]$$

where all symbols are as detailed under E.2.1, except:

DAHR = Average heat rate during hybrid operation (Btu/kWh)

$\overline{SF}$  = Average annual solar fraction (%)

The variable cost,  $V_2$ , corresponding to fossil operation is:

$$V_2 = \left[ \frac{VOM}{10^3} \cdot LF_{O\&M} \right] + \left[ FC \left( \frac{NAHR}{10^6} \right) (LF_{Fuel}) \right]$$

where all symbols are again as detailed in Section B.2.1, except:

NAHR = Average heat rate during fossil operation (Btu/kWh)

$F_1$ , the levelized fixed cost, is computed in the same manner as conventional technology levelized fixed costs.

The sensitivity of hybrid levelized busbar electricity costs to variations in cost/performance and economic parameters was measured by computing the percentage change in levelized busbar costs in response to +1 percent change as a function of capacity factor in the following:

- Capital cost
- Fixed operating and maintenance cost
- Variable operating and maintenance cost
- Daytime average heat rate
- Solar fraction
- Fuel cost
- Discount rate
- Fixed charge rate
- Escalation rates (capital, operating and maintenance, fuel)

Figure B-1 shows the results for the cost components specific to the Advanced Strawman (capital cost, fixed and variable O&M cost, daytime average heat rate, and solar fraction). Since the Advanced Strawman is more capital intensive than the Modified Strawman, it is more sensitive to changes in capital costs related parameters and less sensitive changes in fuel related parameters.

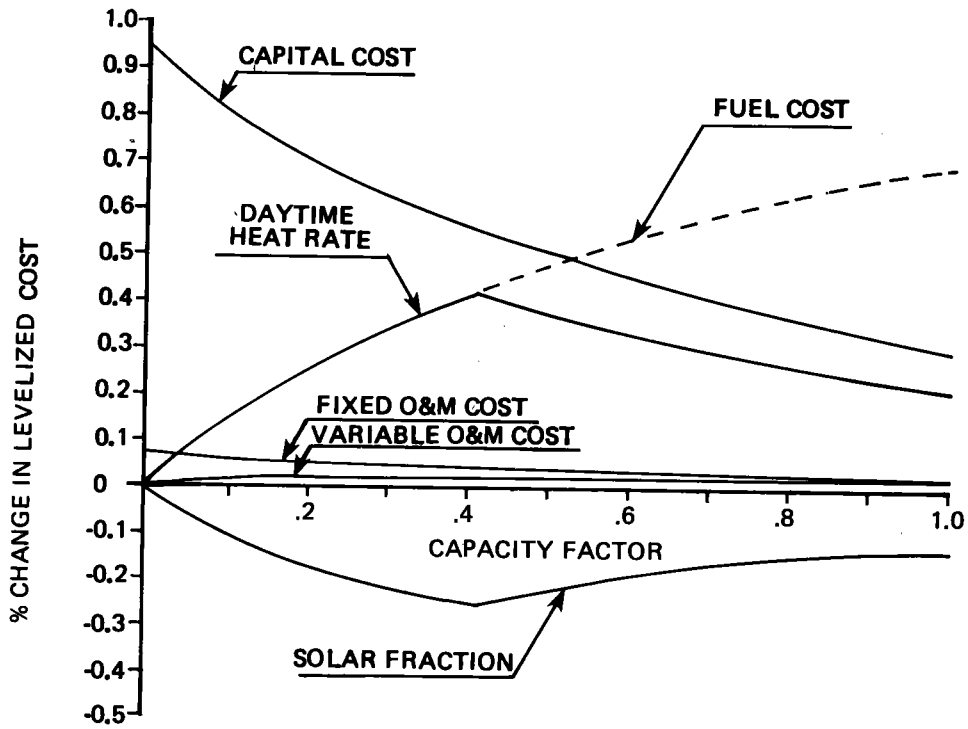


**Figure B-1 SENSITIVITY OF ADVANCED STRAWMAN LEVELIZED BUSBAR COSTS TO +1% VARIATIONS IN COST COMPONENTS SPECIFIC TO HYBRID SYSTEMS**

As capacity factors increase, changes in levelized cost in response to a +1 percent change in capital and fixed operating costs are attenuated, while the percentage change in levelized cost for a +1 percent change in variable O&M cost is increased. Changes in daytime average heat rate and solar fraction reach a maximum at the breakpoint capacity factor of 40.8 percent. The discontinuity in slope for these last two curves reflects the piecewise linear levelized cost function used for the hybrid plants.

Although fuel cost is one of the common cost components, it is also shown in Figure B-1 to emphasize its importance at high capacity factors. It should be noted that a +1 percent change in heat rate has exactly the same effect on levelized cost as a +1 percent change in fuel cost. In fact, if both daytime and nighttime heat rates were changed by +1 percent, the heat rate and fuel cost curves would coincide.

Figure B-2 shows the sensitivity of hybrid levelized busbar costs to variations in levelized cost components common to several of the conventional technologies (fuel cost for oil-fired combustion turbine and combined cycle plants, discount rate, fixed charge rate and escalation rates).

As before, the impact of capacity factor on the results is significant. Levelized costs are more sensitive to variations in fixed cost-related items at lower capacity factors while variable cost-related items are more sensitive at higher capacity factors.

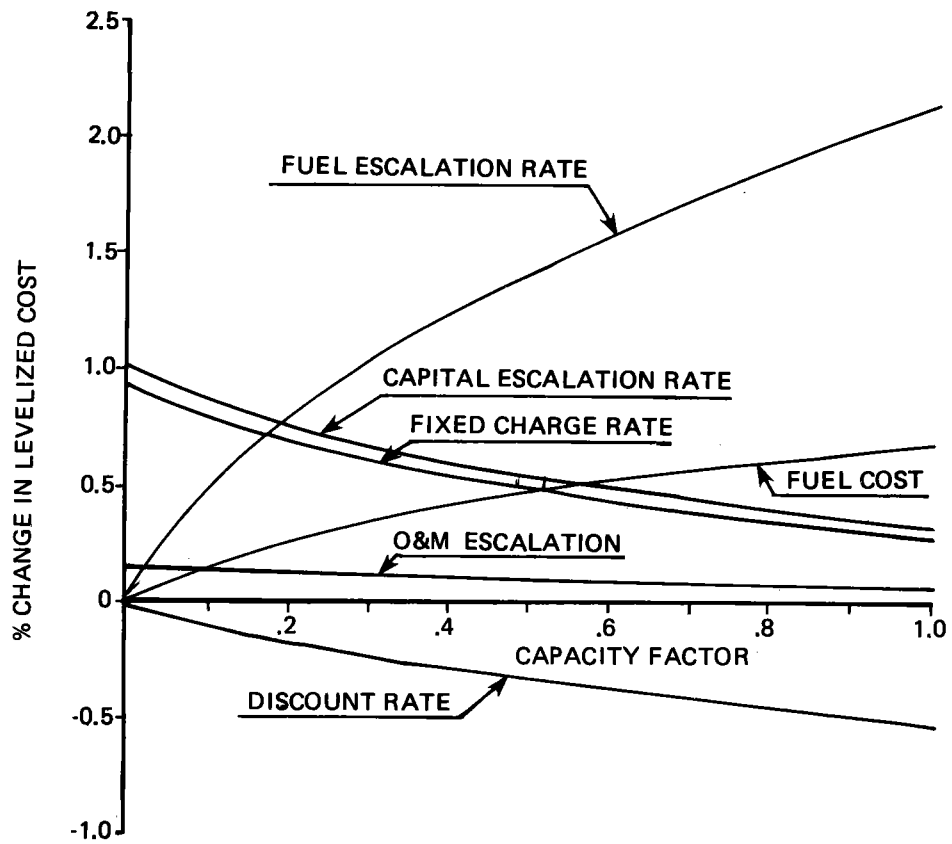


**Figure B-2 SENSITIVITY OF ADVANCED STRAWMAN LEVELIZED BUSBAR COST TO 1% VARIATIONS IN COST COMPONENTS COMMON TO ALL TECHNOLOGIES**

As seen from the figure, fuel escalation rate is the most significant levelized cost component.

For variations of levelized cost components common to all competing technologies, it is instructive to examine not only the changes in hybrid levelized costs, but also the change in hybrid levelized costs relative to the changes in levelized costs for competing technologies. For example, if a 1 percent increase in fuel escalation rate raises hybrid levelized cost by \$1/kW-yr but raises the levelized costs of competing technologies by \$10/kW-yr, the hybrid systems will be more competitive at higher fuel escalation rates. Tables B-7 and B-8 compare the hybrid system with two likely competitors, coal and conventional combined cycle plants. The relative sensitivity measure used is the ratio of the change in hybrid levelized costs to the change in coal or combined cycle levelized costs for a +1 percent change in a common levelized cost component.

For all levelized cost components, except the discount rate, a ratio greater than one implies that the hybrid system benefits (relative to a competitor) from reductions in the levelized cost component, while a ratio less than one implies that the hybrid system benefits from an increase. The opposite is true for the discount rate (as well as any other component, which when increased, decreases levelized cost). That is, a ratio greater than one implies that the hybrid system benefits relative to a competitor from an increase in the levelized cost component while

TABLE B-7

CHANGE IN SOLAR HYBRID LEVELIZED BUSBAR COSTS RELATIVE  
TO COAL LEVELIZED BUSBAR COSTS FOR A + 1% VARIATION  
IN COST COMPONENTS COMMON TO ALL TECHNOLOGIES

Cost Component	Cost Change Ratio For		
	Fixed Cost	Breakpoint Cost	100% Capital Cost
Modified Strawman			
Discount Rate	6.00	1.10	1.39
Fixed Charge Rate	1.71	1.71	1.71
Capital Escalation Rate	1.76	1.76	1.76
O&M Escalation Rate	3.00	0.62	0.04
Advanced Strawman			
Discount Rate	6.00	0.94	1.36
Fixed Charge Rate	1.95	1.95	1.95
Capital Escalation Rate	2.00	2.00	2.00
O&M Escalation Rate	4.00	0.81	0.51



TABLE B-8

CHANGE IN SOLAR HYBRID LEVELIZED BUSBAR COSTS RELATIVE TO THE CHANGE  
IN CONVENTIONAL COMBINED CYCLE LEVELIZED BUSBAR COSTS FOR A + 1%  
VARIATION IN COST COMPONENTS COMMON TO ALL TECHNOLOGIES

Cost Component	Cost Change Ratio For		
	Fixed Cost	Breakpoint Cost	100% Capital Cost
Modified Strawman			
Discount Rate	6.00	0.71	0.88
Fixed Charge Rate	2.12	2.12	2.12
Capital Escalation Rate	2.08	2.08	2.08
O&M Escalation Rate	4.50	2.60	1.73
Fuel Escalation Rate	0	0.68	0.87
Fuel Cost	0	0.68	0.87
Advanced Strawman			
Discount Rate	6.00	0.61	0.87
Fixed Charge Rate	2.41	2.41	2.41
Capital Escalation Rate	2.37	2.37	2.37
O&M Escalation Rate	6.00	3.40	2.18
Fuel Escalation Rate	0	0.59	0.81
Fuel Cost	0	0.59	0.81

a ratio less than one implies that the hybrid system benefits from a reduction.

These results show that the set of levelized cost components favorable to the hybrid systems depends on the type of competing technology. For example, the hybrid systems benefit relative to oil-fired combustion turbine and combined cycle units for:

- Higher fuel oil prices and fuel escalation rates
- Lower discount rate

By contrast, the hybrid systems benefit relative to coal and nuclear plants which use cheaper fuels for:

- Lower fuel oil prices and fuel escalation rates
- Higher discount rate

As they represent the most capital intensive of the competing technologies, the hybrid systems benefit relative to all competitors for lower fixed charge rate and capital escalation rate.

It should be noted that not all of the common levelized cost components are independent. For example, the fixed charge rate is an increasing function of the discount rate. (Fixed charge rate may, however, increase while the discount rate remains constant, as is the case when an investment tax credit is allowed.) Thus the true effect on levelized costs of a 1 percent

change in discount rate is reduced. It should also be recognized that both the absolute and relative sensitivity measures are strictly valid only for small deviations from the baseline parameter set. Since the cost functions are nonlinear in virtually all of the components examined, rates of change also depend on the level of each component. The degree of nonlinearity for small changes, however, is not excessive.

The load duration curve is approximated by the following deterministic function of annual hours of operation:

$$GW(H) = D_3 + \left[ D_4 \cdot 1095 \cdot \sin \frac{2\pi H}{8760} \right] + [D_4 + H]$$

where:

$GW(H)$  = Load duration function

$$D_3 = \frac{D}{(LF \cdot 8760)}$$

$$D_4 = \frac{-2 \cdot D_3 \cdot (1-LF)}{8760}$$

$D$  = Total incremental electricity demand (GWH)

$LF$  = Load factor

$H$  = Annual hours of operation

Regional incremental electricity demand forecasts in thousands of GWH/YR are tabulated in Table B-9. The values are the average over a 2 year period beginning in the years listed in the table.

TABLE B-9  
REGIONAL INCREMENTAL ELECTRICITY DEMAND  
(GWH/YR x 10<sup>3</sup>)

<u>Region</u>	<u>1990</u>	<u>2000</u>	<u>2010</u>	<u>2020</u>
Pacific Southern	13.5	12	12	12
South Mountain	4	6	6	5
South Central	21.5	23.5	22.5	22.5
Middle Atlantic	16.5	21	21.5	19

The regional load factors used in the analyses are tabulated in Table B-10. They are assumed to remain constant over the 1990-2020 time period.

TABLE B-10  
REGIONAL LOAD FACTORS  
(percent)

<u>Region</u>	<u>Load Factor</u>
Pacific Southern	66
South Mountain	65.2
South Central	54.4
Middle Atlantic	62.2

Table B-11 shows projections of incremental coal and nuclear capacity additions as a fraction of total incremental capacity.

TABLE B-11

## INCREMENTAL COAL/NUCLEAR CAPACITY FRACTIONS

<u>Region</u>	<u>1990</u>	<u>2000</u>	<u>2010</u>	<u>2020</u>
Pacific Southern	.7	.69	.76	.93
South Mountain	.71	.88	.84	.84
South Central	1.0	1.0	1.0	1.0
Middle Atlantic	.97	1.0	1.0	1.0

Regional levelized costs in 1990\$ for Modified Strawman (MS), Combined Cycle (CC), and Combusion Turbine (CT) under the three scenarios are tabulated in Tables B-12 to B-14. Cost data for the Modified Strawman are presented for low (L), medium (M), and high (H) ranges.

TABLE B-12

LEVELIZED COSTS IN 1990 \$  
 EPRI REGIONAL COST DATA, DOE/SAN ECONOMIC GUIDELINES  
 FUEL ESCALATION RATE = 12%

Region	CAPITAL COST (\$/kW-yr)			FIXED O & M (\$/kW-yr)			VARIABLE O & M (mills/kW-yr)			FUEL (mills/KW-yr)		
	L	M	H	L	M	H	L	M	H	L	M	H
<u>Pacific Southern</u>												
MS	715.4	794.8	874.3	46.4	51.5	56.7		5.8		301.9	335.4	368.9
CC		183.4			7.7			.9				
GT		97.6			3.3			13.3			611.5	
<u>South Mountain:</u>												
MS	715.4	794.8	874.3	46.4	51.5	56.7		5.8		301.9	335.4	368.9
CC		183.4			7.7			8.2			379.9	
GT		97.6			3.3			13.3			611.5	
<u>South Central:</u>												
MS	691.2	768.0	844.8	44.7	49.7	54.7		5.6		301.9	335.4	368.9
CC		177.2			7.5			7.9			379.9	
GT		94.4			3.3			12.8			611.5	
<u>Middle Atlantic:</u>												
MS	800.4	889.3	978.2	51.8	57.6	63.4		6.5		301.9	335.4	368.9
CC		205.1			8.6			9.3			379.9	
GT		90.2			3.7			14.9			611.5	



TABLE B-13

LEVELIZED COSTS IN 1990 \$  
 EPRI REGIONAL COST DATA, DOE/SAN ECONOMIC GUIDELINES  
 FUEL ESCALATION RATE = 15%

Region	CAPITAL COST (\$/KW-yr)			FIXED O & M (\$/KW-yr)			VARIABLE O & M (mills/KW-yr)			FUEL (mills/KW-yr)		
	L	M	H	L	M	H	L	M	H	L	M	H
<u>Pacific Southern:</u>												
MS	715.4	794.8	874.3	46.4	51.5	56.7		5.8		681.2	756.9	832.6
CC		183.4			7.7			8.2			857.9	
GT		97.6			3.3			13.3			1380.4	
<u>South Mountain:</u>												
MS	715.4	794.8	874.3	46.4	51.5	56.7		5.8		681.2	756.9	832.6
CC		183.4			7.7			8.2			857.9	
GT		97.6			3.3			13.3			1380.4	
<u>South Central:</u>												
MS	691.2	768.0	844.8	44.7	49.7	54.7		5.6		681.2	756.9	832.6
CC		177.2			7.5			7.9			857.9	
GT		94.4			3.3			12.8			1380.2	
<u>Middle Atlantic:</u>												
MS	800.4	889.3	978.2	51.8	57.6	63.4		6.5		681.2	756.9	832.6
CC		205.1			8.6			9.3			857.9	
GT		90.2			3.7			14.9			1380.2	

TABLE B-14

LEVELIZED COSTS IN 1990 \$  
 EPRI REGIONAL COST DATA, BECHTEL ECONOMIC GUIDELINES

Region	CAPITAL COST (\$/kW-yr)			FIXED O & M (\$/kW-yr)			VARIABLE O & M (mills/kW-yr)			FUEL (mills/KW-yr)		
	L	M	H	L	M	H	L	M	H	L	M	H
<u>Pacific Southern:</u>												
MS	368.3	409.2	450.1	29.2	32.5	35.8		3.6		107.5	119.4	131.3
CC		94.3			4.9			5.1			135.4	
GT		50.3			2.1			8.4			217.8	
<u>South Mountain:</u>												
MS	368.3	409.2	450.1	29.2	32.5	35.8		3.6		116.2	129.1	142.0
CC		94.3			4.9			5.1			146.3	
GT		50.3			2.1			8.4			235.3	
<u>South Central:</u>												
MS	355.9	395.4	434.9	28.2	31.3	34.4		3.6		107.5	119.4	131.3
CC		91.1			4.7			5.1			135.4	
GT		48.6			2.1			8.2			217.8	
<u>Middle Atlantic:</u>												
MS	411.9	457.7	503.4	32.7	36.3	39.9		4.2		112.0	124.4	136.8
CC		105.4			5.5			5.9			140.7	
GT		46.3			2.2			9.5			226.6	

APPENDIX C

PARAMETRIC ANALYSIS METHODOLOGY

## CONTENTS

<u>Appendix</u>		<u>Page</u>
C.1	Economic Evaluations	C-3
C.2	Scaling Relationships for Parametric Evaluations	C-9

The capital and operating cost variations resulting from changes in the design and/or operational parameters of the preconceptual baseline were determined after the new design features and performance characteristics had been established. The changes in the capital costs were determined using scaling relationships defined for the individual components based on specific estimates of the point designs. These scaling relationships are discussed in Appendix C.2.

In order to compare the parametric cases on this basis, the direct installed costs for the major portions of the plant in 1978 dollars were estimated. The sum of these costs was then converted to a total capital cost,  $C'$ , in millions of 1990 dollars by the following expression:

$$C' = 1.58 (C_1 + C_2 + C_3) + 1.89 (C_4 + C_5 + C_6 + C_7 + C_8 + C_9)$$

where:

$C_1$  = Heliostat field cost (assumes heliostat cost of \$93.42/m<sup>2</sup>; installed, 1978; this information was provided by Northrup, Inc.)

$C_2$  = Receiver cost

$C_3$  = Tower cost

$C_4$  = Riser/downcomer cost

$C_5$  = Gas turbine-generator cost

$C_6$  = HRSG cost

$C_7$  = Steam turbine-generator and associated equipment cost

$C_8$  = Site, structures, and miscellaneous cost

$C_0$  = Fuel Handling Equipment Cost

The numerical factors 1.58 and 1.89 account for indirect costs, distributables, contingency, and owner's costs. Through the use of the above equation it was possible to identify the capital cost changes caused by a parametric change down to each major part of the plant, as well as the change in the total capital cost. Tables C-1 and C-2 summarize the capital cost changes associated with the parametric evaluations of the Strawman and Advanced Strawman designs.

The cost of fuel consumption over an assumed 30 year operating life was calculated in terms of equivalent capital cost in 1990 dollars. Since the fuel consumption is directly related to the plant heat rate, the incremental equivalent capital costs due to the parametric changes were calculated from the factors listed in Table C-3.

TABLE C-3  
FACTORS FOR CALCULATING THE EQUIVALENT CAPITAL COST  
OF FUEL CONSUMED  
(10<sup>6</sup> dollars in 1990 for 1% change in Heat Rate)

	<u>Fuel Escalation Rate</u>	
	<u>12%</u>	<u>15%</u>
Strawman (daytime, F )	3.76	8.26
(nighttime, F )	1.01	2.23
Advanced Strawman (daytime, F )	2.97	6.53
(nighttime, F )	0.93	2.05

TABLE C-1

## STRAWMAN PARAMETRIC CAPITAL COST BREAKDOWN

Compressor Pressure Ratio	Air System Pressure Drop, PSI $\Delta P$ Total*	Solar Rec'r Pressure Drop, PSI $\Delta P$ Total*	Design Point Solar Fraction	Steam Conditions		Other	$\Delta$ Capital Cost Breakdown (\$ x 10 <sup>6</sup> , 1978)							$\Delta$ C' Total Capital Cost (\$ x 10 <sup>6</sup> , 1990)
				Pressure, PSIG	Temperature, F		C1 Rebo-stat Field	C2 Receiver	C3 Tower	C4 Riser/Downcomer	C5 Gas Turbine Equip.	C6 HRSG Equip.	C7 Steam Turbine Equip.	
PR = 8	8	4	.598	1800	950	-	1.3	-0.8	0.2	-0.5	-1.0	1.9	3.6	26.7
	8	4	.598	1450	950	-	1.5	-0.7	0.2	-0.6	-0.9	1.1	1.7	
PR = 12	8	4	.598	1250	900	-	1.8	-0.5	0.2	-0.5	-0.8	-0.1	1.4	7.4
	8	4	.563	1450	950	-	0.1	-	-	-	-	-0.7	-0.2	-4.9
PR = 16	8	4	.563	850	825	-	-	-	-	-	-	-	-	BASE
	8	4	.530	1250	885	-	0.2	0.1	-	0.3	0.1	-2.0	-	-8.6
PR = 12	8	4	.530	850	885	-	-1.0	1.6	-0.1	0.3	1.7	-1.0	-1.2	1.3
	4	2	.563	1450	950	-	-1.0	1.5	-0.1	0.3	1.7	-2.6	-1.0	-7.5
	4	3	.563	1450	950	-	-0.1	0.6	-	0.7	0.1	-	-0.2	15.5
	12	4	.563	1450	950	-	-0.1	0.6	-	1.8	0.1	-	-0.2	12.6
	12	6	.563	1450	950	-	0.2	0.1	-	-0.6	-0.1	0.1	0.2	-0.9
	16	6	.563	1450	950	-	0.2	-2.3	-	-0.4	-0.1	0.1	3.2	-11.6
	8	2	.563	1450	950	-	0.3	-2.3	-	-0.4	-0.2	0.2	0.3	-10.7
	8	6	.563	1450	950	-	-	2.7	-	-0.5	-	-	-	10.4
PR = 12	8	4	.620	1450	950	Tro=1570F	-	-2.3	-	0.7	-	-	-	-7.2
	8	4	.483	1450	950	Tro=1400F	2.5	3.4	0.3	0.1	-	0.1	-	31.9
PR = 12	8	4	.506	1450	950	Fired HRSG	-3.3	-4.9	-0.4	-0.3	-	0.1	-	-43.8
	8	4	.469	1450	950/950	Fired HRSG Reheat	-2.4	-1.6	-0.3	-0.3	-0.7	2.2	1.5	-5.3
	8	4	.508	1800	950	Fired HRSG	-3.6	-2.5	-0.5	-0.5	-1.0	2.0	3.4	-9.5
	8	4	.465	1800	950/950	Fired HRSG Reheat	-2.5	-1.7	-0.3	-0.3	-0.7	1.2	3.3	10.4
PT = 16			.444	1800	950	Fired HRSG	-3.9	-2.7	-0.5	-0.5	-1.1	2.9	5.7	6.4
	PR = 8	8	.640	1450	950	Fired HRSG	-4.8	-3.1	-0.6	-0.4	0.3	3.3	3.4	-2.9
PR = 12		4	.629	1450	950	Intercool- ed	4.9	1.5	0.6	-0.2	-0.8	1.0	1.0	42.4
		4	.629	1450	950	Intercool- ed	4.5	3.1	0.6	-0.2	0.2	-0.5	0.6	34.6
PR = 16	8	4	.620	850	825	Intercool- ed	4.7	5.7	0.6	-0.1	1.9	-3.1	-1.9	35.5
PR = 12	8	4	.657	1450	950	After Cool- ed 30C F	12.4	8.4	1.4	0.6	1.0	0.3	3.1	139.8
	8	4	.383	1450	950	Parallel Combustor (2000 F)	-7.1	-4.9	-0.7	-0.6	0.1	-	-0.3	-67.7
	8	4	.563	1450	950	Dual Press HRSG	-0.9	-0.6	-0.1	-0.1	-0.3	1.2	1.2	1.2
	8	4	.563	1450	950	Dual Press HRSG Re- heat	-1.0	-0.7	-0.1	-0.1	-0.3	0.8	2.3	7.1

\*To convert to kPa, multiply psi values by 6.89.  
†Tro = Receiver outlet pressure.

TABLE C-2

## ADVANCED STRAWMAN PARAMETRIC CAPITAL COST BREAKDOWN

Compressor Pressure Ratio	Air System Pressure Drop, PSI $\Delta P_{Total}$ *	Solar Rec'r Pressure Drop, PSI $\Delta P_{Total}$ *	Design Point Solar Fraction	Steam Conditions		Other	$\Delta$ Capital Cost Breakdown (\$ x 10 <sup>6</sup> , 1978)							$\Delta C_{Total}$ Capital Cost (\$ x 10 <sup>6</sup> , 1990)
				Pressure, PSIG	Temperature, F		C <sub>1</sub> Heliostat Field	C <sub>2</sub> Receiver	C <sub>3</sub> Tower	C <sub>4</sub> Riser/Down-Comer	C <sub>5</sub> Gas Turbine Equip.	C <sub>6</sub> HRSG Equip.	C <sub>7</sub> Steam Turbine Equip.	
PR=8	15	10	.737	1800	950	-	2.6	4.5	0.4	-0.2	-0.7	-0.1	3.3	51.4
	15	10	.737	1450	950	-	2.9	4.6	0.4	-0.7	-0.6	-0.6	1.3	38.5
	15	10	.737	1250	900	-	3.4	4.9	0.4	-0.2	-0.6	-1.0	1.0	38.9
PR=12	15	10	.719	1800	950	-	-0.2	-0.1	0.1	-	-0.1	0.6	1.8	12.7
	15	10	.719	1450	950	-	-	-	-	-	-	-	-	BASE
	15	10	.719	1250	900	-	0.4	0.2	0.1	-	0.1	-0.6	-0.2	-0.7
PR=16	15	10	.704	1800	950	-	-1.8	-2.7	-0.1	0.4	1.3	1.8	1.0	3.7
	15	10	.704	1450	950	-	-1.6	-2.6	-0.1	0.4	1.3	1.2	-0.6	-7.9
	15	10	.704	1250	900	-	-1.3	-2.4	-0.1	0.4	1.4	0.2	-0.9	-12.5
PR=12	10	5	.719	1450	950	-	-0.3	2.8	-0.3	-	0.1	0.1	-0.1	11.6
	10	8	.719	1450	950	-	-0.3	0.8	-0.1	1.1	0.1	0.1	-0.1	9.2
	20	10	.719	1450	950	-	0.3	0.1	-	-0.7	-0.1	0.1	0.1	-1.6
	20	15	.719	1450	950	-	0.3	-2.1	0.1	-	-0.1	0.1	0.1	-7.9
	15	5	.719	1450	950	-	-	3.0	-0.3	-0.6	-	-	-	10.0
	15	13	.719	1450	950	-	-	-1.3	0.1	1.2	-	-	-	1.2
	25	20	.719	1450	950	-	-	-	-	-	-	-	-	-10.7
PR=12	15	10	.856	1450	950	†Tro=2200F	7.6	14.5	0.5	0.4	-	0.1	-	116.5
	15	10	.590	1450	950	†Tro=1800F	-6.5	10.1	-0.7	-0.4	-	-	-	-89.3
PR=8	15	10	.737	1800	950/950	Reheat	2.6	-4.5	0.4	0.1	0.7	0.6	5.0	67.5
PR=12	15	10	.719	1450	950/950	Reheat	-0.4	-0.2	0.1	-	-0.1	1.2	1.2	11.2
PR= 8	15	10	.759	1450	950	Inter-cooled	5.7	7.3	0.7	0.2	-0.7	-0.7	1.0	67.6
PR=12	15	10	.753	1450	950	Inter-cooled	3.5	1.6	0.4	-	-	-0.1	-0.4	24.6
PR=16	15	10	.753	1450	950	Inter-cooled	2.5	-0.8	-0.4	-0.2	1.4	0.7	-1.3	11.1
PR=12	15	10	.433	1450	950	Parallel Combustor (2400F)	-11.7	-7.6	-1.4	-0.8	0.1	-	-0.2	-109.3

\*To convert to kPa, multiply psi values by 6.89.  
†Tro = Receiver outlet pressure.



The use of these factors required that the fuel requirements for the hybrid, short term fossil and long term fossil operating modes (described in Section 3.5.2, Daily Operational Characteristics) be determined for each parametric case. For daytime operation, a weighted average heat rate was approximated by the expression:

$$DAHR = 0.477 (HR_{STR} - HR_{HYBRID}) + HR_{HYBRID}$$

where:

DAHR = Average heat rate during solar-augmented operation

HR<sub>STR</sub> = Reference heat rate during short-term fossil operation

HR<sub>HYBRID</sub> = Reference heat rate at design point hybrid operation

For nighttime operation, the long-term fossil heat rate was used directly. The equivalent capital cost of the consumed fuel was then calculated as the sum of daytime and nighttime contributions, based on an average daily operation of 12.875 hours, corresponding to a 48 percent capacity factor and 90 percent availability. The expression for the incremental equivalent capital cost of fuel ( $\Delta ECC$ ), in  $10^6$  dollars in 1990, is given by:

$$\Delta \text{ECC} = (\Delta \text{HR}_{\text{LTF}}) (\text{FN}) + (100) \frac{\text{DAHR} (1-\text{sef}) - \text{DAHR}_{\text{BASE}} (1-\text{sef}_{\text{BASE}})}{\text{DAHR}_{\text{BASE}} (1-\text{sef}_{\text{BASE}})}$$

where:

- $\Delta \text{HR}$  = Change in long-term fossil heat rate
- $\text{DAHR}$  = Average heat rate during hybrid operation
- $F_N$  = Fuel escalation factor, nighttime  
(Table C-3)
- $\text{sef}$  = Solar energy fraction

Based on systems analysis and market potential discussions with utilities, the baseline fuel escalation rate for the parametric analysis was chosen to be 12 percent. A fuel escalation rate of 15 percent was also calculated to check the sensitivity to changes in fuel escalation rate.

## C.2 SCALING RELATIONSHIPS FOR PARAMETRIC EVALUATIONS

The methodology for economic evaluation of the parametric cases is described in Section 3.1.3. In order to implement this methodology, a series of scaling relationships were developed so that changes from the baseline case could be evaluated with the level of accuracy necessary for the first broad screening of the concept. The cost components which were individually evaluated for each parametric case were:

- $C_1$  = Heliostat field cost
- $C_2$  = Receiver cost
- $C_3$  = Tower cost
- $C_4$  = Riser/downcomer cost
- $C_5$  = Gas turbine-generator cost
- $C_6$  = HRSG cost
- $C_7$  = Steam turbine-generator and associated equipment cost

The costs of the site, auxiliary structures, fuel handling equipment and miscellaneous items were considered invariant and were not scaled for the evaluation.

### C.2.1 Collector Field

To account for the changes in geometric efficiency as the number of heliostats varied in the parametric cases, it was assumed that

the incremental number of heliostats ( $\Delta N_H$ ) was proportional to the 1.05 power of the receiver thermal power increment ( $\Delta P_R$ ).

The field-tower relationship was held constant during the scaling by maintaining the same rim angle for the field. A further simplifying assumption was that the area of the field is proportional to the number of heliostats. For small changes in field size, this assumption is accurate enough for the analysis.

The change in tower height ( $\Delta h_{TOWER}$ ) required for a given number of heliostats was then calculated from percentage changes by the equation:

$$\Delta h_{TOWER} = (\Delta N_H)^{0.5} = \Delta(P_R)^{0.525}$$

By using these geometric similarities for the parametric cases, the geometric efficiency of the collector subsystem was preserved. The change in atmospheric attenuation was considered negligible for this type of analysis. The elliptical field was used as the reference arrangement in the parametric studies.

### C.2.2 Receiver

Point designs were developed for seven different cases by Foster Wheeler Development Corp. for each receiver type. This information was used to develop cost and weight scaling relationships in the form:

$\Delta$  Receiver cost  $\propto (\Delta P_R)^a$

$\Delta$  Receiver weight  $\propto (\Delta P_R)^b$

where the exponents were found to be;  $a = 1.0$  and  $b = 1.07$  for the heat-pipe receiver and;  $a = 0.525$  and  $b = 1.22$  for the ceramic tube receiver.

The receiver efficiency also had to be evaluated for those cases where the receiver outlet temperature was different than the baseline value. A curve fit was used, based on information supplied by Foster Wheeler, to estimate the receiver efficiencies for the parametric cases.

The receiver costs were based on the delivery of the large components at the Barstow site. The installation cost was estimated from Bechtel experience on heavy construction of overhead structures. The estimated installation cost for the Strawman receiver was \$1.25/lb. This was based on an average manpower requirement of 100 manhours/ton. This value generally agrees with estimates by Foster Wheeler on the earlier Dynatherm work. The same value was used for the Advanced Strawman receiver although the uncertainty of the installation cost is considerably higher.

### C.2.3 Tower

The cost of the tower was calculated using an equation provided by Sandia Laboratories. This equation does not include allowances for the weight of the riser and downcomer piping.

### C.2.4 Riser/Downcomer

Changes from the baseline diameter  $\Delta d$  for the conceptual piping layout were calculated from the relationship:

$$\Delta d \propto \left[ \frac{(\Delta G)^2}{\Delta \zeta - \Delta P} \right]^{0.2}$$

For each case, the change in air mass flow rate ( $\Delta G$ ), air density ( $\Delta \zeta$ ) and allowable pressure losses ( $\Delta P$ ) were calculated separately for the riser and downcomer. For the purpose of parametric analysis, equal pressure losses were assumed for the riser and downcomer.

Because of the piping layout, the length was not directly evaluated with the above equation. The piping length was related instead to tower height using point designs developed for tower heights from 122 meters (400 feet) to 325 meters (1100 feet).

The piping cost equations were developed from point designs. The direct costs in millions of 1978 dollars were found by the expressions:

$$\text{Strawman Riser Cost} = (30931 t_R + 2503) (\phi_R) (F_{TH})$$

$$\text{Strawman Downcomer Cost} = (26883 t_D + 3561) (\phi_D) (F_{TH})$$

$$\text{Adv. Strawman Riser Cost} = (35019 t_R + 2847) (\phi_R) (F_{TH})$$

$$\text{Adv. Strawman Downcomer Cost} = (31045 t_D + 9680) (\phi_D) (F_{TH})$$

where:

$t$  = pipe wall thickness, inches

$\phi$  = pipe diameter, inches

$F_{TH}$  = tower height cost factor

The subscripts R and D refer to riser and downcomer, respectively.

The tower height cost factors were defined from the relations:

$$\text{Strawman } F_{TH} \propto (\Delta h_{TOWER})^{0.97}$$

$$\text{Advanced Strawman } F_{TH} \propto (\Delta h_{TOWER})^{0.97}$$

All diameters in the cost equations were based on the pressure boundary steel pipes. Thus for the downcomer piping with internal insulation, the inside diameter of the pipe was based on a fixed insulation thickness.

The thickness of the pipe wall was estimated from the standard ASME piping code equation with a 68.9 MPa (10,000 psi) pressure stress assumed and a minimum corrosion allowance of 0.16 cm (0.0625 in.). The calculated wall thicknesses were rounded up to the nearest 31.8 cm (0.125 in.) but the pipe diameters calculated

from the scaling relationships were not adjusted to compensate for this correction.

#### C.2.5 Combined Cycle EPGS

For scaling purposes, the combined cycle portion of the EPGS was divided into three components, namely, the gas turbine generator, the HRSG and the steam turbine generator and its associated equipment. The cost for the baseline plants was scaled using these three pieces from more detailed cost estimates of larger plant sizes. The scaling parameters are based on the Energy Conversion Alternative Study (ECAS) reports by General Electric and Westinghouse (Refs. C-1 and C-2), and on Bechtel's experience gained from extensive work on combined cycle power plant design and cost estimating.

#### C.2.6 Gas Turbine-Generator

The costs included in this category represent not only the gas turbine, but essentially a gas turbine peaking power plant. The cost of the gas turbine itself is closely tied to specific power. However, the cost of a peaking power plant, over a narrow range, is expected to vary as the rated power with an exponent of 0.8.

The exponent to be used for large changes (a factor of two or larger) in MWe rating is close to 1.0 since these larger plants use a modular arrangement with multiple gas turbines.



Other scaling relationships for the gas turbines are shown in Table C-4.

TABLE C-4  
SCALING RELATIONSHIPS FOR GAS TURBINE POWER PLANTS

<u>Parameter</u>	<u>Value</u>	<u>\$/kW Factor</u>
Compressor Pressure Ratio =	8	0.98
	12	1.0
	16	1.15
Turbine Inlet Temperature	1093C (2000F)	1.0
	1316C (2400F)	0.9
Intercooler	with	0.85
	without	1.0

The procedure for estimating the change in cost of the gas turbine portion of the plant is based on the application of the power related scaling relationship as modified by the factors in Table C-4. The cost of an intercooler or aftercooler was estimated separately, using the method outlined below for the HRSG and added to the gas turbine cost for the appropriate cases.

#### C.2.7 Heat Recovery Steam Generator

The usual method for scaling the cost of a heat exchangers is based on cost changes proportional to the heat transfer surface area. In accordance with common estimating practice for such equipment, the cost of the heat exchange equipment was assumed to vary with the 0.8 power of the heat transfer surface area. To estimate the heat transfer surfaces for each parametric case, it

was assumed that the overall heat transfer coefficient,  $\mu$ , remains constant over the explored range. With this assumption the heat transfer surface area becomes directly proportional to the heat transfer duty/log mean temperature ratio.

The additional factors, given in Table C-5, were applied where appropriate to take into account the effects of varying system conditions.

TABLE C-5  
SCALING RELATIONSHIPS FOR HEAT RECOVERY STEAM GENERATORS

<u>Parameter</u>	<u>Parametric case</u>	<u>Cost Factor</u>
Supplemental Firing	no	1.0
	yes	1.10
Steam Pressure	5.86 MPa (850 psia)	0.73
	8.62 MPa (1250 psia)	0.92
	10.0 Mpa (1450 psia)	1.0
	12.4 Mpa (1800 psia)	1.08
Multiple Steam Pressure	Single Pressure	1.0
	Dual Pressure	1.05

The HRSG steam flow at the parametric conditions was estimated from the expression, derived from heat exchanger effectiveness equation:

$$\dot{m}_s = m_g \text{ BASE} \left( \frac{\dot{m}_g}{\dot{m}_g \text{ BASE}} \right) \left( \frac{T_1 - T_2}{T_1 \text{ BASE} - T_2 \text{ BASE}} \right)$$

where:

$\dot{m}_s$  = steam flow rate

$\dot{m}_g$  = HRSG gas flow rate

$T_1$  = HRSG gas inlet temperature

$T_2$  = HRSG steam evaporator temperature

$\dot{m}_g$  BASE',  $T_1$  BASE', and  $T_2$  BASE represent the values in the preconceptual baseline design.

### C.2.8 Steam Turbine-Generator

The third category for the combined cycle plant was the steam turbine-generator and associated equipment. It actually includes all equipment necessary to the operation of the power cycle, except the gas turbine-generator, the HRSG and the fuel handling system. Therefore the scaling relationship is approximately that for a small fossil fired steam power plant without the boiler. For scaling purposes the cost of this set of equipment was assumed to vary according to the 0.8 power of the power output.

In addition, several factors given in Table C-6 were used to modify the basic relationship for the appropriate cases.

TABLE C-6

SCALING RELATIONSHIPS FOR STEAM TURBINE-GENERATOR AND  
ASSOCIATED EQUIPMENT

<u>Parameter</u>	<u>Value</u>	<u>\$/kW</u> <u>Cost Factor</u>
Steam Pressure, MPa (psig)	5.5 (750-850)	1.03
	9.3 (1250-1450)	1.0
	11.7 (1600-1800)	1.17
Steam Temperature, C (F)	399-441 (750-825)	0.98
	441-482 (826-900)	0.99
	482-510 (901-950)	1.0
	510-538 (951-1000)	1.02
Steam Reheat		1.10

APPENDIX C: REFERENCES

- C-1 Brown, D.H. and Corman, J.C. (General Electric Co. Schenectady, N.Y.), Energy Conversion Alternatives Study (ECAS), General Electric Phase I Final Report, Volume II, Part 1, Open Cycle Gas Turbines, Contract No. NAS 3-19406, February 1976.
- C-2 Amos, D.J. and Grube, J.E. (Westinghouse Gas Turbine Engine Div., Lester, Pa.), Energy Conversion Alternatives Study (ECAS), Westinghouse Phase I Final Report, Volume IV - Open Recuperated and Bottomed Gas Turbine Cycles, Contract No.: NAS 3-19407, February 12, 1976.

APPENDIX D  
EPGS SYSTEMS DESCRIPTIONS

## CONTENTS

<u>Section</u>		<u>Page</u>
D.1	Main, Secondary, and Bypass Steam Systems	D-3
D.2	Condensate and Feedwater System	D-5
D.3	Condenser Vacuum System	D-7
D.4	Auxiliary Steam System	D-7
D.5	Service Water System	D-10
D.6	Auxiliary Closed Cooling Water System	D-11
D.7	Turbine Gland Seal Steam System	D-13
D.8	Lube Oil Storage, Transfer, and Purification System	D-17
D.9	Demineralized Water Makeup, Storage, and Transfer System	D-17
D.10	Compressed Air System	D-19
D.11	HVAC System	D-19
D.12	Fire Protection System	D-21
D.13	Sampling System	D-22
D.14	Raw Water Makeup System	D-23
D.15	HRSO Chemistry Control System	D-23

The main and secondary steam systems carry steam from the HRSG high-pressure, and low-pressure superheater outlets, respectively, to the steam turbine. The main steam piping routes steam from the high-pressure (HP) superheater outlet to the HP cylinder of the turbine. The secondary steam piping routes steam from the low pressure (LP) superheater outlet to an intermediate section of the turbine, thereby admitting steam to the intermediate- and low-pressure stages of the turbine.

The main/secondary steam bypass provides the capability of bypassing the steam turbine and routing steam directly to the condenser during startup. The main steam desuperheating station is located near the HRSG high-pressure superheater outlet, while the low-pressure desuperheating station is located close to the main condenser. Desuperheating sprays to the HP and LP stations supplied from the main feedpump and condensate pump discharges, respectively.

Steam supply for the auxiliary steam system is supplied from the main steam header and is the primary source for plant auxiliaries requiring process steam.

The main/secondary steam system diagram is presented in Figure D-1.





The condensate system supplies condensate from the condenser hotwell through the demineralizers and the gland seal steam condenser to the constant-pressure deaerator. This system maintains a stable condensate level in the deaerator over the entire load range of the steam cycle plant operation, as well as providing condensate for other miscellaneous services such as desuperheating spray, main feedwater pump seal water, and turbine exhaust hood sprays. Condensate flow to the deaerator is regulated by two deaerator control valves arranged in parallel, which are controlled by a two-element deaerator level control system that monitors deaerator level and condensate flow into the deaerator.

The feedwater system provides feedwater from the deaerator storage tank by means of the feedwater booster pumps through the IP economizer to the LP steam drum. The booster pumps also provide suction to the main feedwater pumps which supply feedwater through the HP economizer to the HP steam drum.

Flow measuring devices for actuating pump recirculation systems are provided in the feed pump suction lines and the booster pump discharge lines. Recirculation lines to the deaerator storage tank are sized for an assumed recirculation capacity of 50 percent full flow to allow for continuous pump operation at full flow. A condensate-feedwater system diagram is shown in Figure D-2.



### D.3 CONDENSER VACUUM SYSTEM

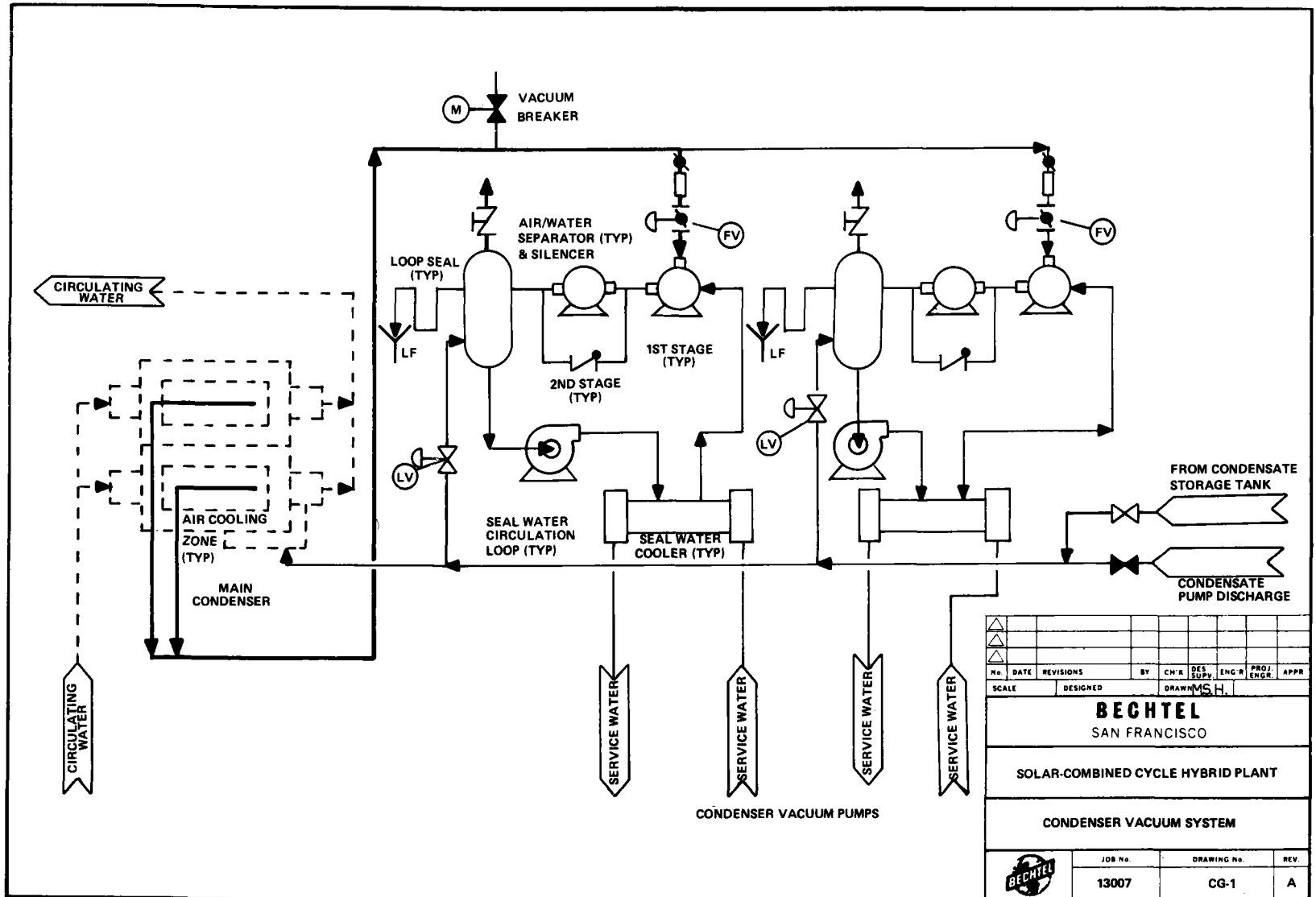
The condenser vacuum system removes air and other noncondensable gases from the main condenser and exhausts them to atmosphere. The system consists of two full-capacity vacuum pumps of the rotating liquid ring type. The pumps are installed in parallel and may be operated individually or together, as shown in Figure D-3. The system is designed so that only one pump is required for the hogging (evacuation) and holding operation. To accelerate the condenser evacuation process, both pumps can be operated, which minimizes the plant startup time.

A seal water system is provided as an integral part of the vacuum pump and consists of an air/water separator, a pump, and seal water cooler. This system provides the necessary flow of cold water to the rotary liquid ring vacuum pumps with the seal water cooler connected to the plant service water system, or chilled water system if service water is too hot.

### D.4 AUXILIARY STEAM SYSTEM

The auxiliary steam system receives, conditions, and distributes steam to secondary users during various modes of power plant operation. The auxiliary steam system, as shown in Figure D-4 consists of a common steam distribution header with various branch connections for receiving and supplying steam. Depending on the operating mode and load condition of the plant, the auxiliary steam system receives its steam from either the HP main

8-D



No.	DATE	REVISIONS	BY	CHK'D	DES. SUPV.	ENGR.	PROJ. ENGR.	APPR.
SCALE		DESIGNED		DRAWN MS.H.				
<b>BECHTEL</b> SAN FRANCISCO								
SOLAR-COMBINED CYCLE HYBRID PLANT								
CONDENSER VACUUM SYSTEM								
JOB No.			DRAWING No.			REV.		
13007			CG-1			A		

Figure D-3 CONDENSER VACUUM SYSTEM

6-9

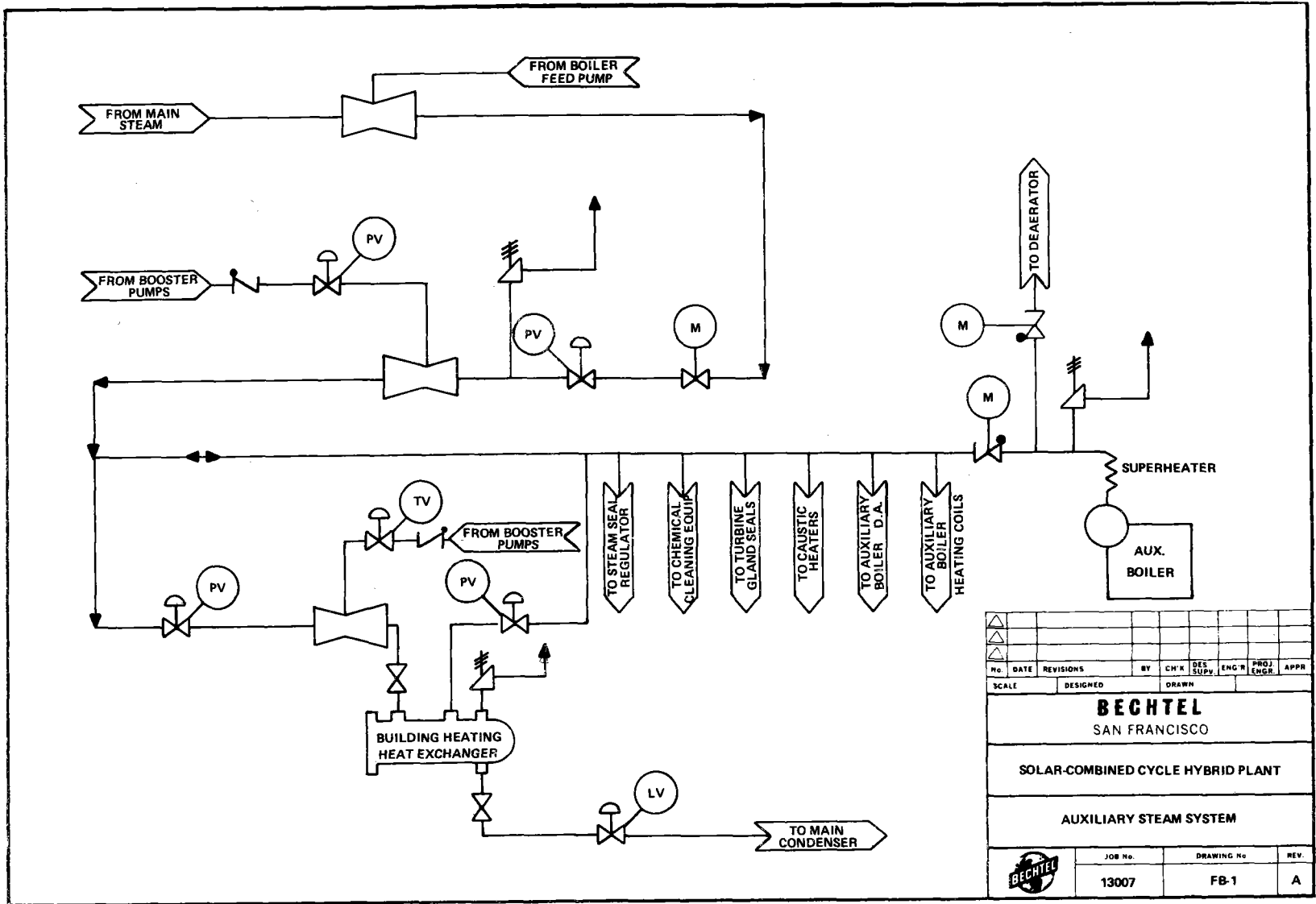


Figure D-4 AUXILIARY STEAM SYSTEM

steam header or the auxiliary boiler. The auxiliary boiler will produce 2.5 kg/sec (20,000 lb/hr) steam at 1.7 MPa (265 psig) and approximately 260C (500F). Superheat capability is dictated by gland seal maintenance on the steam turbine.

The auxiliary steam distribution header supplies steam for the following services:

- Auxiliary boiler deaerator
- Auxiliary boiler heating coils
- Building heating heat exchanger
- Caustic dilution water heaters
- Chemical cleaning equipment
- Steam seal regulator (aux. supply)
- Turbine gland seals

The main deaerator has a direct connection to the auxiliary boiler only, since deaerating steam during plant operation is supplied by a separate low-pressure evaporator within the HRSG.

#### D.5 SERVICE WATER SYSTEM

The service water system provides cooling water to the turbine generator auxiliaries. The heat exchangers to which service water is supplied are as follows:

- Generator exciter coolers (both steam and gas turbine generator)
- Generator stator coolers

- Turbine lube oil coolers
- Generator hydrogen coolers
- Main condenser vacuum pump cooler
- Auxiliary cooling water system heat exchangers

A schematic illustration of the service water system is shown in Figure D-5. It should be noted that auxiliaries associated with the gas turbine-generator will also be water cooled, and service water supplied to those auxiliaries is implied in the figure with the exception of the gas turbine lube oil coolers.

The two nominal half capacity service water pumps are the horizontal centrifugal type and take suction from the main circulating water system. The warm water side of the system returns to the hot leg of the circulating water system. The circulating water system is described in Volume II, Section 5.6.6.

#### D.6 AUXILIARY CLOSED COOLING WATER SYSTEM

The auxiliary closed cooling water system provides cooling water to various plant and yard auxiliaries and rejects heat to the service water system at the auxiliary cooling water heat exchanger interface. Corrosion-inhibited condensate is used as a cooling medium in this system which is continuously circulated in the closed-loop system. Auxiliaries that comprise this system include:



D-12

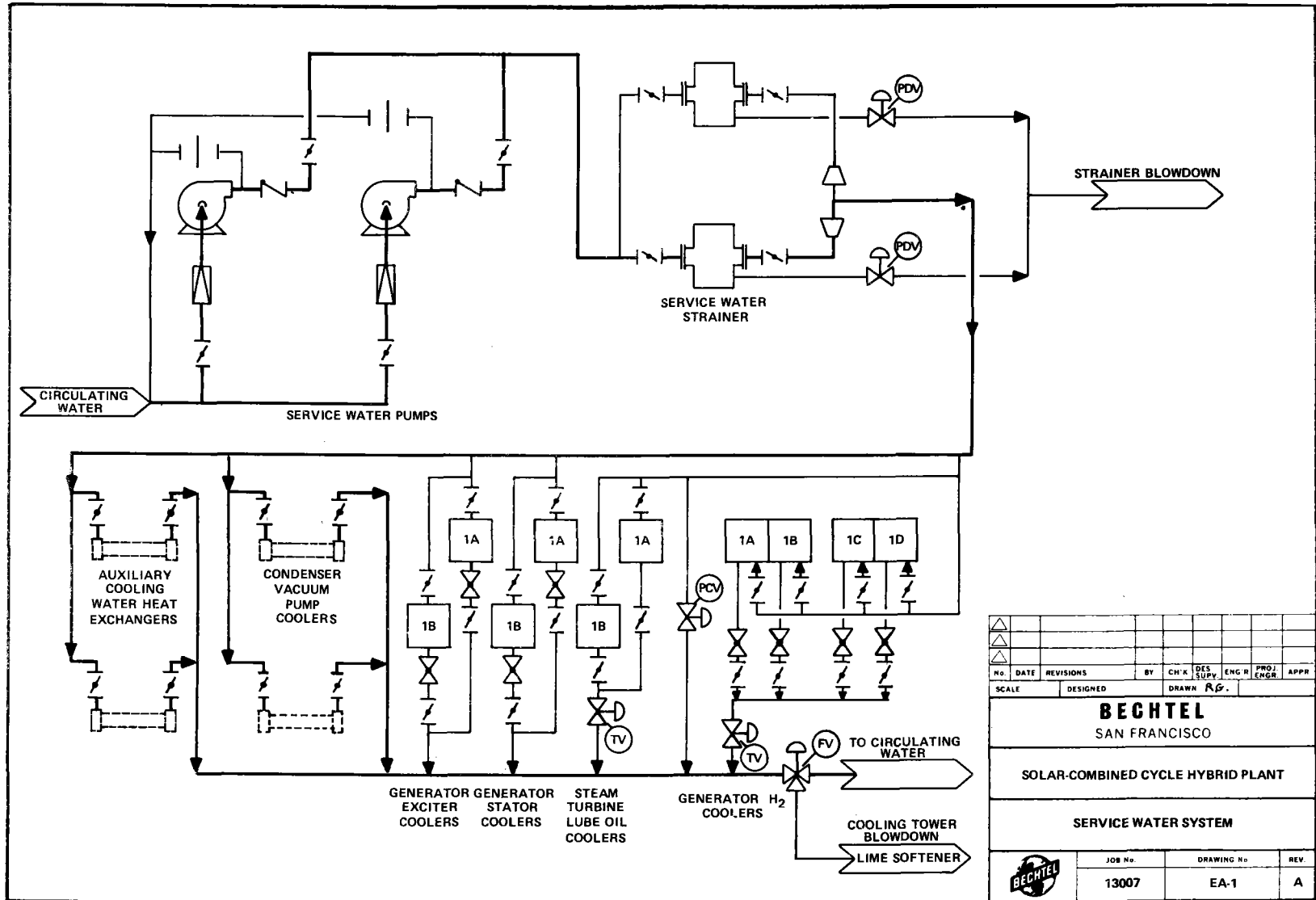


Figure D-5 SERVICE WATER SYSTEM

- Electrohydraulic fluid coolers
- Gas turbine lube oil coolers
- Hydrogen seal oil unit coolers
- Main steam grab sample cooler
- Secondary steam grab sample cooler
- Imphase bus duct cooler
- Air compressor coolers
- Sample cooling rack
- Sample chiller coolers

An auxiliary cooling water head tank is included as part of this system and is located on the deaerator platform on the heat recovery steam generator. The purpose of this tank is to accommodate thermal expansion and contraction of the cooling medium and provide surge protection for the system. Condensate makeup to this system is made via this tank. As shown in Figure D-6, two nominal half-capacity horizontal centrifugal pumps are used to circulate the condensate.

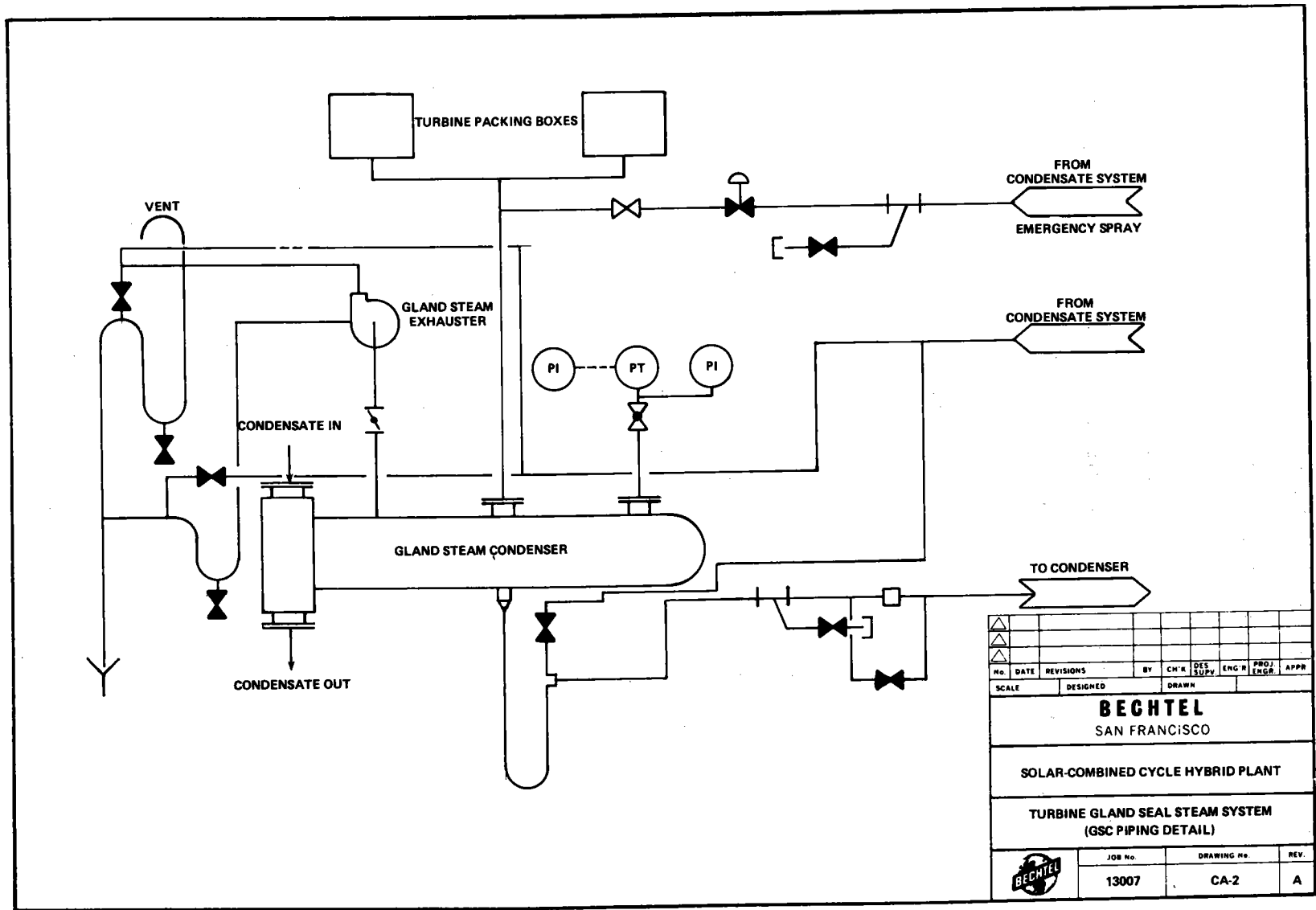
#### D.7 TURBINE GLAND SEAL STEAM SYSTEM

Figure D-7 and D-8 show representative schematics of the turbine gland seal steam system. As indicated, the primary sealing steam source is the main steam header which supplies steam to the steam seal regulator and subsequently to the turbine glands. Also shown is the auxiliary steam connection which provides a backup source of sealing steam to the system. The auxiliary steam source is used mainly during startup and for maintaining turbine





D-16



NO.	DATE	REVISIONS	BY	CHK	DES	ENGR	PROJ	APPR
SCALE	DESIGNED		DRAWN					
<b>BECHTEL</b> SAN FRANCISCO								
SOLAR-COMBINED CYCLE HYBRID PLANT								
TURBINE GLAND SEAL STEAM SYSTEM (GSC PIPING DETAIL)								
JOB No.			DRAWING No.			REV.		
13007			CA-2			A		

Figure D-8 TURBINE GLAND SEAL STEAM SYSTEM (GSC PIPING DETAIL)

gland seals during short duration shutdown if desirable.

First-stage shell, inner valve steam leakoff, and packing leakoff drains are routed directly to the main condenser. Gland seal steam from the turbine packing boxes is condensed in the gland steam condenser which uses condensate-feedwater as a cooling medium returned to the main condenser.

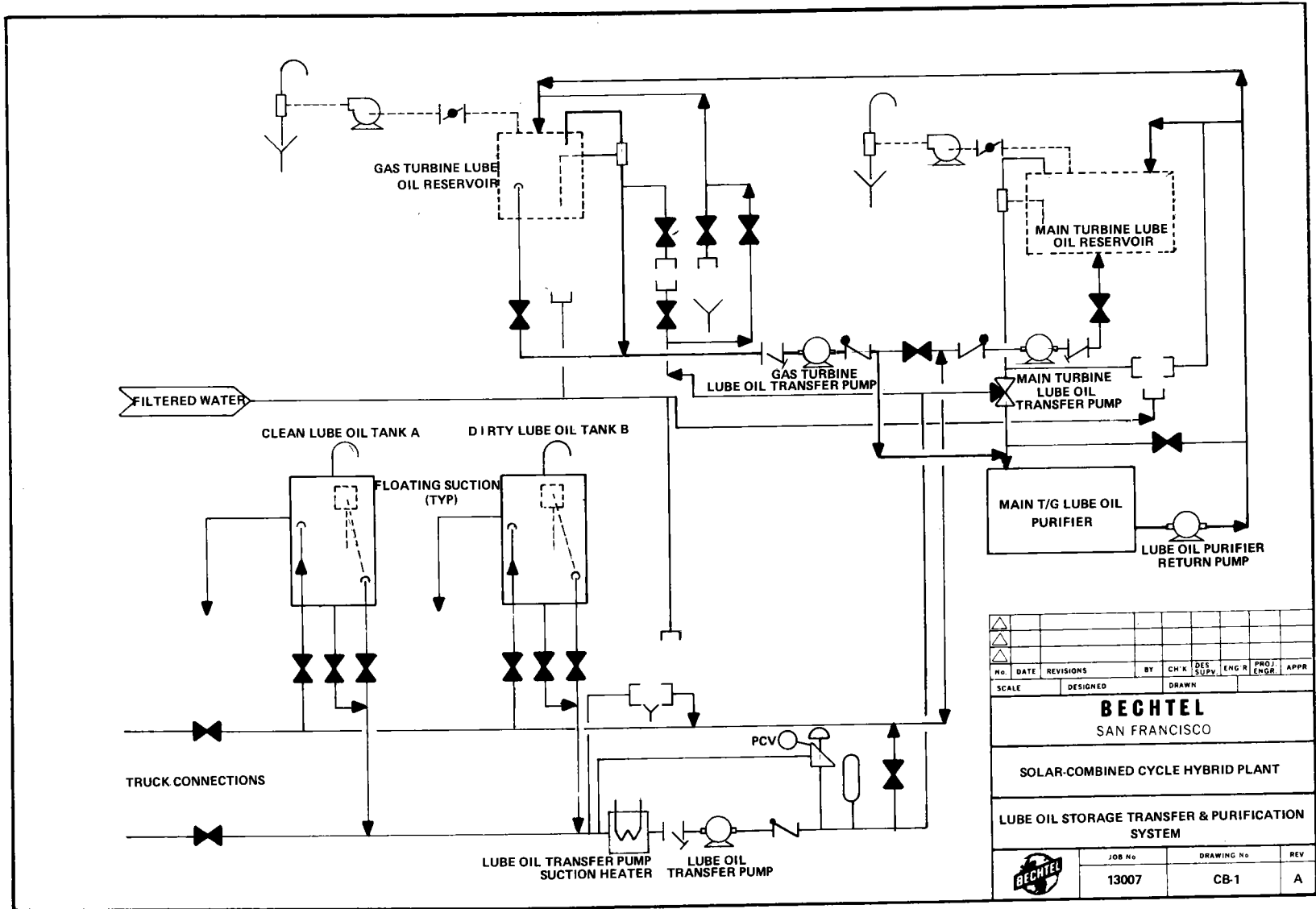
#### D.8 LUBE OIL STORAGE, TRANSFER, AND PURIFICATION SYSTEM

The lube oil system is designed to provide lube oil storage, transfer, and purification. The system will include two lube oil storage tanks, a main turbine generator oil purifier, and two lube oil reservoirs and the necessary transfer pumps. A schematic representation of the gas turbine/steam turbine shared lube oil system is shown in Figure D-9. The clean and dirty oil tanks are each sized for one change of lube oil for the gas and steam turbine lube oil reservoirs. The lube oil purifier is installed near the main reservoir, taking suction through a nonsyphoning overflow and returning the purified oil to the top of the reservoir.

#### D.9 DEMINERALIZED WATER MAKEUP, STORAGE, AND TRANSFER SYSTEM

This system receives, stores, and supplies chemically treated condensate to the condenser deaerating sections and has other miscellaneous uses within the plant. The system also transfers and removes condensate and chemical flushing fluids during

D-18



No.	DATE	REVISIONS	BY	CH'K	DES	ENGR	PROJ	APPR
SCALE	DESIGNED	DRAWN						
<b>BECHTEL</b> SAN FRANCISCO								
SOLAR-COMBINED CYCLE HYBRID PLANT								
LUBE OIL STORAGE TRANSFER & PURIFICATION SYSTEM								
		JOB No	DRAWING No		REV			
		13007	CB-1		A			

Figure D-9 LUBE OIL STORAGE TRANSFER AND PURIFICATION SYSTEM

startup and maintenance operations. During normal operation, if the water level rises above the normal level in the condenser hotwell, the excess water is pumped through the condensate reject valve to the condensate storage tank. In meeting the condensate requirements of the auxiliary boiler, the condensate storage tank header will supply or receive condensate from the auxiliary boiler deaerator. The system is shown schematically in Figure D-10.

#### D.10 COMPRESSED AIR SYSTEM

The compressed air system furnishes instrument and service air in quantities and at pressures required for proper functioning of the plant through all modes of plant operation. All compressors are of the multistage centrifugal type and the system is designed to maintain a minimum pressure of 689 kPa (100 psig) at the inlet of the plant equipment or instruments. The system includes an air dryer provided to satisfy plant requirements for dry air and inlet filter-silencer intercoolers, aftercoolers, controls, and cooling water accessories.

#### D.11 HVAC SYSTEM

The plant heating and ventilating system is designed to provide adequate ventilation to dissipate heat rejected from operating equipment and to maintain space temperatures for various modes of plant operation including shutdown. Filtered ventilation air is supplied by this system to minimize airborne dust and removes



D-20

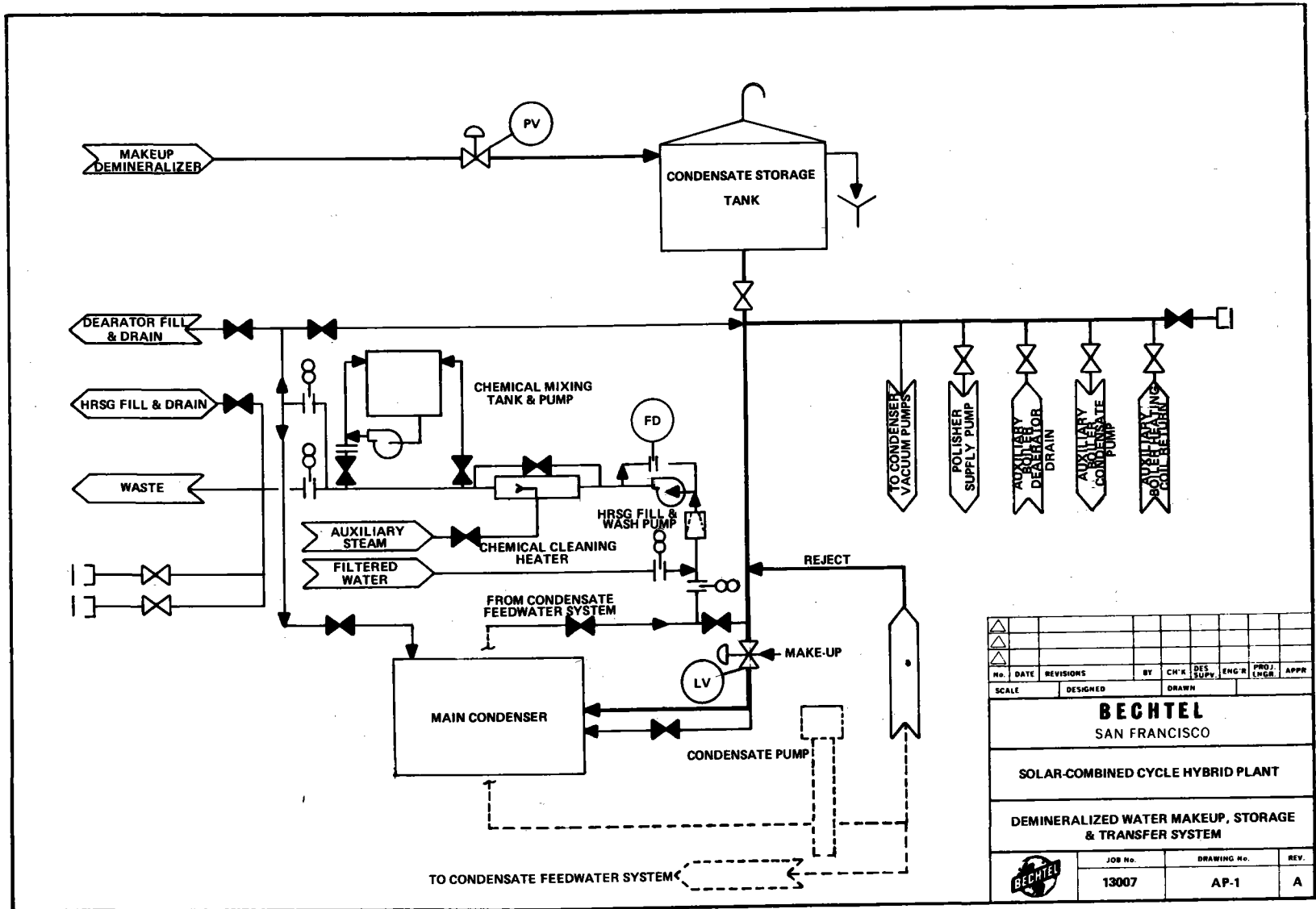


Figure D-10 DEMINERALIZED WATER MAKEUP, STORAGE AND TRANSFER SYSTEM

contaminated air to eliminate health hazards, nuisance, and fire danger.

The control room and administration building HVAC is designed to maintain appropriate temperature and humidity conditions in these areas during all modes of plant operation, thereby insuring control room habitability and equipment operability. A positive air pressure will be maintained in the control room to minimize dust infiltration.

#### D. 12 FIRE PROTECTION SYSTEM

The fire protection system is comprised of automatic sprinkler, deluge, and carbon dioxide systems as applicable. Standpipes and hose reels are provided throughout normally accessible areas of the plant so that no area is more than 30 m (100 ft) from a standpipe. Manual, ABC, fire extinguishers are provided for first aid fire protection. Selection, placement, and spacing of fire monitoring detection and alarm devices is based on consideration of the design, configuration, and employment of the area, together with draft conditions due to natural or mechanical ventilation.

The fire protection water supply system consists of an adequate and reliable source of water, two fire pumps (one motor driven, one engine driven), and a jockey pump to maintain system pressure. The yard main is looped around the plant to provide fire protection for all buildings and enclosures. Hydrants

complete with hose houses are located at approximately 76 m (250 ft) intervals along the yard main.

#### D. 13 SAMPLING SYSTEM

The sampling system consists of an array of indicators, recorders, and analyzers that monitor pressure, temperature, conductivity, flowrate, and chemical breakdown of selected fluids associated with the steam/water cycle. Those fluids sampled include:

- Auxiliary boiler inlet
- Auxiliary boiler blowdown
- Auxiliary boiler steam
- HRSG blowdown (low- and high-pressure drums)
- Superheater inlet steam (low- and high-pressure)
- Superheater outlet steam (low- and high-pressure)
- LP evaporator inlet
- Condensate storage

Sampling and analysis of the water systems provided input to the chemical control necessary to ensure that properly conditioned water is maintained in the fluid portions of the cycle.

#### D.14 RAW WATER MAKEUP SYSTEM

The raw water makeup system provides water to the water treatment system, which supplies treated water to the demineralizers, the domestic water treatment system, the fire protection system, and cooling tower makeup water system.

The system is designed to supply water to the various systems either continuously or intermittently, year round regardless of power plant status. The domestic water and fire protection systems have independent pumping and distribution systems.

Raw water source is assumed to be deep wells. The system includes pumps piping, surge tanks, and distribution headers as appropriate.

#### D.15 HRSG CHEMISTRY CONTROL SYSTEM

The HRSG chemistry control system removes impurities in the condensate feedwater system during startup and normal operation to meet feedwater quality requirements recommended by the HRSG and steam turbine manufacturers. This system provides high-purity demineralized water in the feedwater system by removing dissolved and suspended solids utilizing mixed bed cation-anion exchange resins vessels.

Chemical injection (such as amine and hydrazine) are performed in the condensate portion of the feedwater-condensate system between

the demineralizer outlet and the gland seal condenser inlet. Chemical injection and demineralization is used for pH control, oxygen scavenging, and general feedwater quality and purity control. Feedwater chemistry is monitored by the sampling systems.

APPENDIX E  
COMMERCIAL-SCALE SOLAR HYBRID  
POWER SYSTEM ASSESSMENT

## CONTENTS

<u>Section</u>	<u>Page</u>
E.1 Energy Storage Reassessment	E-3
E.2 Development Activities in Catalytic Combustion Systems	E-31
E.3 Assessment of Ceramic Receiver Concepts	E-34
E.4 Utility Questionnaire	E-56

## E.1 ENERGY STORAGE REASSESSMENT

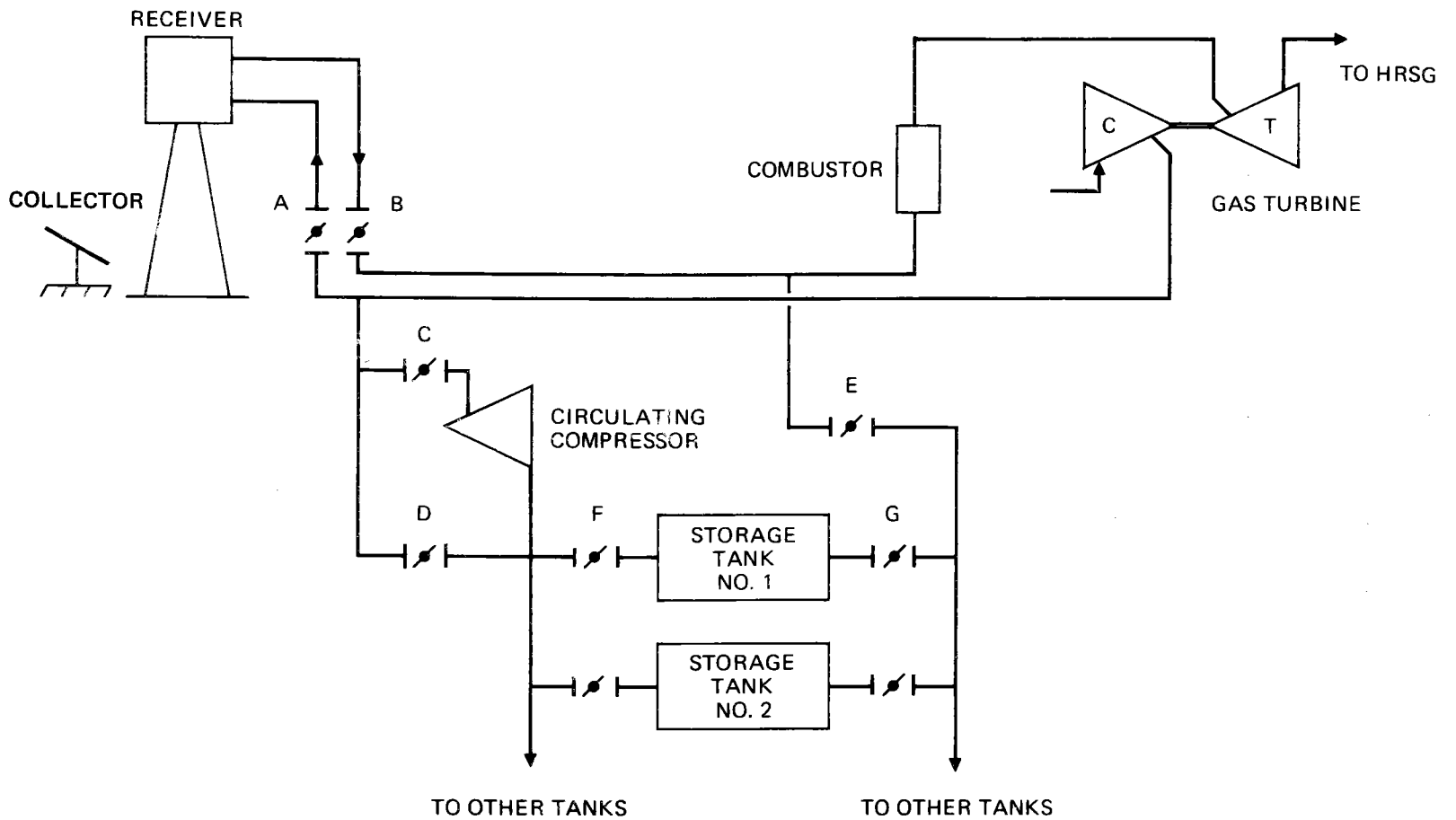
The schematic of the energy storage concept is shown in Figure 6-1. It consists of internally insulated steel tanks filled with alumina which are shaped and stacked to form passages for air flow during charging and discharging. The number of tanks depends on the desired storage capacity. A high-temperature, moderate-pressure ratio axial compressor is used to circulate part of the receiver discharge air through the storage tanks during the charging cycle. Valves and connecting piping similar in design to those used in the basic hybrid system control flow direction and internal system connections, as well as connections to the riser and downcomer piping near the foot of the receiver tower.

### E.1.1 Daily Operating Cycle

A typical daily operating cycle of the storage subsystem, using valve designations from Figure E-1, may be described as follows:

- System Startup. In the early morning hours, when only limited insolation is available, air is circulated through the receiver with valves A and B open, and C, D and E closed. When the receiver outlet air reaches a predetermined level, just below the design peak of 843C (1550F), the circulating compressor is started and valves C and E are opened. This initiates the charging operation.
- Storage Charging. It is assumed that the storage is being charged concurrent with normal operation of the hybrid power system. During the charging cycle the air flow through the storage tanks is controlled by adjusting the circulating compressor speed. When the storage is depleted, the compressor operates at higher





E-4

Figure E-1 ENERGY STORAGE SUBSYSTEM SCHEMATIC

speeds and is gradually stowed down as the storage approaches fully charged status. During this latter phase the receiver outlet temperature is monitored and heliostats are defocused if the temperature becomes excessive. If the storage becomes fully charged before the system can use any of the stored energy, the circulating compressor is shut off and the subsystem is isolated by closing valves C and E.

- Storage Discharging. As insolation declines in the afternoon, energy can be extracted from storage. To discharge from storage, the circulating compressor is shut off, valve C is closed, and valve D is opened. This results in a reverse air circulation through the storage tanks, bypassing a part of the main compressor discharge around the receiver. The bypassed air flow is regulated to maintain the receiver temperature within safe limits. When direct solar energy is no longer available, valves A and E are closed and all the air flows through the storage tanks until the storage outlet temperature falls to the level of the main compressor outlet temperature. At this point both the receiver and storage subsystems are bypassed and the plant operates on fossil fuel only.

While the energy storage subsystem was designed for augmentation of solar energy input to power generation, with some modifications it could also be used for system preheating in the morning. This mode was not considered, however. Design characteristics of the energy storage subsystem were defined for 1, 2, and 3 hours of average storage capacity. These characteristics are listed in Table E-1.

A schematic daily power map, Figure E-2, shows the effects of the above sequence on the relative solar and fossil fueled operation.

Figure E-3 shows the relationship between hours of storage at a 70 percent turnaround efficiency to the "H" field multiple for the conceptual design. The hours of storage are defined as the

TABLE E-1

## ENERGY STORAGE CONCEPTUAL DESIGN SIZING DATA

Data Item	Base System	Hours of Storage		
		1	2	3
Field multiple	1.0	1.315	1.53	1.73
Receiver air flow, kg/s	257.6	338.74	394.13	445.6
lb/s	568.0	746.9	869.1	982.7
Riser pipe ID, m	1.52	1.75	1.88	2.00
in.	60	69	74	79
Downcomer pipe ID, m	1.44	1.66	1.79	1.90
in.	57	65	71	75
Storage system air flow, kg/s	--	81.14	136.53	188.0
lb/s	--	179	301	415
No. of storage tanks		2	3	4
Storage tank dimensions				
Diameter, m	--	6.23	6.23	6.23
in.	--	245.3	245.3	245.3
Length, m	--	30.79	37.38	40.88
ft	--	101.0	122.6	134.1
Weight of alumina, metric tons	--	3175	3855	4215

E-7

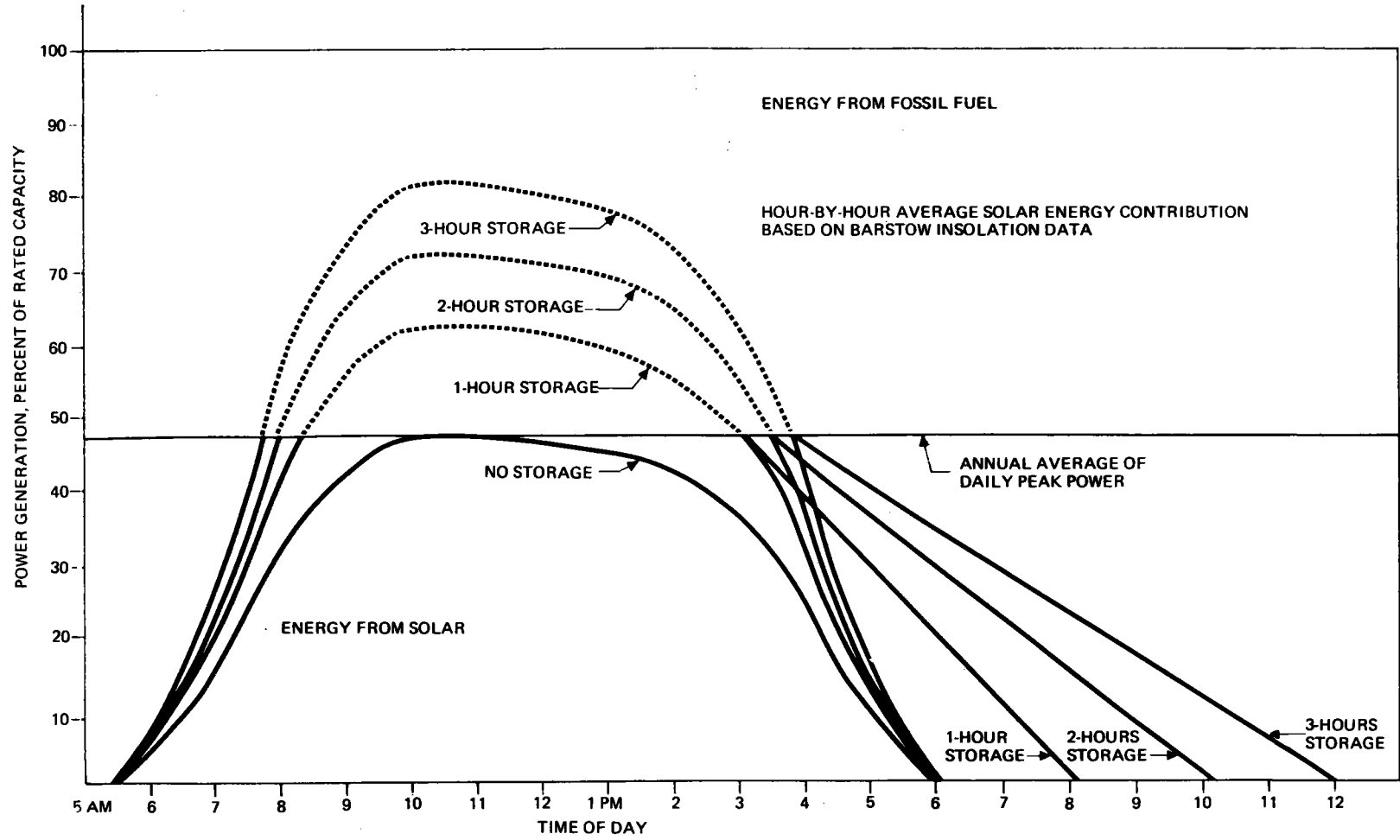


Figure E-2 FOSSIL FUEL DISPLACEMENT EFFECTS OF ENERGY STORAGE

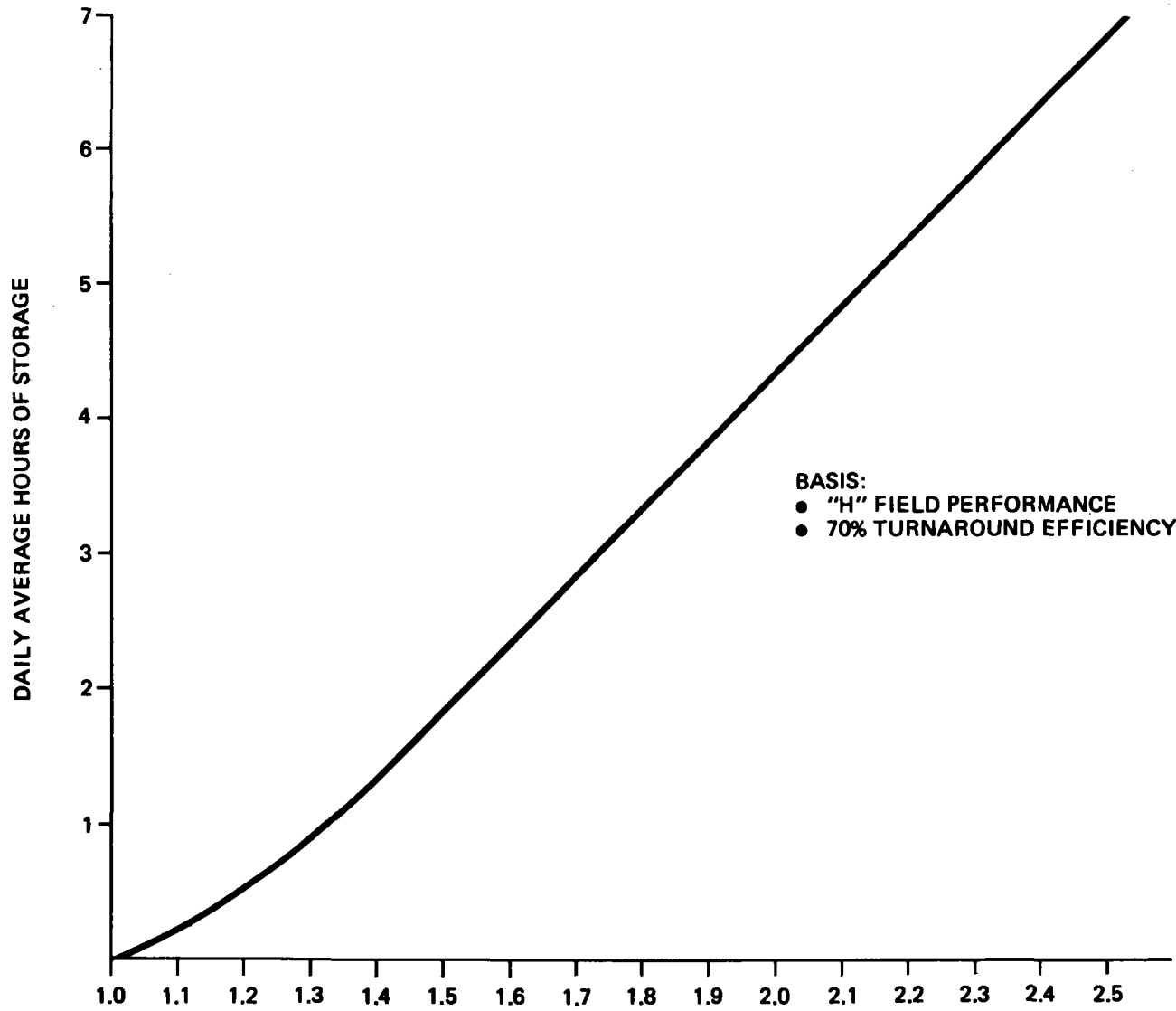


Figure E-3 HOURS OF STORAGE AS A FUNCTION OF FIELD MULTIPLE

average annual daily storage capability, where sensible heat begins charging the storage at about 47.4 MWe, the year-round average of the daily peak solar power generation. The information is based on a reference Barstow weather tape for the design point year.

The necessary field multiple is determined as a function of the required number of hours of storage as defined for Figure E-3. Figure E-2 represents the annual average hourly solar megawatt generation for three study cases - 1, 2, and 3 hours of storage capability.

As evident from Figure E-2, fossil fuel energy savings result from displacement of fossil energy during the day, specifically peak insolation hours in addition to the displacement of fossil energy in the evening by the energy storage system. Figure E-2 also shows that the solar input decreases with time. This is due to temperature degradation in the storage tank. Since the solar fraction can also be defined as the percentage of energy requirement supplied by the sun, the benefit of energy storage to improve the plant solar fraction depends strongly on the daily loading curves of specific utility grids.

### E. 1.2 Energy Storage Subsystem Equipment

The storage tanks required for the study cases are scaled from Boeing's design (Ref. E-1). The storage tanks are direct-contact using aluminum oxide refractory. The refractory is contained in an insulated cylindrical steel pressure tank. The domed ends of the tanks are filled with alumina spheres and Inconel grating to provide a diffuser and prevent large pieces of refractory material from blowing out of the tank if it fractures.

Line pressure drop rates are treated as constant and line sizes were scaled as the square of the difference of the flow rate of the riser/downcomer piping. The pressure drop through the energy storage tank was estimated to be .165 MPa (24 psi). The circulating compressor, used to compensate for this pressure drop, may be of axial or centrifugal type and must have variable speed capability. Inlet temperature to the circulating compressor will range from 371 to 538C (700 to 1000F). Figure E-4 indicates the design and daily average power requirements to operate the circulating pump and its effect on the daily average net plant heat rate.

### E. 1.3 Collector Subsystem

An enlarged, radially-staggered "I" field was designed to collect solar energy for normal hybrid operation, plus an average daily energy surplus which would allow an additional 3 hours of post-

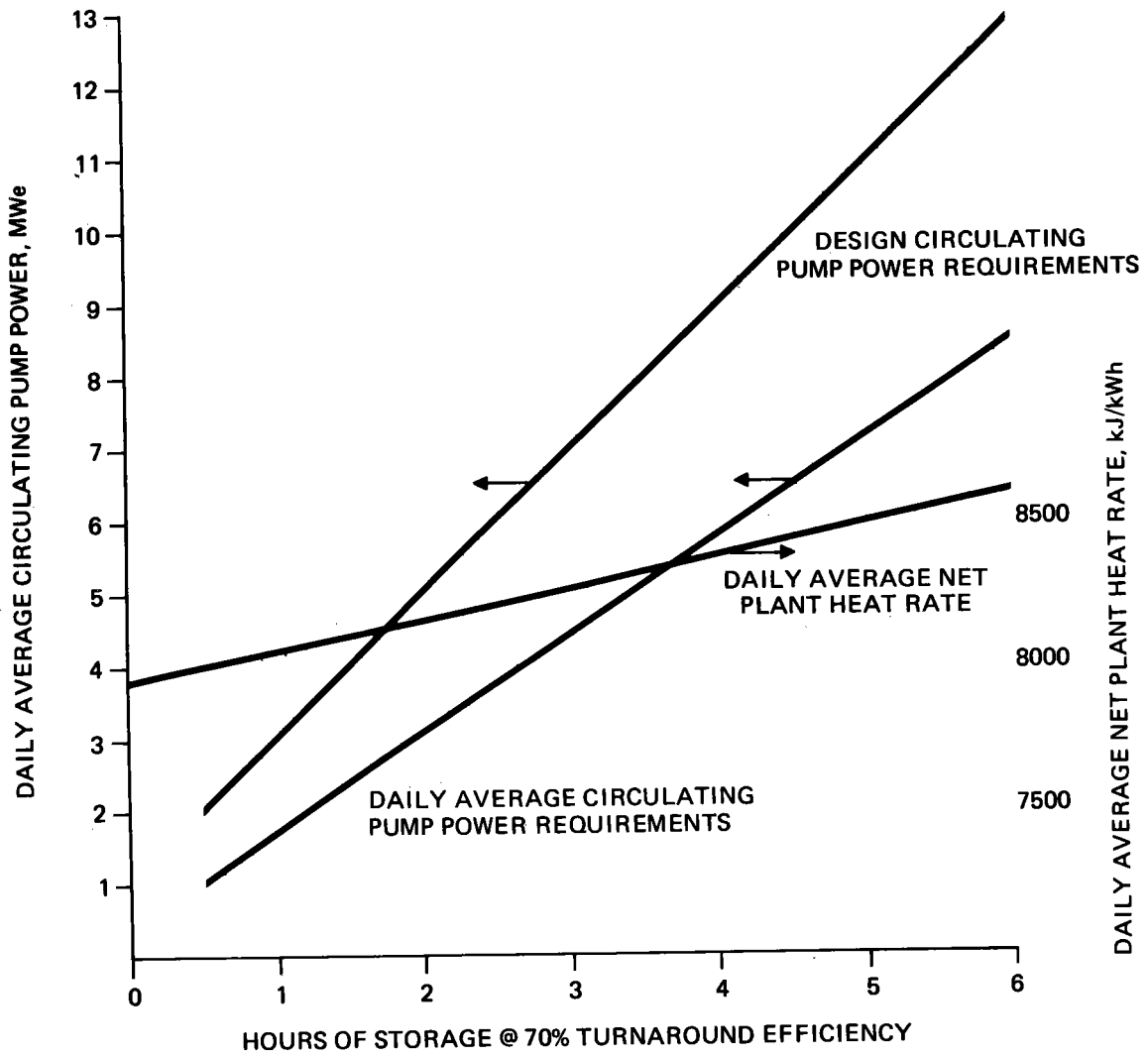


**Figure E-4 CIRCULATING COMPRESSOR POWER REQUIREMENTS AND EFFECT ON NET PLANT HEAT RATE**



collection operation. The field was sized using the following baseline performance parameters:

Cosine Efficiency = 88 percent

Mirror Reflectivity = 87 percent

Blocking Efficiency = 99.9 percent

Shading Efficiency = 95 percent

Attenuation Efficiency = 93 percent

Aperture Spillage Efficiency = 96 percent

Average Daily Collection Period = 7 hours

Based on these design criteria, it was found that a field size containing 8800 heliostats, each having a mirror area of 50.54 m<sup>2</sup> (544 ft<sup>2</sup>), would be required.

The radial stagger field layout, based on minimum blockage, was established using the Northrup "LAYRAD" computer code. The receiver tower is 210 m (689 ft) high, and is located 232.5 m (763 ft) south of the east-west field axis. The ellipse has a major axis of 2011.4 m (6599.0 ft) and a minor axis of 1551.8 m (5091.4 ft). The corresponding slant range limits are 242.5 m (795.5 ft) to 1077.7 m (3535.6 ft). The field average atmospheric attenuation is 6.74 percent. The complete heliostat layout for the enlarged "I" field is illustrated in Figure 6-1 of Volume II.

#### E.1.4 Economics of Energy Storage

As the cost of electric energy produced by alternative sources rises, the economic viability of solar power will improve. The viability of long-term storage of solar energy, as a means to displace costly fuel during generating periods when solar energy is not available, is also more likely as solar plants become economic. The value analyses performed earlier in the project (see Section 4) indicate that a zero cost storage would break even by 1990 for nominal distillate oil escalation rates of about 14 percent. Long-term energy storage is therefore a likely future improvement to the solar hybrid power system. With this in mind, the earlier "value of storage" or breakeven analyses were expanded to a more detailed parametric optimization study.

Under the assumptions set forth below, optimal capacities for a sensible heat storage system compatible with the hybrid power plant have been determined over a range of distillate oil escalation rates. The optimal storage capacity was defined as that which results in the lowest levelized busbar electricity cost. Cost components affected in the analyses include:

- Fuel cost savings
- Solar system capital charges
- Capital charges associated with the storage equipment itself
- Incremental operating and maintenance costs

The annual electricity produced with stored solar thermal energy was computed using an hour-by-hour computer simulation based on weather conditions at Barstow, California.

The computer program and insolation data used in the previous simulation were modified to reflect:

- A radial stagger field layout with a 145 meter tower at zero storage
- Receiver efficiency variation with power levels
- Storage compressor power requirements
- The power level at which solar thermal input would be diverted to storage

Consistent with the conceptual design, heliostat turndown occurs when field power densities exceed  $950 \text{ W/m}^2$ , and no solar energy is collected when the insolation level is below  $500 \text{ W/m}^2$ . The  $500 \text{ W/m}^2$  cutoff point was found to have negligible impact on average annual solar fraction. A revised schematic representation of the incremental solar thermal energy contributions due to a storage system are shown in Figure E-5. The effects of declining receiver efficiency and storage compressor losses are also indicated. As before, a portion of the incremental solar thermal input (labeled A) is used immediately while the remainder (labeled B) is diverted to thermal storage and used to displace distillate oil during the late afternoon and early evening. Annual electric energy production using both the direct and stored thermal energy

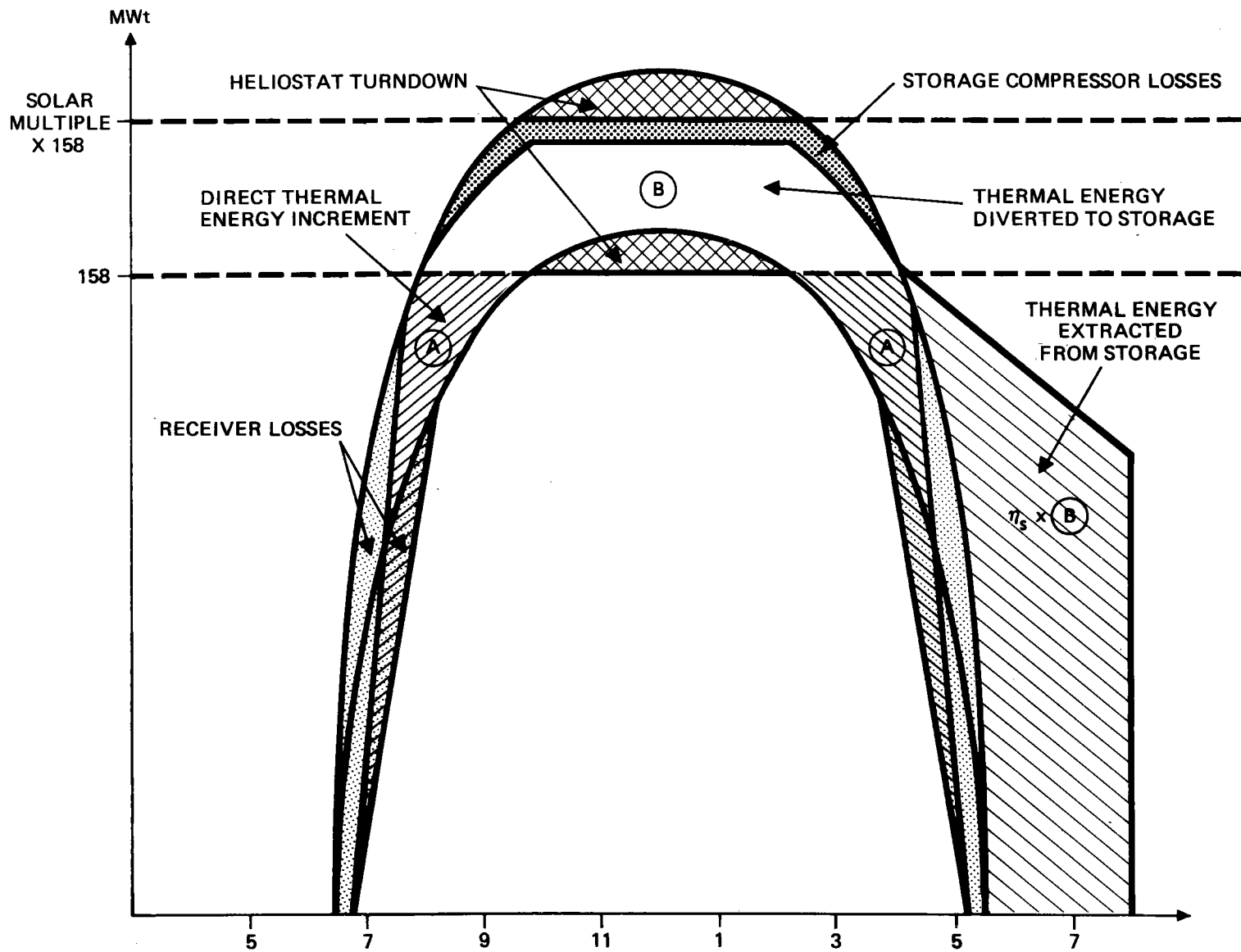


Figure E-5 REVISED STORAGE SCHEMATIC

increments is shown in Figure E-6 for ranges of collector field multiples and storage efficiencies.

The net effect of the modifications described above was to slightly increase storage contributions at all solar multiples and storage efficiencies. The increase is less pronounced at higher solar multiples because of the compressor losses.

Determination of the fuel cost savings corresponding to the storage-related electric energy production over the life of the hybrid plant is complicated by the stochastic nature of insolation profiles, the manner in which the stored energy is used, and the fuels and power cycles being displaced by the stored energy. To simplify the analysis, it was assumed that the 1976 weather data is repeated every year during the 1900 to 2020 time frame.

The dollar value of the incremental solar thermal input is the sum of the value of fuel displaced by the direct increment and the value of that displaced by the stored increment. Since it was assumed that all of the stored energy is used during periods when the hybrid plant would normally be scheduled for operation (i.e., within the baseline 48 percent capacity factor), the annual value of both the direct and stored increments is directly proportional to the product of:

- The number of MWe produced by incremental solar thermal input during the year

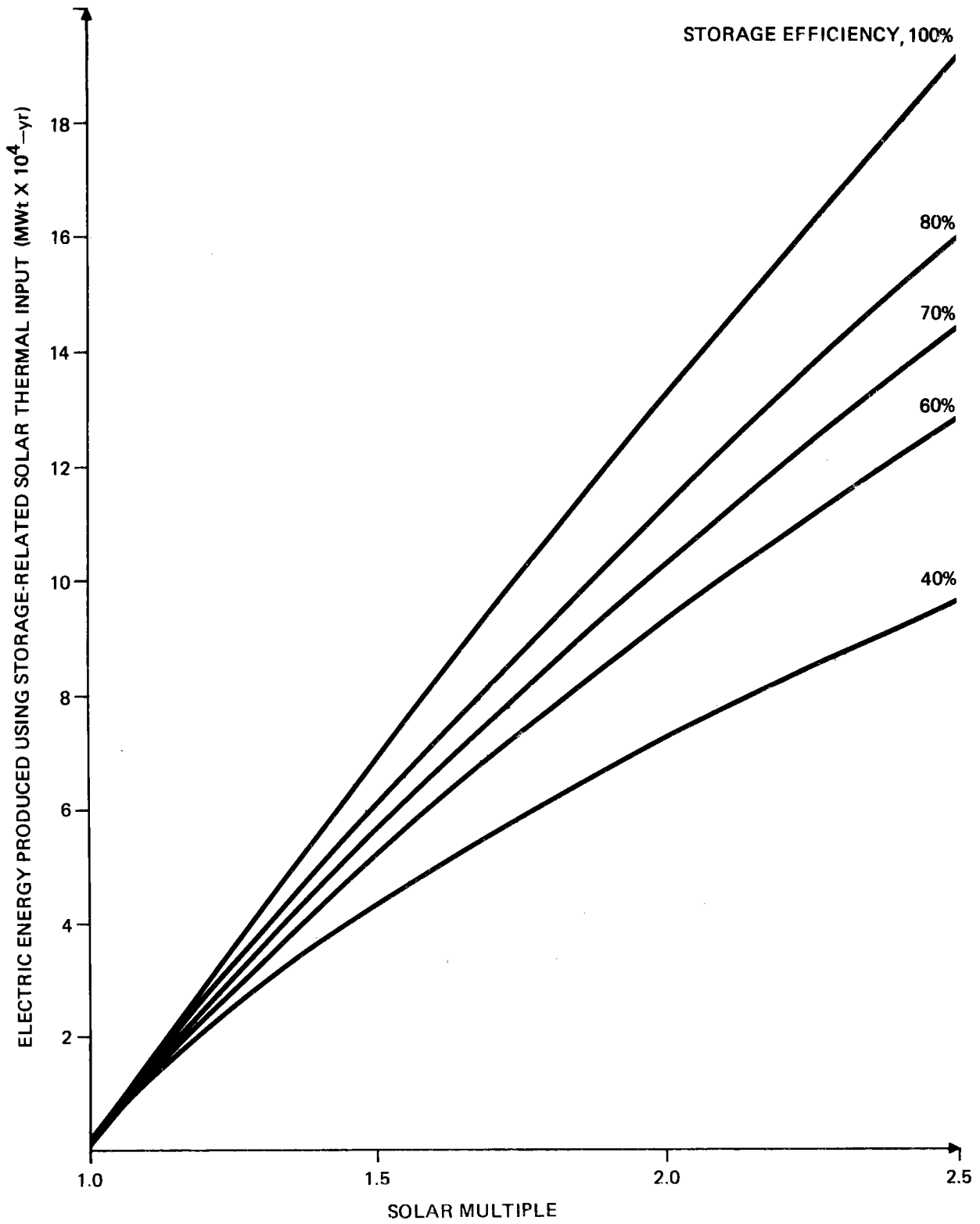


Figure E-6 INCREMENTAL ANNUAL POWER PRODUCTION

- The average heat rate of the hybrid plant
- The projected price of distillate oil

The fixed capacity factor of 48 percent limits possible storage discharge to between 2 and 3 hours on average. But this assumption is not as restrictive as it appears, since the value of stored thermal energy declines sharply when it is used to displace low-cost fuel in base-load plants. Moreover, since the plant cannot operate without fossil input, there can be severe cost penalties associated with nonsolar output when the plant is operated at higher capacity factors.

However, several alternatives could be considered to the passive storage dispatch strategy described above. For example, storage could be charged during the morning hours (the rest of the hybrid plant remaining idle) and used selectively for peak shaving in the afternoon or early evening. This could even be accomplished without the excess solar system capacity required by the passive strategy. Some of the complications involved in evaluating storage under this and similar "active" dispatch strategies are discussed later. The passive strategy, however, is adequate for establishing an upper bound on possible busbar electricity cost reductions.

Reductions in levelized cost resulting from storage-related distillate oil displacement are shown in Figure E-7 for ranges of solar multiples and distillate oil escalation rates. Assumptions used in the calculations included 70 percent turnaround

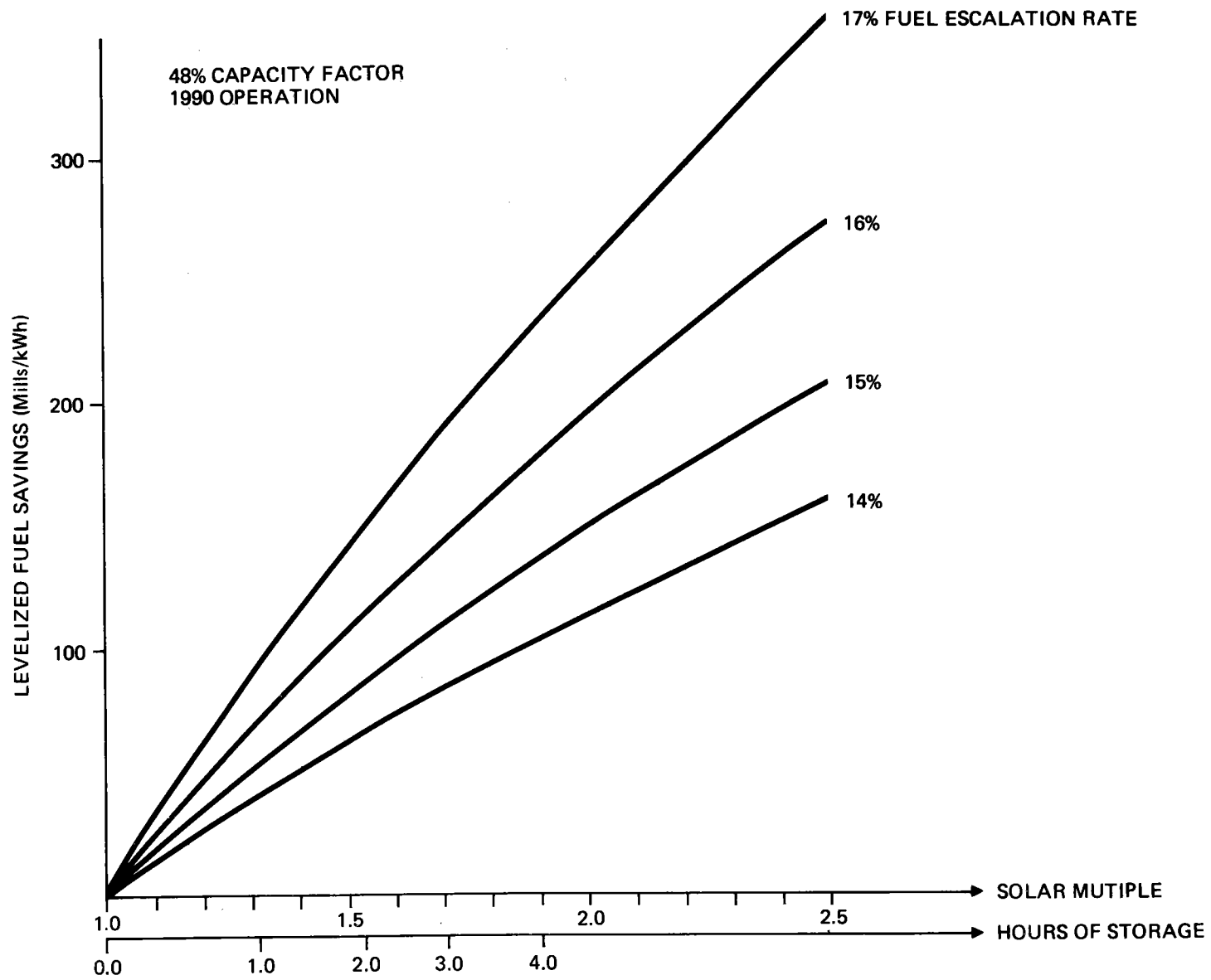


Figure E-7 VALUE OF FUEL SAVINGS



efficiency for the storage tanks, a base distillate oil price of \$2.35 per MBtu (1978 dollars), a first operational year of 1990, 90 percent availability, and an average heat rate of 8412 kJ/kWh (7978 Btu/kWh).

Offsetting the levelized cost savings resulting from distillate oil displacement are the levelized capital charges for the storage subsystem equipment, and the levelized incremental operating and maintenance costs.

Incremental solar equipment costs are based on the conceptual estimate. They include the cost of additional collector area, receiver capacity, tower height, riser/downcomer piping, controls, and structures. The parametric equations relating incremental cost to solar multiple for each of these components have been revised as follows:

$$\text{Collector Field: } \Delta C_1 (\text{SM}) = K_1 [ (\text{SM})^{1.03} - 1 ]$$

$$\text{Receiver: } \Delta C_2 (\text{SM}) = K_2 [ \text{SM} - 1 ]$$

$$\text{Tower: } \Delta C_3 (\text{SM}) = K_3 ( f_S [ H (\text{SM}), W (\text{SM}) ] - f [ H_0, W_0 ] )$$

$$\text{Plant Support Structures: } \Delta C_4 (\text{SM}) = K_4 [ (\text{SM})^{0.5} - 1 ]$$

$$\text{Controls: } \Delta C_5 (\text{SM}) = K_5 + (K_6 \cdot \text{SM})$$

Where:

SM = Solar multiple (Parametric thermal power input) / (reference thermal power input)

H<sub>0</sub> = Tower height under the conceptual design

W<sub>0</sub> = Receiver weight under the conceptual design

H (SM)	=	Tower height at field multiple SM
	=	$H_0 \cdot (SM)^{0.5}$
W (SM)	=	Receiver weight at field multiple SM
	=	$W_0 \cdot (SM)^{1.07}$
f (H,W)	=	Sandia tower cost equation for height H and weight W
$\Delta C_1$ (SM)	=	Change in collector field capital cost
$\Delta C_2$ (SM)	=	Change in receiver in capital cost
$\Delta C_3$ (SM)	=	Change in tower capital cost
$\Delta C_4$ (SM)	=	Change in support structure cost
$\Delta C_5$ (SM)	=	Change in control system cost
$K_1, K_2, K_3, K_4, K_5, K_6$	=	Constants

The energy storage capital costs, shown in Figure E-8, were estimated for the sensible heat energy storage concept. The curve was fitted from costs of point designs with 1, 2, and 3 hours of storage capacity, and corresponding capital cost estimates. These costs estimates include an allowance for additional riser/downcomer piping.

The total change in levelized capital charges was obtained by escalating the sum of incremental solar system and energy storage capital costs to 1990 and applying an 18 percent fixed charge rate. Incremental annual operating and maintenance costs are assumed to be proportional to incremental capital investment. They are levelized and added to the incremental levelized capital charges to give the total increase in levelized cost due to storage-related capital investment.

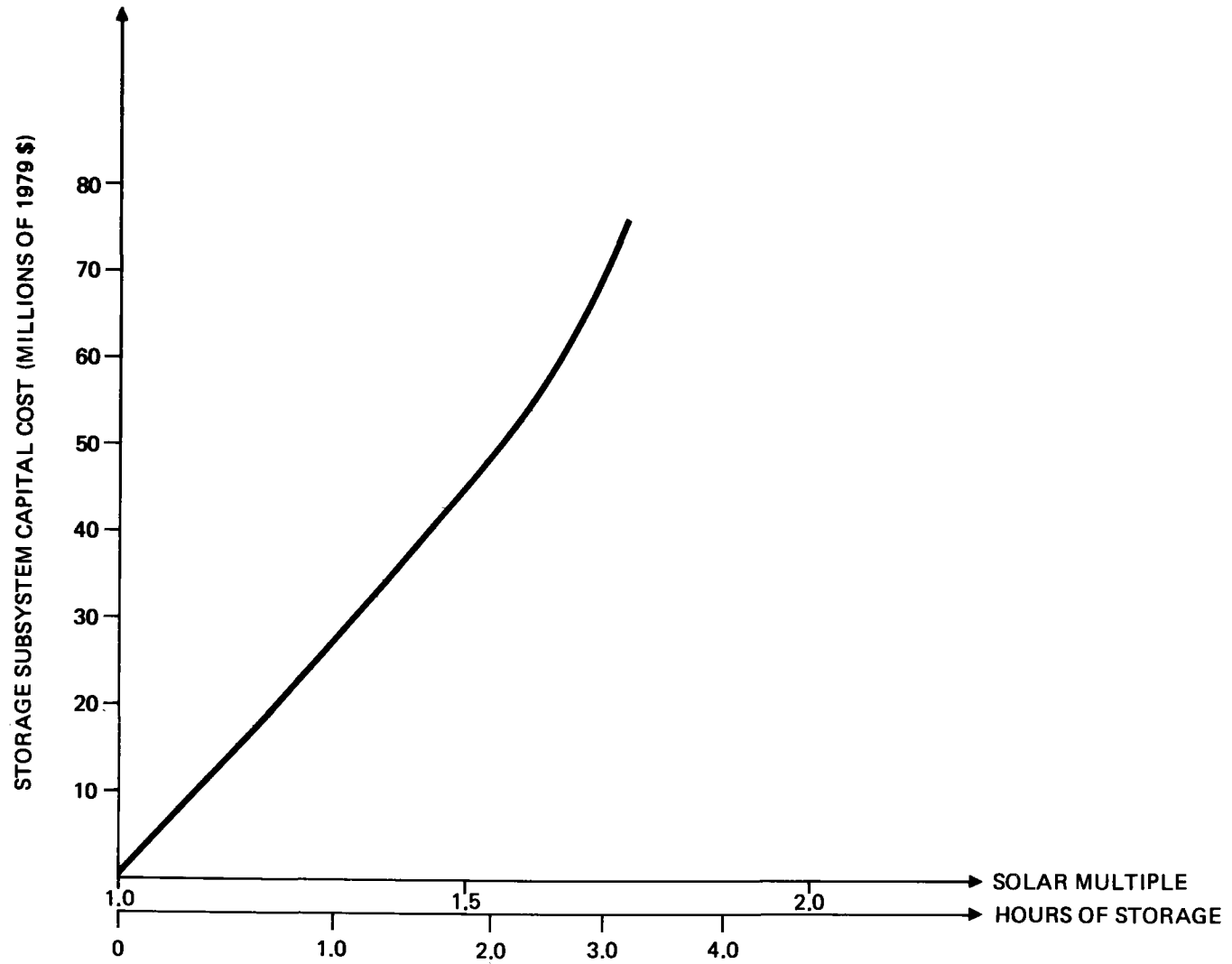


Figure E-8 CAPITAL COST OF ENERGY STORAGE

Figure E-9 shows the net change in levelized cost of electricity as a function of solar multiple and fuel escalation rate. The cost reductions were computed using the VALSTOR computer program. Under the assumptions described above, the sensible heat storage system breaks even for nominal fuel escalation rates exceeding 15 percent.

Figure E-10 is a plot of the optimal storage capacities (expressed in terms of hours of storage and solar multiple) at various fuel escalation rates. It shows that storage actually breaks even at a 15.5 percent escalation rate. This result is consistent with the value analysis in Section 4, which indicated that "free" storage equipment would break even between 13 and 14 percent.

In view of the 10 to 16 percent near term and 7 to 11 percent long range distillate fuel escalation rates expected by many electric utilities, these results imply that storage systems may be of limited value when used under a passive dispatch strategy in the hybrid power plant. The value of fuel displaced by stored thermal energy can never exceed the maximum value of displacement in intermediate-load plants. This is true because the hybrid plant will always be dispatched as an intermediate-load combined cycle plant (with or without solar thermal input) before peaking combustion turbines or less efficient oil-fired intermediate plants. Therefore, it is not realistic to expect significant peak shaving under any operating strategies.

E-24

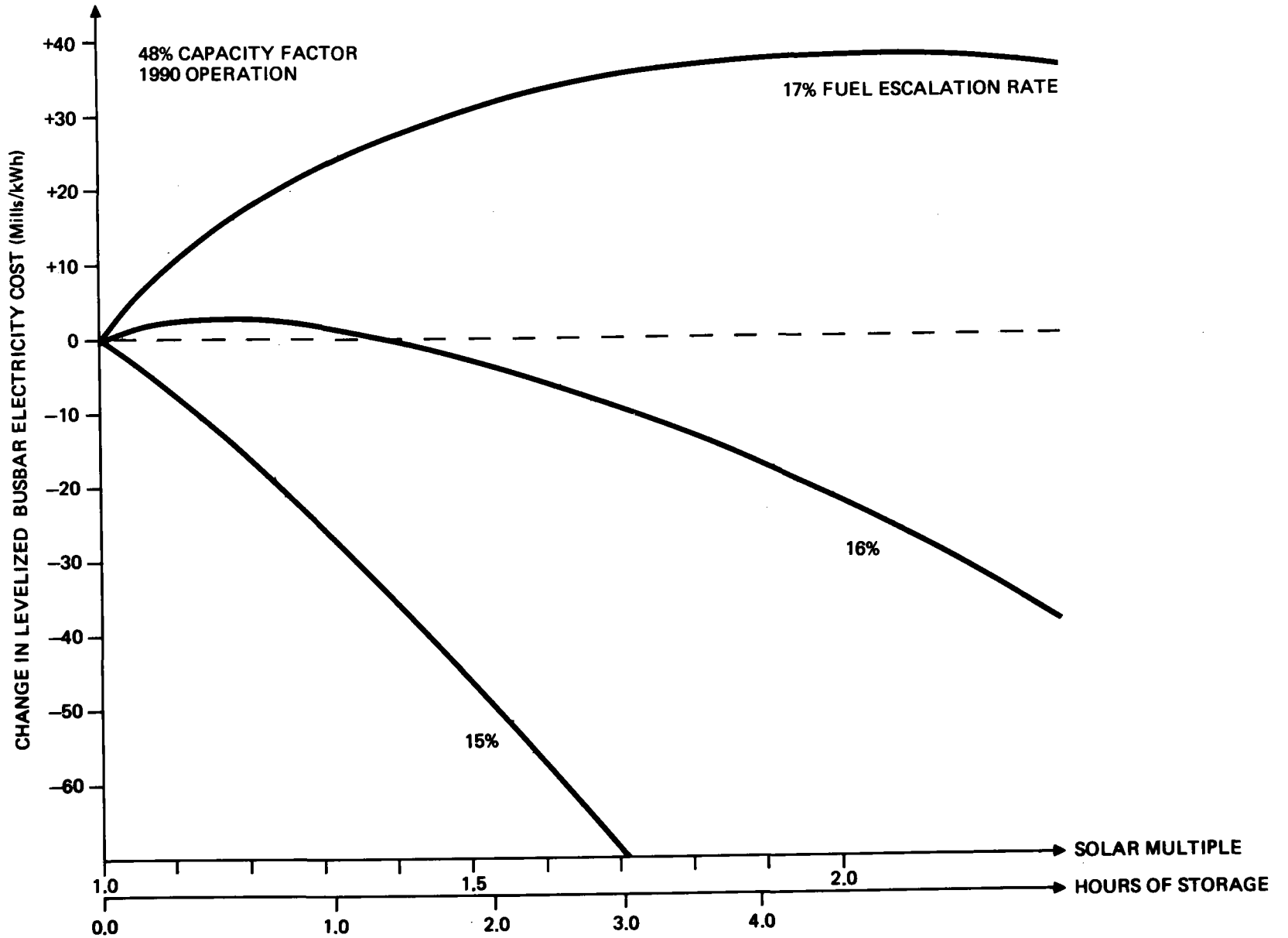


Figure E-9 ELECTRICITY COST SAVINGS WITH ENERGY STORAGE

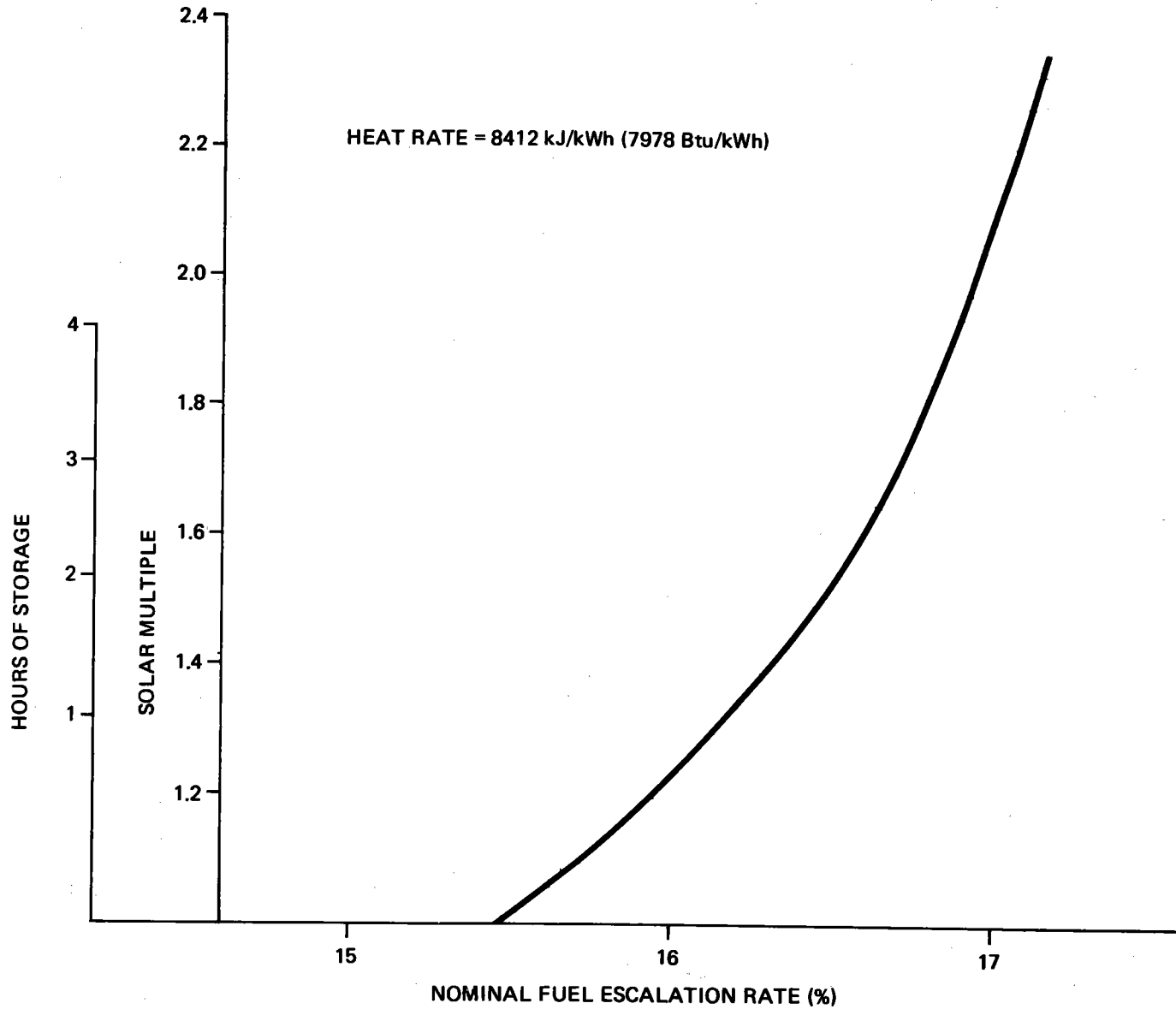


Figure E-10 OPTIMUM STORAGE CAPACITY AS FUNCTION OF FUEL COST ESCALATION RATES

The value of fuel displacement, however, could be slightly higher than the value of distillate oil displacement in the hybrid plant if the instantaneous reductions in fuel cost due to extraction of thermal energy from storage allows the hybrid plant to be dispatched ahead of another intermediate-load plant. For example, if variable operating and maintenance costs are neglected, the instantaneous marginal cost of the hybrid plant in mills/kWh is:

$$\left(1 - \frac{SF(t)}{100}\right) \cdot FC_1 \cdot \frac{HR_1(SF)}{1000}$$

Where:

SF(t) = The instantaneous solar fraction in the hybrid plant (%)

FC<sub>1</sub> = The cost of distillate oil (\$/MBtu)

HR<sub>1</sub>(SF) = The instantaneous heat rate of the hybrid plant (Btu/kWh),  $\delta HR / \delta SF < 0$

If the solar fraction, SF(t), is sufficient to allow the hybrid plant to economically meet a load requirement that would have been allocated to another unit, if SF(t) were zero, the instantaneous value of fuel displacement in the hybrid plant in terms of mills/kWh increases by:

$$f \left\{ \left[ \left(1 - \frac{SF(t)}{100}\right) \cdot FC_1 \cdot \frac{HR_1(SF)}{1000} \right] - \left[ FC_2 \cdot \frac{HR_2}{1000} \right] \right\}$$

$$f(0) = 0, \quad \left. \frac{f(x)}{x} \right|_{x=0} > 0$$

where  $FC_2$  and  $HR_2$  are the fuel cost (\$/MBtu) and heat rate (Btu/kWh) of the unit which would have been dispatched in the absence of thermal input from storage.

Thus, it is possible that even under the passive dispatch strategy, the value of stored thermal energy may be greater (and the breakeven distillate oil escalation rate lower) than indicated by the results of the storage optimization study. To examine the possible increases in the value of stored thermal energy, breakeven analyses were performed for a range of effective heat rates for the aggregate of units in which fuel, specifically distillate oil, might be displaced. Figure E-11 shows the results. Clearly, the distillate oil escalation rate at which storage breaks even is not a strong function of the efficiency of the units in which displacements occur; even when the effective heat rate is doubled, which is unlikely, the breakeven rate drops only by about 15 percent. Thus, energy storage under the pure fuel displacement passive dispatch strategy appears to have limited benefits even under the most optimistic assumptions.

As mentioned earlier, strategies other than pure displacement are possible. For example, a "pure load shifting strategy" could be envisioned in which no additional fuel is displaced but possible cost penalties are avoided associated with dispatching hybrid plant under offpeak conditions just to use insolation. (In fact, in this strategy less fuel is displaced when the roundtrip efficiency of storage is accounted for.) When the hybrid plant



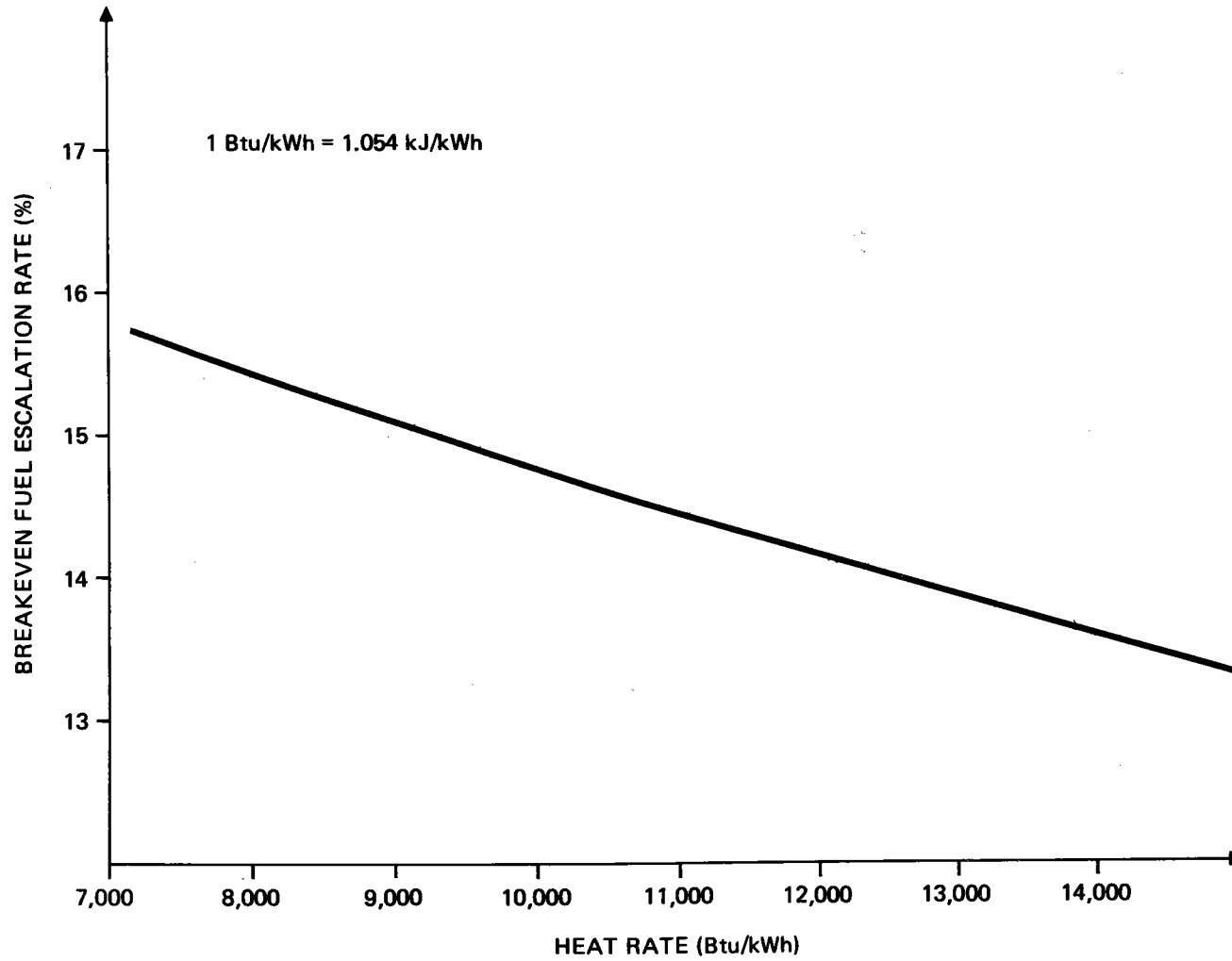


Figure E-11 SENSITIVITY OF THE BREAKEVEN ESCALATION RATE FOR STORAGE TO THE VALUE OF FUEL DISPLACED

is dispatched to use insolation during periods when only base-loaded plants would normally be operating, a cost penalty is incurred. Negating operating and maintenance cost differentials, the cost penalty in terms of mills/kWh has an instantaneous value of:

$$\left[ \left( 1 - \frac{SF(t)}{100} \right) \cdot FC_1 \cdot \frac{HR_1(SF)}{1000} \right] - \left[ \sum_I K_i(t) \cdot FC_i \cdot \frac{HR_i}{1000} \right]$$

where:

- SF(t) = The instantaneous solar fraction of the solar hybrid plant
- FC<sub>1</sub> = The cost of distillate oil (\$/MBtu)
- HR<sub>1</sub>(SF) = The instantaneous heat rate of solar hybrid plant
- I = The set of other power generation units shut down or throttled to allow the hybrid plant to absorb load up to its rated capacity
- K<sub>i</sub>(t) = The fraction of the hybrid plant's rated output (112.6 MWe) which normally would have been filled by power generation unit i,  $\sum_I K_i(t) = 1$
- FC<sub>i</sub> = Fuel cost for the i<sup>th</sup> unit
- HR<sub>i</sub> = Heat rate for the i<sup>th</sup> unit

If on other hand, the solar energy can be collected and used when it is actually needed, this penalty can be avoided.

A way to accomplish this would be to size the collector and receiver subsystems for hybrid operation but to provide an energy storage subsystem as well to allow collection when the combined

cycle part of the plant is not operating. The evaluation of such an arrangement is complex. Since the benefits depend primarily on insolation profiles, load profiles, and systemwide dispatching procedures, the sample approach used to evaluate the pure fuel displacement strategy is inadequate. Since  $SF(t)$  and all of the  $K(t)$  are time-varying, both in terms of short-term fluctuations and long-term trends, the true value of cost penalties avoided can only be evaluated through a detailed production costing simulation. Moreover, the results would not necessarily apply for all utility systems. For example, this type of strategy would probably be more valuable to winter peaking utilities whose load and insolation profiles would not coincide for a large part of the year. Conversely, it would probably be of limited value for a summer peaking utility.

## E.2 DEVELOPMENT ACTIVITIES IN CATALYTIC COMBUSTION SYSTEMS

Development of a catalytic combustion system for gas turbines has been under way since the early 1970's. Parallel activities are currently under contract for aircraft, automotive and stationary applications. The main sources of funding besides corporate funds are the Department of Energy, the Air Force, the Environmental Protection Agency, and the Electric Power Research Institute. The technical manager for most government-funded activities is NASA-Lewis Research Center.

Westinghouse has been pursuing internally-funded development of catalytic combustors since about 1973 in cooperation with Engelhard Industries. The result is that a full-scale catalytic combustor is expected to begin testing in the Westinghouse laboratory before the end of 1979. At least three other development programs are important to note in relation to the solar hybrid system. DOE, through NASA-Lewis, is funding five contractors (Westinghouse, General Electric, Pratt & Whitney/UTC, Solar Turbine, and Detroit Diesel-Allison) to evaluate many types of new combustion systems, some catalytic, for both fuel and emission capabilities. This one and a half year Phase I program begun recently is funded with approximately \$5 million. The remaining phases are planned to conclude with engine testing of the most promising concepts by 1983.

In another program, Acurex is being funded by EPA and DOE for more than \$1 million to develop promising catalytic combustion designs and to do catalytic performance testing.

The most important program is being considered for funding by EPRI. The goal of this three-phase program is to complete a field test of a catalytic combustion system on an existing utility gas turbine by 1985. The funding for the first phase is approximately \$1 million, and the contracts should be started by January 1980. The emphasis of this program is on clean distillate fuel applications for utilities in states like California, where coal and nuclear generation are under great political pressure. The solar hybrid system has an advantage for this application because of the solar exemption to the requirements of the National Energy Act of 1978.

Other programs to develop catalytic systems for aircraft and automotive systems may help the development of the combustion system for the solar hybrid system in a more indirect manner.

Two feasible scenarios are apparent for development of a solar hybrid combustor. In the first, current development activities for conventional gas turbines can be monitored and the specific modifications necessary to meet the solar hybrid requirements can be made after the demonstration of a catalytic combustion system for a conventional gas turbine. In the second, with a small increase in funding, the solar hybrid requirements would be added as a parallel development activity to those currently under way.

The first scenario would probably result in the hardware necessary for a demonstration solar hybrid plant being available by 1990. The second scenario could result in the necessary hardware by 1985 or at least before 1990.

E.3.1 Introduction

As a result of the solar hybrid combined cycle system study performed for DOE during FY 1979, the potential advantages of a solar receiver capable of operating in the 1000 to 1100C (1800 to 2000F) temperature range were identified. This range is beyond the capabilities of receivers using metallic superalloys and represents an advanced state of receiver development.

The following advantages were identified for the solar hybrid system using a high-temperature receiver:

- High solar fraction, resulting in increased displacement of fossil fuel
- High system efficiency, resulting in reduced fossil fuel input when used with an advanced combustion turbine
- Reduced dependence on imported superalloy constituents, such as cobalt and molybdenum
- Increased thermodynamic availability of solar thermal energy for processes other than power generation.

To evaluate the potential of several proposed high-temperature receiver concepts, a systematic review of their relative advantages and disadvantages was conducted, limited to their applicability to Bechtel's solar hybrid combined cycle system. Six concepts were reviewed:

- Black & Veatch/Electric Power Research Institute (EPRI) Ceramic Tube Receiver

- Sanders Ceramic Honeycomb Receiver
- Massachusetts Institute of Technology (MIT)/Lincoln Laboratory Ceramic Dome Receiver
- Naval Research Laboratory (NRL) Solchem Receiver
- Lawrence Berkeley Laboratory (LBL) Black Particle Concept
- Los Alamos Scientific Laboratory (LASL) Ceramic Heat Pipe Concept.

### E.3.2 System Requirements

The receiver for the solar hybrid combined cycle system absorbs focused solar energy from the heliostat field and transfers the resultant thermal energy to the compressed air working fluid. A diagram of the overall system is given in Figure E-12.

The following receiver characteristics have been determined from the economic analyses performed for a hybrid system:

- Receiver inlet air temperature - 290 to 450C (550 to 850F)
- Receiver outlet air temperature - 1000 to 1100C (1800 to 2000F)
- Receiver operating pressure - 0.7 to 1.5 MPa (100 to 220 psia)
- Receiver pressure loss - less than 0.08 MPa (10 psi)
- Receiver capacity - 150 to 800 Mwt total with multiple cavities.

In addition, it is desirable for the receiver to be low in cost and weight, small in physical size, and able to withstand the most severe thermal transients due to variations in solar input.



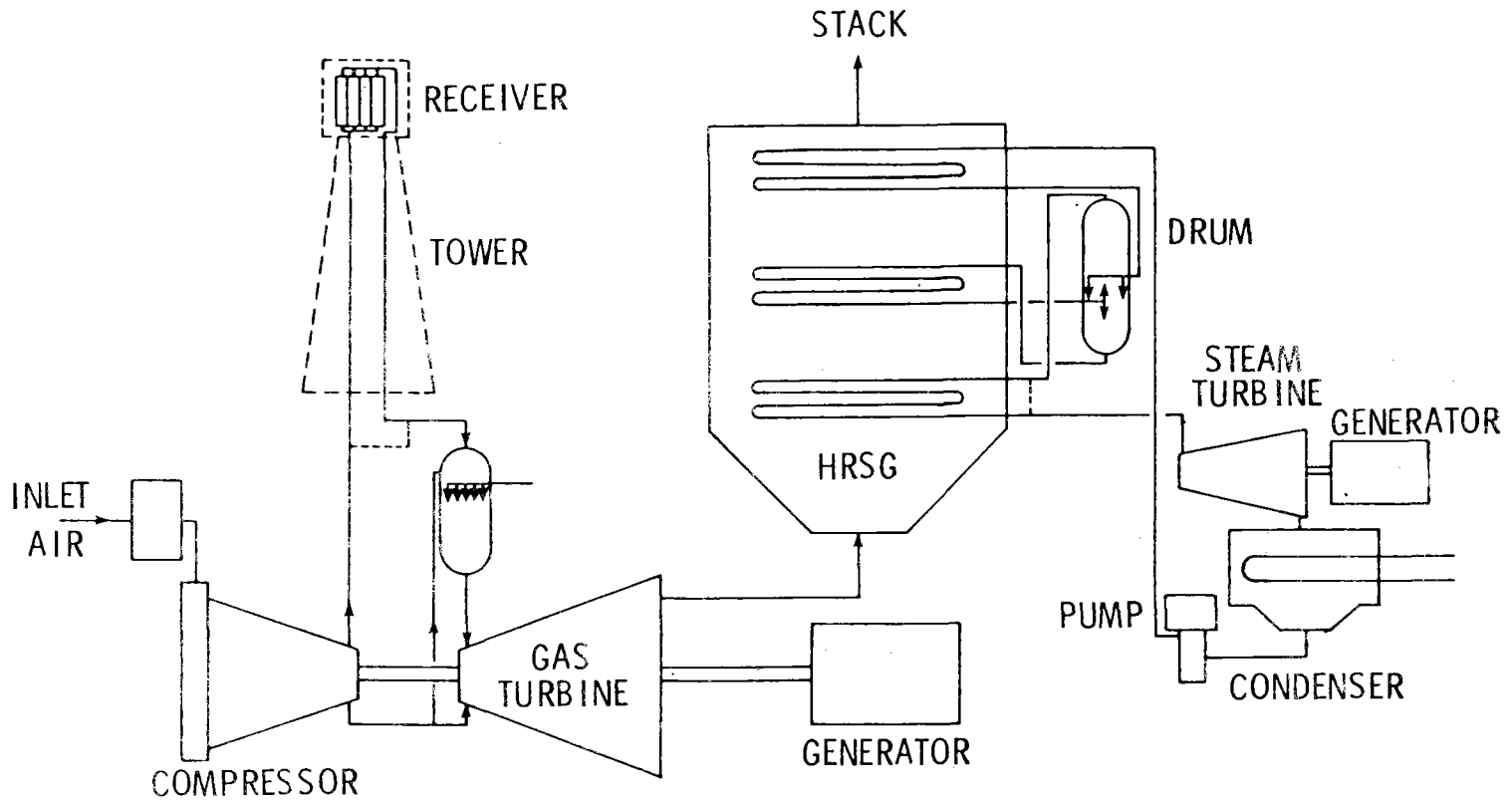


Figure E-12 SOLAR COMBINED CYCLE HYBRID SYSTEM FLOW DIAGRAM

### E.3.3 Assessment of Ceramic Receiver Concepts

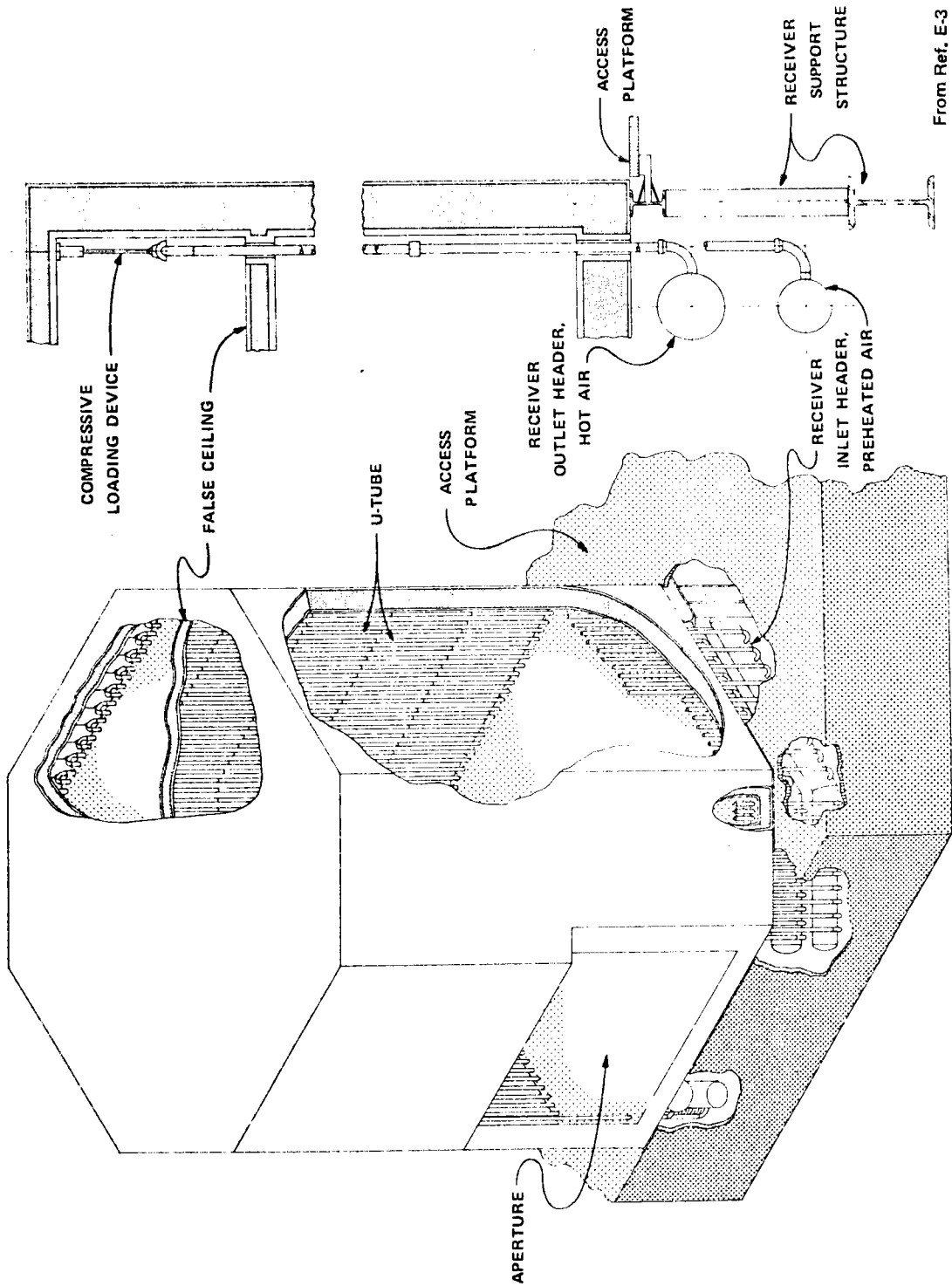
Each of the proposed concepts has been compared to the requirements of the solar hybrid combined cycle system. This section summarizes the results of this assessment.

#### E.3.3.1 Black & Veatch/EPRI Ceramic Tube Receiver

Concept. The Black & Veatch/EPRI concept uses vertical U-tubes of silicon carbide (SiC) arranged in parallel adjacent to the rear wall of the receiver cavity (Refs. E-2 and E-3). Tube pitch and distance from the wall are carefully determined to give reasonably uniform flux to the tube circumference. Air makes two passes through the cavity, since the inlet and outlet headers are located below the tubes. This concept was used as a preconceptual baseline in Bechtel's solar hybrid study. Figure E-13 shows a receiver cavity for this concept.

Status. Several early conceptual designs have been prepared for cavities in the 30 to 60 MWt range of power delivered to the air. Individual U-tubes have been tested for heat transfer and cycling. A 1 MWt module is expected to undergo testing at the 5 MWt solar test facility in Albuquerque shortly. This is the most developed of the six ceramic receiver concepts.

Assessment. Table E-2 summarizes the assessment of the Black & Veatch/EPRI Ceramic Tube Receiver. It appears feasible to use this concept for the design of a high-temperature air-cooled



From Ref. E-3

Figure E-13 BLACK AND VEATCH/EPRI CERAMIC TUBE RECEIVER

TABLE E-2

SUMMARY ASSESSMENT - BLACK & VEATCH/EPRI CERAMIC TUBE RECEIVER

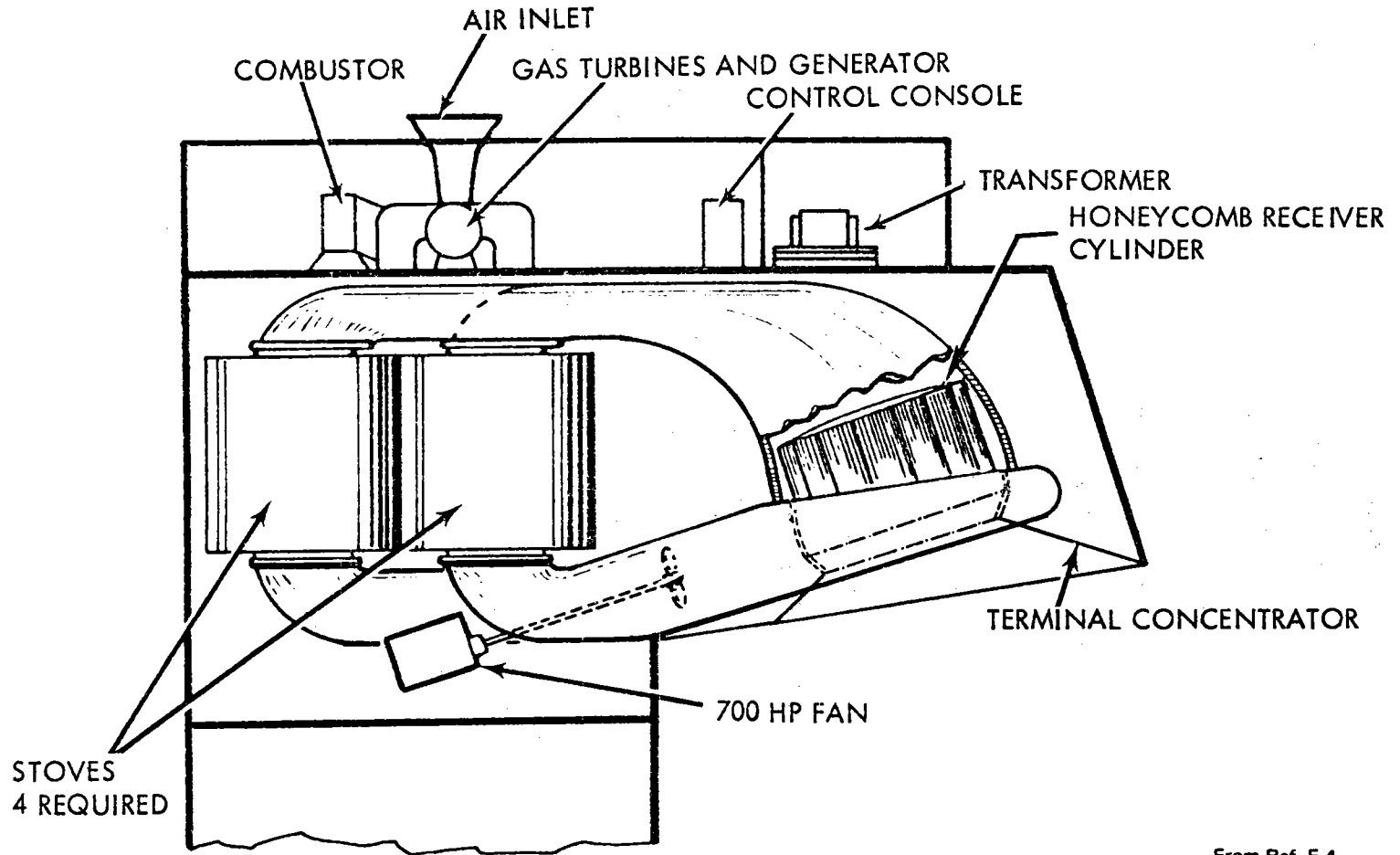
CATEGORY	ASSESSMENT		Remarks
	POSITIVE	NEGATIVE	
Operating Temperature	X		Can handle air outlet 1200C (2200F)
Operating Pressure	X		Can handle compressor pressure ratio of 16
Pressure Drop		X	Higher ΔP yields system performance penalty
Solar Flux		X	Limited to 200-225 kW/m <sup>2</sup>
Size and weight		X	Large and heavy due to heat flux limit
Leakage	X		All joints sealed
Scalability	X		No apparent limitation
Complexity	X		Simple, except allowance for relative thermal growth
Consequence of critical failure	X		Single tube failure not severe but causes shutdown

receiver, although the high pressure drop and the large size and weight of this receiver are drawbacks. The direct installed cost is estimated to be approximately \$140/kWt (1978\$) delivered to the air for a 50 MWt cavity. This cost is very sensitive to outlet air temperature and design pressure drop. The many tube joints required due to the maximum tube length of 2.5 m (8 ft) are a distinct disadvantage. The main advantage of this concept is the relatively advanced state of development.

#### E.3.3.2 Sanders Ceramic Honeycomb Receiver

Concept. The Sanders concept uses a ceramic honeycomb matrix to absorb the focussed solar flux (Refs. E-2 and E-4).

Unpressurized air is blown through the honeycomb to remove the thermal energy. Design variations include either a window on the aperture or an intermediate air-to-air heat exchanger to allow the heating of pressurized air. Figure E-14 shows the Sanders 100 MWe conceptual receiver design using indirect heating through stove-type storage units.



From Ref. E-4

Figure E-14 SANDERS 100 MWe RECEIVER CONCEPTUAL DESIGN WITH ENERGY STORAGE

Status. A conceptual design has been developed for a 100 MWe receiver but most hardware developmental work has been concentrated in the 10-75 kWt range. Some small scale testing has been done at the White Sands facility and Georgia Institute of Technology.

Assessment. Table E-3 summarizes the assessment of the Sanders ceramic honeycomb receiver. The use of this concept for small distributed systems, where windows are feasible, is more likely than its application to large power systems, where indirect heating of the working fluid appears necessary. Sanders estimated the direct cost of a 200 MWt receiver at approximately \$170/kWt in 1973 dollars or \$270/kWt in 1978 dollars. The estimated weight per kWt was approximately three times that for the ceramic tube receiver.

#### E.3.3.3 MIT/Lincoln Laboratory Ceramic Dome Receiver

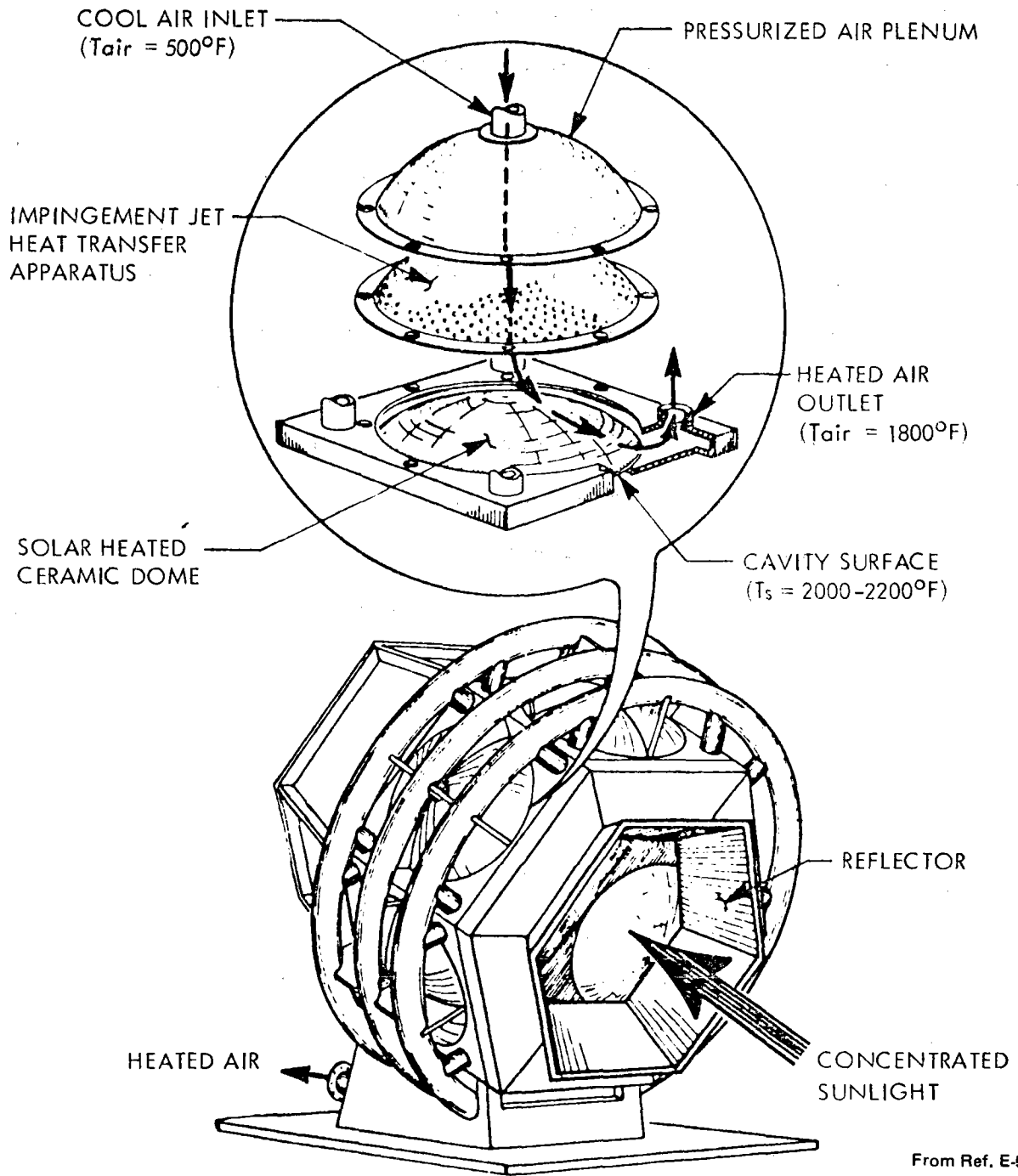
Concept. The MIT/Lincoln Laboratory concept uses a SiC dome to absorb the solar input (Refs. E-2, E-5, and E-6). The concave side is oriented toward the receiver cavity and air pressure is applied to the convex side, resulting in compressive loading of the ceramic. Impingement air jets are used to remove the heat from the dome. Multiple domes would be needed for a large multimegawatt receiver. Figure E-15 shows the conceptual design of a 1 MWt ceramic dome receiver.

TABLE E-3

## SUMMARY ASSESSMENT - SANDERS CERAMIC HONEYCOMB RECEIVER

CATEGORY	ASSESSMENT		Remarks
	POSITIVE	NEGATIVE	
Operating Temperature	X		Counterflow design, with 1100-1200C (2000-2200F) claimed
Operating Pressure		X	Window limits design pressure
Pressure Drop	X		Very low in honeycomb
Solar Flux	X		High fluxes possible
Size & weight		X	Larger and heavier than tube-type
Leakage	X		Window eliminates leakage
Scalability		X	Large window is very difficult
Complexity	X		Simple design
Consequence of critical failure		X	Window failure would be severe





From Ref. E-5

**Figure E-15 ARTIST'S CONCEPT OF A MIT/LL 1 MWt CERAMIC DOME RECEIVER**

Status. Conceptual designs have been prepared for small 1 Mwt receivers. Individual domes up to 0.3 m (12 in.) diameter have been tested under laboratory conditions.

Assessment. Table E-4 summarizes the assessment of the MIT/Lincoln Laboratory ceramic dome receiver. Although this concept is not conceptually advanced for large receivers, few drawbacks were found in the comparative evaluation. The possibility of higher fluxes than the Black & Veatch/EPRI tube-type receiver promises a savings in both cost and weight. A small amount of leakage can be tolerated in an open Brayton cycle. The structural design and air distribution need further definition in a conceptual design before a definitive evaluation can be made.

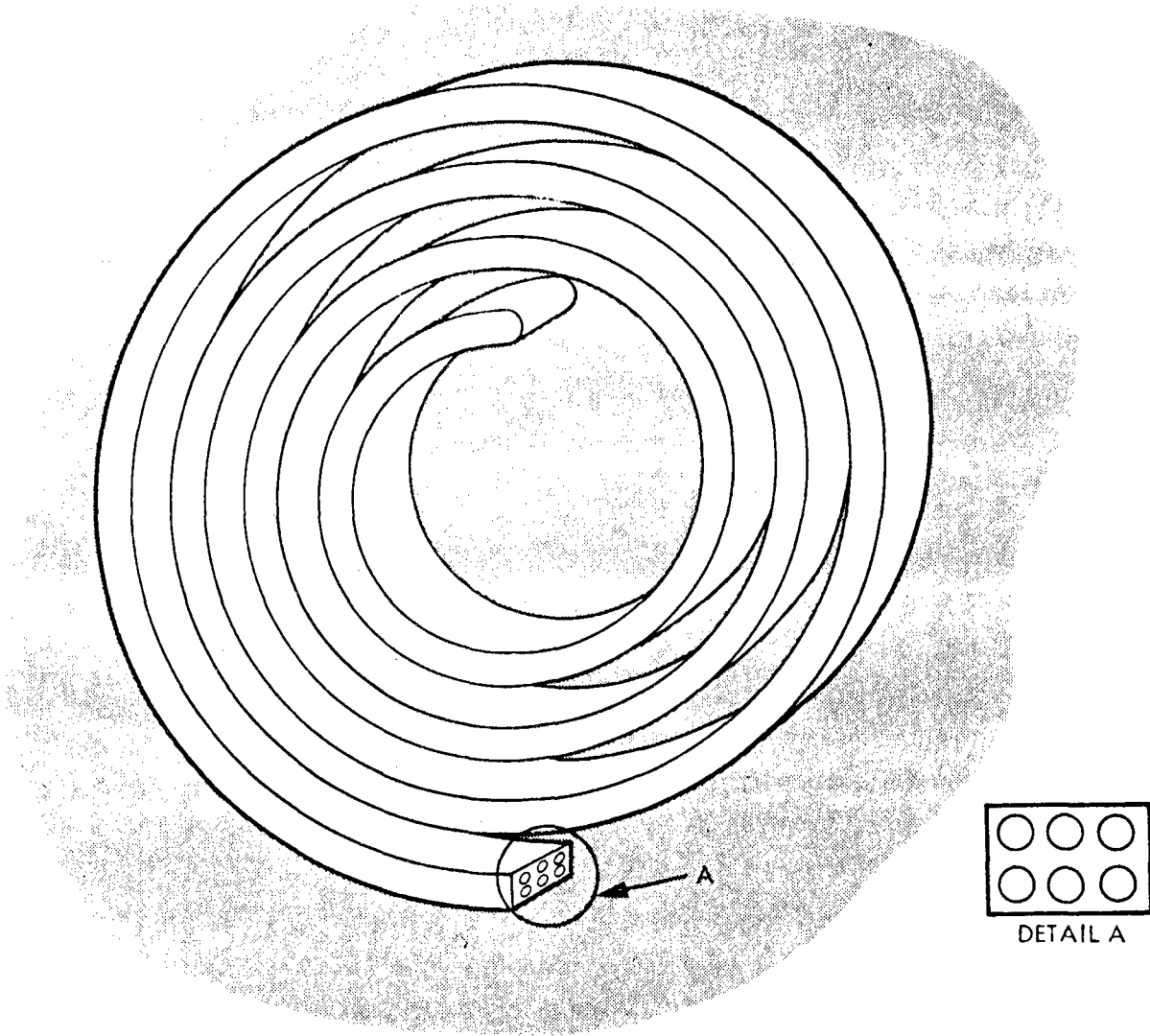
#### E.3.3.4 NRL Solchem Receiver

Concept. The Naval Research Laboratory Solchem concept was developed to convert solar energy into chemical energy (Refs. E-2 and E-7). It uses a coiled ceramic element with several intergral flow passages. The regenerative design has the high-temperature region at the center of the coil and both inlet and outlet on the outside of the coil. The direct heating of a working fluid may also be possible. Figure E-16 shows a typical coiled element of the Solchem receiver.

TABLE E-4

## SUMMARY ASSESSMENT - MIT/LINCOLN LABORATORY CERAMIC DOME RECEIVER

CATEGORY	ASSESSMENT		Remarks
	POSITIVE	NEGATIVE	
Operating Temperature	X		1200C (2200F) possible
Operating Pressure	X		Pressure ratio of 16 possible
Pressure Drop	X		<35 kPa (5 psi)
Solar Flux	X		0.75 to 1 MWt/m <sup>2</sup>
Size & weight	X		Higher flux yields smaller receiver
Leakage		X	<1% leakage at dome joint
Scalability	X		Many domes for large receiver
Complexity		X	Complex piping for air distribution
Consequence of critical failure	X		Dome failure not severe but causes shutdown



From Ref. E-2

Figure E-16 NRL SOLCHEM RECEIVER ELEMENT

Status. Several coils for small distributed receivers have been made and tested in the laboratory. Quality control for this type of ceramic construction has been a problem.

Assessment. Table E-5 summarizes the assessment of the NRL Solchem receiver. This concept was developed chiefly for small distributed receivers. It shows extremely limited potential for large receivers with air cooling.

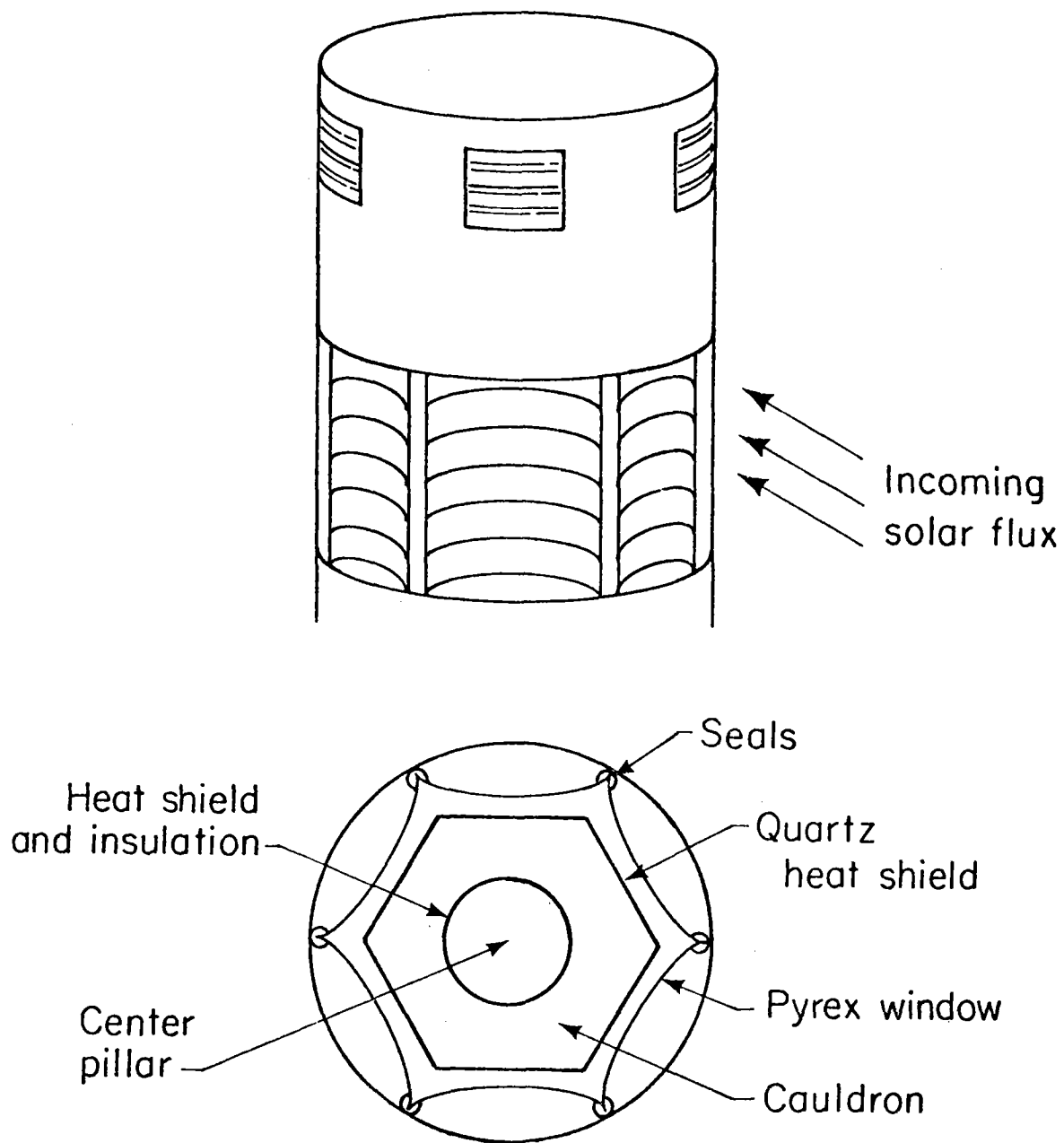
#### E.3.3.5 LBL Black Particle Receiver

Concept. The Lawrence Berkeley Laboratory concept uses sub-micron graphite particles suspended in an air stream to absorb solar energy (Ref. E-8). These particles quickly release heat to the air because of their large ratio of surface to volume. A window is used as a pressure boundary and to contain the particles. The receiver for this concept is merely a chamber with transparent walls. At the temperatures of interest, the graphite particles are sublimed, making it necessary to produce them at the rate consumed by the receiver. Figure E-17 shows a preliminary concept of a black particle receiver.

TABLE E-5

## SUMMARY ASSESSMENT - NRL SOLCHEM RECEIVER

CATEGORY	ASSESSMENT		Remarks
	POSITIVE	NEGATIVE	
Operating Temperature		X	Limited by regenerative design
Operating Pressure		X	Low Design pressure
Pressure Drop		X	High due to long flow path
Solar Flux		X	Small area exposed to peak flux
Size and weight			Unknown
Leakage		X	Delicate, brittle sections
Scalability		X	Much work needed to quantify
Complexity		X	Complex air distribution & thermal growth designs required
Consequence of critical failure		X	Coil breakage would be severe



From Ref. E-8

XBL787-2595

Figure E-17 BLACK PARTICLE RECEIVER CONCEPT

Status. Some laboratory tests of the ability of suspended black particles to absorb radiant energy have been performed at low temperature rises.

Assessment. Table E-6 summarizes the assessment of the LBL black particle receiver. This concept has not been fully defined although it is elegantly simple. The negligible thermal capacity of the receiver makes reliable particle production critical. Operating costs for particle production is unknown and may offset the apparent advantage of small receiver size. It is possible that cleaned coal particles could be used instead of graphite to minimize cost.

#### E.3.3.6 LASL Ceramic Heat Pipes

Concept. Preliminary unpublished work at Los Alamos Scientific Laboratory has produced SiC heat pipes with sodium as a working fluid. These could potentially be used to design a ceramic receiver analogous to the metallic heat pipe design of Dynatherm. The heat pipes efficiently transfer energy from the cavity through the pressure boundary and release the energy into the air stream.

The characteristics of a potential receiver using ceramic heat pipes could be similar to those of the metallic heat pipe receiver but have not been determined.



TABLE E-6

## SUMMARY ASSESSMENT - LBL BLACK PARTICLE RECEIVER

CATEGORY	ASSESSMENT		Remarks
	POSITIVE	NEGATIVE	
Operating Temperature	X		High temperatures possible
Operating Pressure		X	Limited by window
Pressure Drop	X		Very low
Solar Flux	X		High fluxes possible
Size & weight	X		Compact and light
Leakage	X		Window eliminates leakage
Scalability		X	Limited by window
Complexity	X		Very simple design
Consequence of critical failure		X	Loss of particle production would be disastrous

Status. A few heat pipes using a tantalum plug for a sealing device have been tested. Manufacturability studies are under way.

Assessment. At this early stage of development, assessment can only be speculative. A ceramic heat pipe receiver should satisfy all the system requirements, but sealing of the pipes, ceramic panel design and interface connection between pipes and the panel may present difficult problems. Design heat fluxes of  $1.2 \text{ MWt/m}^2$  are used for the metallic heat pipe receiver, and should be achievable by the ceramic equivalent.

#### E.3.4 Summary Assessment

There are several generic problems associated with ceramic receiver concepts:

- Ceramic materials generally have limited tensile strength and are susceptible to brittle fracture.
- All require metal-to-nonmetal pressure joints which must limit leakage at elevated temperature.
- All are susceptible to thermal shock damage, though in varying degrees.

Those concepts which minimize these drawbacks while meeting the system requirement have the most promise for application to the solar hybrid system.

The two concepts which are most promising are the Black & Veatch/EPRI tube-type and the MIT/Lincoln Laboratory dome-type receivers. Both concepts appear to be compatible with the solar hybrid system, although the tube-type receiver has achieved a much higher state of development. Comparing the two concepts, the ceramic dome receiver has the following advantages:

- Better application of the basic material properties of ceramic materials (i.e. compression loading)
- Fewer metal-to-nonmetal pressure joints
- Higher allowable surface heat flux (factor of 3 to 4) meaning smaller size, lighter weight and potentially lower cost
- Lower air pressure drop (determined by economic tradeoff) meaning better system performance

On the negative side, the ceramic dome receiver has a small leakage of air and a complex and possibly expensive air distribution piping network. Before a more definitive and conclusive comparative assessment can be made, the ceramic dome receiver must be brought to a more advanced state of development both in component testing and, in the development of a good conceptual design for a large power system application.

The other four receiver concepts are less suitable for the solar hybrid system application in the near term. The Sanders and black particle concepts, because of the required window, are expected to be useful in large power systems only for low pressure ratio regenerative Brayton cycles. The Solchem concept may never be applied to large receivers, especially with high air

outlet temperatures. The ceramic heat pipe concept, if brought to the same state of development as its Dynatherm counterpart, may be promising, although the expected heat flux capability is not much higher than that of the ceramic dome concept.

As a result of this comparative investigation, it is recommended that the MIT/Lincoln Laboratory ceramic dome receiver concept be further developed so that a definitive comparison on technical and economic bases can be made between it and the currently more advanced Black & Veatch/EPRI ceramic tube receiver.

#### E. 4 UTILITY QUESTIONNAIRE

The Solar Energy Research Institute (SERI) and the following eight utility companies were requested to respond to the questionnaire shown in Figure E-18:

- Middle Atlantic Region: Pennsylvania Power and Light Company
- South Central Region: Texas Electric Service Company
- South Mountain Region: Public Service Company of New Mexico  
Nevada Power Company  
Arizona Public Service Company
- Pacific Southern Region: Southern California Edison  
Pacific Gas & Electric Company

A draft of the executive summary of this report was included with the questionnaire to provide background information on the solar hybrid plant concept. Both written and oral responses were received from the utility companies. Since some of these responses contained proprietary data, they have not been reproduced in full. Instead, comments have been summarized.

##### E. 4.1 Expected Use of Solar Energy

Utility companies in the South Mountain region were of the opinion that there may be a good demand for combined cycle solar hybrid plants in their region after the year 2000. Stand-alone solar plants would probably displace hybrid plants after the year

2020, although demand for solar energy would increase markedly in the late 1990s to displace scarce and more expensive fuels. In the opinion of these utilities, the question of economic competitiveness would resolve itself, provided a heliostat production base is established. Utilities from the other three regions did not foresee widespread commercial use of solar energy before the year 2020.

SERI and all the utilities emphasized that solar energy, if adopted, would be used primarily for intermediate loads with limited use in peaking units. Market penetration forecasts of solar energy ranged from 2 percent to a maximum of 10 percent in the early 2000s.

#### E.4.2 Energy Storage

It is SERI's opinion that solar energy storage depends entirely on economics, while some of the utility companies felt that buffer storage (30 to 60 minutes) would be necessary. The Arizona Public Service Company plans to use thermal storage of 11 to 18 hours (tube-in-molten salt bath) for both the advanced receiver stand-alone and solar hybrid systems being considered.

#### E.4.3 Technologies Competing with Solar

Besides coal and nuclear generation mixes, some utilities considered pumped hydro as a major competitor to solar energy in the intermediate-load service. Pennsylvania Power and Light

Company expressed a strong interest in cogeneration, but only Pacific Gas and Electric Company and Southern California Edison included cogeneration as an option in their future generation capacity mix forecasts. In addition to cogeneration, PG&E and Southern California Edison are considering gas turbine, combined cycle, nuclear, hydro, and geothermal. Southern California Edison also includes wind and fuel cells.

#### E.4.4 Solar Plant Compatibility with Load Profiles

Arizona Public Service Company and the Public Service Company of New Mexico felt that solar plants would be quite compatible with their grid system and load requirements. Since these utilities have peak demand in the summer, the solar energy availability tracks their load demand very well. However, this is not the case for Pennsylvania Power and Light Company, since their peak load occurs in the winter when solar energy is least available.

#### E.4.5 Potential Limitations to Widespread Use of Solar Power Systems

All utilities expressed concern about some common issues. Items that have a major impact on decisions regarding implementation of solar energy include taxes, solar investment tax credit, unequal parity of tax credit on fossil fuel versus solar energy, and land availability.

Another major impediment to expanded solar use could be the position of utility regulatory commissions toward the value of fuel oil savings and how that value is to be treated with respect to customer rates. With the present generally accepted fuel cost pass-through provisions, there is little or no incentive for utilities to pursue fuel savings, except as may be required by the National Energy Act of 1978.

New legislation would have to be enacted both at state and federal levels to help commercialize solar energy. Five of the seven utilities noted that environmental considerations, particularly land use, could hinder solar plant construction. However, Arizona Public Service Company noted that according to their studies, land constraints were minimal, and environmental laws would not hinder solar plant construction in their region.

#### E.4.6 Summary

It appears that as solar energy becomes economically competitive with other available energy sources, the utility companies will be looking to the government for incentives. As PG&E points out, "Developing a resource from technological immaturity to commercial availability requires large financial commitments and investment risks," and the utilities are not prepared to undertake this commitment on their own. The extent of market penetration will be directly related to the amount of government financial support.



The utilities did agree that the solar energy market would increase significantly if fuel escalation rates were much higher than projected and if nuclear plant construction was constrained in the future. Advanced technologies, including wind, photovoltaic cells, and ocean thermal energy conversion (OTEC), were not included in the future generation capacity forecasts for any of the utilities, except Southern California Edison, which included wind as a future generation capacity.

UTILITY QUESTIONNAIRE

(Response to be used as input data for Market Potential Analysis)

A. Economic Analysis

1. What is your cost of fuel in 1979? (No. 2 oil, No. 6 oil, coal, LWR), \$/mmBtu.
2. What escalation rates do you use for each of the above types of fuel? (%)
3. What escalation rates do you use for:
  - Capital cost (%)
  - Operation and Maintenance Costs (%)
4. What discount rate do you use? (%)
5. What fixed charge rate do you use? (%)

B. Expansion Plans/Methodology

1. What is the present generating capacity mix of your system? (MW)
2. What is the future generation capacity forecast by technology (e.g., coal, nuclear, etc.) for your system (1980-2020)?
3. What methods do you use for generation planning and production costing?
4. What method do you use in forecasting incremental demand?
5. Have you compared your results with historical performance? If so, how well did it compare?

C. Plant Characteristics

1. What is the average heat rate for your system (Btu/kWhr) for:
  - Oil
  - Coal
  - LWR
  - Combined-Cycle
  - Average Mix

Do you expect it to change?

Figure E-18 UTILITY QUESTIONNAIRE WITH ACCOMPANYING LETTER

2. What is the economic life of your plants?
  - Oil
  - Coal
  - LWR
  - Combined-Cycle
  - Average Mix
  
3. What is your expected:
  - Fixed operation and maintenance costs? (\$/kW-yr)
  - Variable operation and maintenance costs? (mills/kWhr)
  - Capital costs and estimated year of expenditure? (\$/kW)  
(for Gas Turbine, Combined-Cycle, Coal, LWR)

(Note: If fixed and variable O&M costs are not available could you estimate them as a percentage of capital costs?)
  
4. What is the expected cost of your average standing inventory?
  
5. What is your projected cost of power generation (1980-2020) for:
  - Oil
  - Coal
  - LWR
  - Combined-Cycle
  - Average Mix
  
6. What is the incremental electricity demand forecast for your region? (GWH/yr x 10<sup>3</sup>)
  
7. What is the production forecast for your system?
  
8. What is the expected capacity factor forecast for your system for oil, coal, LWR, nuclear, combined-cycle, etc.?
  
9. What is the expected load factor forecast for your system? (up to year 2020)
  
10. What is the shape of your existing and projected load duration curve?
  
11. What is the annual retirement rate per year of the installed capacity of your system?
  
12. What are your basic reserve requirements? How are they established (present and future) for oil, coal, LWR, nuclear, and combined-cycle?

Figure E-18 (Continued)

D. Solar

1. What are some of the factors/characteristics of your system that you think may influence the inclusion or not of solar energy technology? (e.g., Institutional restrictions, government regulations and/or inducement of State and local laws, etc.)
2. Do you see any potential for solar energy in your system? What would you estimate to be the upper limit of this potential in percent to 1990, to 2020, of annual energy?
3. What existing and/or future technologies do you see as a major competitor of solar energy (i.e., cogeneration, etc.)?
4. How would you utilize solar energy if you elected to use it? (i.e., combined-cycle, intermediate load range, etc). How does solar energy impact your grid requirement? Compatible? Would energy storage be utilized? Method?

E. MARKET PENETRATION

1. We would appreciate any comments you may have on the Executive Summary of the Project Topical Report enclosed, especially with regard to the market penetration analysis methodology.

# Bechtel National, Inc.

Engineers - Constructors

Fifty Beale Street  
San Francisco, California

Mail Address: P. O. Box 3985, San Francisco, CA 94119

July 19, 1979

Job 13007



Dear

I am enclosing a list of questions that Ann Saha mentioned to you in her telephone conversation with you on July 17, 1979. Your response will be used in a market potential analysis for a combined cycle solar hybrid plant. This analysis is part of a study being conducted by Bechtel National, Inc., San Francisco, for the U.S. Department of Energy, San Francisco Operation.

The study is aimed at selecting a solar hybrid system concept of maximum potential worth to a utility. This worth is analyzed in terms of minimum cost of power generated and savings in capital costs, operation and maintenance costs and displacement of fossil fuels over conventional power generation systems.

In the solar hybrid concept under study by Bechtel, solar energy is used to supply part of the energy required for a combined cycle power plant, slated for use in the intermediate load range. The market potential study will help us to identify the marketability of this solar hybrid system. In order to provide you some background information on our concept, we are also enclosing a copy of the Executive Summary of the project Topical Report.

We would like to start our Market Potential Analysis as soon as possible, and would therefore, like to be able to call you in 3-4 days for your responses to the questions. We would appreciate your sending us a typed copy of your answers as a follow-up, so that we may include these in our report to DOE/SAN.

If you feel that you may not be able to provide this information gratuitously or if you have any questions, please call Ann Saha at (415) 768-8769. We sincerely appreciate your cooperation in this matter.

Very truly yours,

A handwritten signature in dark ink, appearing to read "Ernest Y. Lam". The signature is fluid and cursive, written over a light background.

Ernest Y. Lam  
Solar Technology Supervisor  
Research and Engineering

EYL/AS/fed  
Encl.

Figure E-18 (Continued)

## APPENDIX E: REFERENCES

- E-1 Davidson, W. S. et al. (Boeing Engineering and Construction Co., Seattle, WA), Closed Brayton Cycle Advanced Central Receiver Solar-Electric Power System, Final Report, November 1978.
- E-2 Ewing, J. and Zwissler, J. (Jet Propulsion Laboratory Pasadena, CA), Performance Prediction Evaluation of Ceramic Materials in Point-Focusing Solar Receivers, DOE/JPL-1060-23, June 1, 1979.
- E-3 Grosskreutz, J.C., et al. (Black & Veatch Consulting Engineers, Kansas City, MO), Solar-Thermal Conversion to Electricity Utilizing a Central Receiver, Open-Cycle, Gas Turbine Design, Final Report, EPRI ER-652, March 1978.
- E-4 (Sanders Associates, Inc., Nashua, NH), Final Report for a 10 kWt Solar Energy Receiver, submitted to DOE/COO, December 1978.
- E-5 Jarvinen, P.O. (MIT/Lincoln Laboratory, Lexington, MA), "Solar Heated Air Cavity Receiver Development (SHARE)," presented at the Focus on Solar Technology -- A Review of Advanced Solar Thermal Power Systems Meeting, Denver, CO, November 15-17, 1978.
- E-6 Jarvinen, P.O. (MIT/Lincoln Laboratory, Lexington, MA), "Ceramic Receivers for Solar Power Conversion," presented at the AIAA Terrestrial Energy Systems Conference, Orlando, FL, June 4-6, 1979.
- E-7 Chubb, T.A., Nemecek, J.J., and Simmons, D.E. (Naval Research Laboratory, Washington, DC), "Design of a Small Thermochemical Receiver for Solar Thermal Power," presented at the 1978 Annual Meeting of the American Section of ISES, Denver, CO, August 28-31, 1978.
- E-8 Hunt, A.J. (Lawrence Berkeley Laboratory, Berkeley, CA), A New Solar Thermal Receiver Utilizing a Small Particle Heat Exchanger, LBL-8520, April 1979.

APPENDIX F  
CONCEPTUAL DESIGN DATA LISTS

## CONTENTS

<u>Section</u>		<u>Page</u>
F.1	Collector Sybsystem	F-3
F.2	Heat Pipe Receiver	F-6
F.3	Electric Power Generation Subsystem	F-11



F.1. COLLECTOR SUBSYSTEM

A. Design Characteristics

1. Field Geometry and Size, m (ft) Modified elipitical field, eliminating all heliostats in a 120 degree arc south of the tower position
- |  |             |
|--|-------------|
| Major diameter                                 | 1534 (5034) |
| Minor diameter                                 | 1184 (3884) |
| Distance from major axis to south offset tower | 177.4 (582) |
2. Field Layout
- |                                |  |
|--------------------------------|--|
| Heliostat layout               | Radial stagger grid within ellipse   |
| South to north spacing, m (ft) | From 13.1 (43) at the southern extremity to 17.1 (56) at the north end                     |
| East to west spacing, m (ft)   | From 13.7 (45) at the center of the field to 28.0 (92) at the east and west field extremes |
3. Field Oversizing, MWt
- |  |  |
|--|--|
| Desired power to the receiver at peak conditions | 156.4  |
| Power provided by field                          | 164.0 (allows 5 percent of field to be down) |

## 4. Beam Pointing Accuracy and Error Budget, mrad

Beam pointing accuracy	1.5
Dead band allowed by control system	0.6
Undisturbed standard deviation	0.01
Maximum deflection, normal operating winds	2.31
Elevation drive	2.31
Azimuth	1.52
Beam pointing error, 12 m/sec (27 mph) wind	2.77

(Thermal distortion of the mirror must be determined in Phase II from the component experiments, because of the unreliability of the thermal analysis.)

## 5. Heliostat Beam Quality and Error Budget

Attainment of the specified beam quality of 90 percent of the energy falling within the theoretical solar core (9.3 mrad) plus a 1.4 mrad wide fringe ring is accomplished by using canted flat 1.2 x 1.2 m facets

Error due to environmental effects,  
21C (70F) ambient temperature, mrad

No wind	0
12 m/sec (27 mph) wind	2.66

6. Heliostat Geometry and Size, m (ft)

Rectangular, 7.38 (24.21) wide by 7.42 (24.33) tall

7. Number of Heliostats

5121

B. Operating Characteristics

1. Auxiliary Power Required  $W/m^2$

2.47 (tracking and standby)

2. Heliostat Operating Modes

Tracking, slewing, standby (alignment)

3. Control System Characteristics

See Section 5.7.2

4. Operation and Survival

Heliostat and field will conform to the operating and survival conditions specified by SLL in AL 0772 dated 10/12/78

F.2 HEAT PIPE RECEIVER

	<u>One Cavity</u>	<u>Total (3 Cavities)</u>
<b>A. <u>Design Characteristics</u></b>		
1. Cavity height, m (ft)	17.6 (57.7)	--
Cavity width, m (ft)	12.8 (42.0)	--
Cavity depth, m (ft)	8.3 (27.2)	--
2. Area of aperture, m <sup>2</sup> (ft <sup>2</sup> )	82.8 (891.3)	248.4 (2,673.9)
Exposed heat pipe area m <sup>2</sup> (ft <sup>2</sup> )	765.6 (8,241.0)	2,296.8 (24,723)
Panel area, m <sup>2</sup> (ft <sup>2</sup> )	143.0 (1,539.3)	429.0 (4,618)
3. Heat pipe O.D., mm (in.)	60.3 (2.375)	--
Heat pipe I.D., mm (in.)	52.7 to 54.9 (2.075 to 2.160)	--
Heat pipe wall, mm (in.)	2.8 to 3.81 (0.110 to 0.150)	--
4. Heat pipe length, m (ft)	0.91 (3.0)	--
5. Number of panels	11.0	33.0
Number of heat pipes	12,628.0	37,884.0
Number of heat pipes per panel	1,148.0	--
6. Panel material	Inconel 617	--
Total mass of panels, kg (lb)	38,433.0 (84,553)	115,300.0 (253,660)
Mass per panel, kg (lb)	3,494.0 (7,687)	--
7. Heat pipe material	Inconel 617	--
Mass of heat pipes, kg (lb)	96,061.0 (211,333)	288,182.0 (634,000)
Mass per heat pipe, kg (lb), average	7.6 (16.7)	--
Fins per cm (in.), average	1.2 (3.0)	--
8. Inlet header material	Carbon Steel	--
Outlet header material	Incoloy 800H	--
Mass of headers, kg (lb)	16,485.0 (36,267)	49,454.0 (108,800)
9. Insulation materials	Fiberfrax and mineral fiber	--
Mass of insulation, kg (lb)	9,341.0 (20,550)	28,023.0 (61,650)

	<u>Characteristics</u>	<u>One Cavity</u>	<u>Totals (3 Cavities)</u>
10.	Structure material Total mass of structure, kg (lb)	Carbon steel, stainless steel 76,235.0 (167,717)	— 228,705.0 (503,150)
11.	Support Material, total mass, kg (lb)	Included in 10	Included in 10
12.	Total mass of piping material, kg (lb) (excluding riser/downcomer)	See item 31	See Item 31
13.	Valve material Number of receiver valves Mass of receiver valves, kg (lb)	Carbon steel 11.0 850.0 (1,870)	Inconel 617 33.0 2,550.0 (5,610)
14.	Not applicable		
15.	Total mass of other misc. items, kg (lb)	4,000.0 (8,800) (allowance)	12,000 (26,400) (allowance)
16.	Total dry mass on top of tower, kg (lb)	—	742,564 (1,637,046)
17.	Mass of receiver working fluid, kg (lb)	41.0 (90)	123.0 (270)
18.	Receiver operational seismic load, g's Vertical Horizontal	2.15 4.14	Same Same
19.	Receiver survival seismic load, g's Vertical Horizontal	3.58 (est.) 6.90 (est.)	Same Same
20.	ASME code	Section VIII, Divisions 1 & 2 (with modifications for solar applications)	
21.	Emissivity Absorptivity	0.90 0.95	
22.	Receiver pressure drop correlations	Appendix B	
23.	Receiver heat transfer correlations	Appendix B	
24.	Receiver losses equations	Section 3.3.4	
25.	Tower construction Height to top of tower, m (ft)	Steel (pipe sections) 140 (459)	

<u>Characteristics</u>	<u>Riser</u>	<u>Downcomer</u>
26. Tower piping material	Carbon Steel	Carbon Steel with Inconel 617 liner
Outside diameter, mm (in.)	1327 (52.3)	Pipe: 1676 (66) Liner: 1460 (57.5)
Inside diameter, mm (in.)	1295 (51)	Pipe: 1638 (64.5) Liner: 1448 (57)
Wall thickness, mm (in.)	16 (.625)	Pipe: 19 (.75) Liner: 6 (.25)
27. Tower piping, total length, m (ft)	146 (480)	146 (480)
28. Tower piping mass, kg (lb)	74,150 (163,500)	145,000 (320,000)
29. Tower piping insulation thickness, mm (in.)	51 (2)	89 (3.5)
30. Insulation mass, kg (lb)	2,060 (4540)	8,110 (17,900)
31. Total mass of other miscellaneous items in tower, kg (lb)		
a) Piping and Insulation	3,600 (8,000)	18,200 (40,000)
b) Valves and Actuators	11,000 (24,000)	2,700 (6,000)
c) Expansion joints, hangers, etc.	(included in totals above)	
d) Crane	22,700 (50,000)	
32. Horizontal piping material/OD/ID/wall	(same as Item 26 above)	
33. Total horizontal length, m (ft)	36 (120)	36 (120)
34. Horizontal piping mass, kg (lb)	18,600 (41,000)	36,400 (80,000)
35. Horizontal piping insulation thickness, mm (in.)	(same as Item 29 above)	

<u>Characteristics</u>	<u>Riser</u>	<u>Downcomer</u>
36. Mass of horizontal piping insulation, kg, (lb)	520 (1140)	2000 (4,400)
37. Ground level valve material	Carbon Steel	Lined Carbon Steel with 321 SS internals
Size, mm (in.)	1,295 (51)	1,448 (57)
38. Ground level valve number	2	1
39. Receiver pumps		N/A
40. Receiver pump characteristics		N/A
41. Steam generator characteristics		N/A

F-9

B. Receiver Operating Characteristics (Design Conditions)

1. Incident power @ aperture plane, MWt	170.90
@ panel surfaces, MWt	162.11
2. Absorbed power, MWt	141.18
Per panel values	Table F-1
3. Flux maps	Table 5-7
4. Peak flux absorbed, MWt/m <sup>2</sup>	1.093 (panel 6, north cavity)
5. Average flux absorbed, MWt/m <sup>2</sup>	0.329
6. Working fluid inlet temp., C (F)	363.9 (687)
Working fluid outlet temp., C (F)	843.3 (1550)

<u>Characteristics</u>		<u>Value</u>
7.	Working fluid inlet press., MPa (psi)	1.055 (153)
	Working fluid outlet press., MPa (psi)	1.014 (147)
8.	Working fluid flow rates, kg/h (lb/h)	927,360.0 (2,044,800)
9.	Working fluid velocities, m/s (ft/s)	
	Panel Inlet	2.6 to 9.3 (8.5 to 30.4)
	Panel Outlet	4.7 to 16.3 (15.3 to 53.3)
10.	Losses (% of total incident power to receiver)	
	Wind speed m/s (MPH)	6.7 (15.0)
	Reflection, %	1.40
	Reradiation, %	7.64
	Convection, %	2.67
	Conduction, %	0.52
	Total, %	12.23
11.	Peak metal temp., C (F)	888.5 (1631.4)
	Location	Panel No. 6, 10 m (30 ft) above inlet
12.	Peak working stress, MPa (psi)	See Table 5-10
13.	Fatigue life	
	Number of cycles	13,000.0
	Design life (years)	30.0
14.	Heat transfer coefficients $W/m^2-C$ (Btu/h-ft <sup>2</sup> -F)	
	Working fluid (air)	109.5 to 308.1 (19.3 to 54.3)
	Heat pipe working fluid	28,372.0 (5,000)
	Overall	56.2 to 102.1 (9.9 to 18.0)



F.3 ELECTRIC POWER GENERATION SUBSYSTEM

	<u>Gas Turbine</u>	<u>Steam Turbine</u>
A. <u>Design Characteristics</u>		
1a. Turbine generator type	Westinghouse W-501 (modified)	Westinghouse single flow, condensing, 23"LSL
1b. Nameplate rating	85.6 MWe, 143 MVA, 0.9 pf	45.9 MWe, 2.5" HgA, 0% MV
2. Turbine inlet conditions:		
Temperature, C(F)	1085 (1985)	510/316 (950/600)
Pressure, MPa (psia)	0.945 (137)	6.9/117 (1000/250)
Flow Rate:		
Maximum kg/hr (lb/hr)	1,196,000 (2,637,000)	142,200/25,100 (313,600/55,300)
Design kg/hr (lb/hr)	1,202,000 (2,430,000)	129,700/24,500 (286,000/54,000)
Minimum kg/hr (lb/hr)	1,102,000 (2,430,000)	55,700/19,500 (122,800/43,000)
3. Turbine reheat conditions		Not applicable
4. Number and location of feedwater heating extractions		None
5. Condenser type and configuration		Two pass, single-pressure, divided waterbox, 5 minute storage hotwell
6. Feedwater/Feedwater Booster Pump stages		8/3
7. Auxiliary steam supply package boiler, kg/hr (lb/hr), Mpa(psig)		9072 (20,000), 1.72 (250)
8. Sealing steam requirements, kg/hr (lb/hr)		680 (1500)

9. Turbine startup (cold, warm, and hot start) and shutdown characteristics	See Table F-2
10. Nonsolar energy source design interface	At combustor inlet
11. Nonsolar emission level limited for Distillate Oil No. 2, lb per million Btu	
NO <sub>x</sub>	0.3
SO <sub>x</sub>	0.8
Particulates	Negligible

F-12

B. Operational Characteristics

1. See Table F-2	
2. Nonsolar energy fuel(s)	Distillate Oil No.2
3. Fuel characteristics	See Table 3-18
4. Fuel heating value (as fired), kJ/kg (Btu/lb)	8291 (19,300)
5. Fuel burning rate	See Table F-2
6. Nonsolar discharge rate	
Maximum, MWt	272.8
Design, MWt	119.2
Minimum, MWt	~0

7. Combustor/heater gas operating temperatures (in/out)	<u>In</u>	<u>Out</u>
Maximum, C (F)	839/1173	(1542/2144)
Design, C (F)	839/1173	(1542/2144)
Minimum, C (F)	368/1173	(695/2144)
8. HRSG water/steam operating temperatures (in/out)		
Maximum, C (F)	121/510 & 316	(250/950 & 600)
Design, C (F)	121/510 & 316	(250/950 & 600)
Minimum, C (F)	121/349 & 218	(250/660 & 425)
9. HRSG steam/water operating pressures (in/out)		
Maximum, MPa (psia)	0.2/6.9 & 1.7	(30/1000 & 250)
Design, MPa (psia)	0.2/6.9 & 1.7	(30/1000 & 250)
Minimum, MPa (psia)	0.2/3.45 & 1.35	(30/500 & 125)
10. Steam flow rates	<u>Main Steam</u>	<u>Secondary Steam (No Reheat)</u>
Maximum, kg/hr (lb/hr)	142,200 (313,600)	25,100 (55,300)
Design, kg/hr (lb/hr)	129,700 (286,000)	24,500 (54,000)
Minimum, kg/hr (lb/hr)	55,800 (123,000)	19,500 (43,000)
11. Nonsolar heat losses (provide fuel heating value and other pertinent factors used as a basis for calculations)	<u>HRSG</u>	<u>Gas Turbine</u>
Design power		
Radiation, %	0.5	0.5

	<u>HRSG</u>	<u>Gas Turbine</u>
Hydrogen and moisture in fuel, %	Not applicable	12.5/0.0
Moisture in air, %	68.0 RH	68.8 RH
Unburned combustibles, %	0.0	0.0

TABLE F-1

## NET POWER TO PANEL ZONES

(MW  
(thousand Btu/hr)

m ft		PANEL NUMBER					
		6	5 & 7	4 & 8	3 & 9	2 & 10	1 & 11
40		0.1867 637.	0.1443 492.	0.1072 366.	0.0821 280.	0.0477 163.	0.0199 68.
		0.2939 1003.	0.2635 899.	0.2304 786.	0.1986 678.	0.1430 488.	0.0715 244.
30		0.7322 2498.	0.6858 2340.	0.5945 2028.	0.4740 1617.	0.3164 1080.	0.1668 569.
		1.3677 4667.	1.3041 4450.	1.1466 3912.	0.9149 3122.	0.6302 2150.	0.3614 1233.
20		1.6655 5683.	1.5993 5457.	1.4140 4825.	1.1373 3881.	0.8050 2747.	0.4899 1671.
		1.3412 4576.	1.2909 4405.	1.1479 3917.	0.9307 3176.	0.6739 2299.	0.4276 1459.
10		0.7586 2589.	0.7308 2494.	0.6... 2232.	0.5349 1825.	0.3945 1346.	0.2595 885.
		0.3138 1071.	0.3032 1035.	0.2727 931.	0.2251 768.	0.1681 574.	0.1139 389.
0		0.0483 165.	0.0470 160.	0.0424 145.	0.0351 120.	0.0271 93.	0.0185 63.
		6.7078 22888.	6.3689 21732.	5.6096 19141.	4.5326 15466.	3.2060 10939.	1.9290 6582.
		13.42	12.74	11.22	9.07	6.41	3.86

TABLE F-2  
EPGS PERFORMANCE

	<u>Hybrid Mode</u>	<u>Solar-Only Mode</u>	<u>Long-Term Fossil Mode</u>
Gross cycle efficiency, %	45.1	31.2	43.0
Net cycle efficiency, %	43.8	29.8	42.1
Solar fraction <sup>a</sup>	.537	1.0	0.0
Gross cycle heat rate, kJ/kWh (Btu/kWh)	7,987 (7,570)	11,524 (10,923)	8,362 (7,926)
Net cycle heat rate, kJ/kWh (Btu/kWh)	8,229 (7,794)	12,069 (11,431)	8,618 (8,162)
Turbine exhaust pressure, mm (in. HgA)	63.5 (2.5)	63.5 (2.5)	63.5 (2.5)
Feedwater temperature, C(F)	295 (563)	247 (477)	295 (563)
Flow rate to turbine, kg/hr (lb/hr):			
HP	129,700 (286,000)	55,800 (123,000)	128,800 (284,000)
LP	24,500 (54,000)	19,500 (43,000)	23,900 (52,600)
Total	154,200 (340,000)	75,200 (165,800)	152,700 (336,600)
Auxiliary power requirements, kW:			
Gas turbine auxiliaries	370	150	400
Boiler feed water booster pump	130	65	130
Boiler feed pump	450	225	450
Condensate pumps	100	50	100
Circulating water pumps	710	350	710
Suction water pumps	70	35	70
Cooling tower fans	410	200	410
Heliostat tracking	640	640	0
Miscellaneous auxiliaries	290	200	290
Total	3,340	1,915	2,730
Fuel Burn Rate kg/hr (lb/hr)	9,560 (21,075)	0	21,670 (47,778)

TABLE F-3

## HRGS DATA

Service	H.P. Superheater	I.P. Superheater	H.P. Evaporator	H.P. Economizer	I.P. Evaporator	I.P. Economizer	L.P. Evaporator
Numer required	1	1	1	1	1	1	1
Type	Straight Finned Tube						
Orientation	Vertical Tubes, Horizontal Gas Flow						
Number of shell passes	1	1	1	1	1	1	1
Number of tube passes	2	2	2	4	2	4	2
Tube side fluid	Steam	Steam	Feedwater Steam	Feedwater	Feedwater Steam	Feedwater	Feedwater Steam
Shell side fluid	Gas Turbine Exhaust						
Tube side material	Alloy Steel	Alloy Steel	Carbon Steel	Carbon Steel	Carbon Steel	Carbon Steel	Carbon Steel
Shell material	Carbon Steel with Inner Liner						
Number of tubes	540	162	1,296	594	702	594	702
Tube O.D./I.D./wall, mm (in.)	50.8 nom/~50.8/3.05 min (2.0 nom/~2.0/0.12 min)						
Tube layout and pitch dimension	Two rows of tubes per module						
Unit size, m (ft)	32.4 x 12 x 18.3 (106'-2" x 39'-3" x 60'-0" high)						
Total external surface area, including finned area, m <sup>2</sup> (ft <sup>2</sup> )	9,104 (98,000)	2,694 (29,000)	2,179 (234,000)	9,940 (107,000)	11,798 (127,000)	9,940 (107,000)	11,798 (127,000)
Inactive external surface area	Not Available						
LMTD, C(F)	71 (128)	31 (56.3)	55 (98.3)	31 (55.2)	20 (36.8)	33 (60.1)	28 (49.9)
Pinch point $\Delta T$ C(F) (design mode)	-	-	9 (16.2)	11.9 (21.4)	8.4 (15.1)	12.1 (21.8)	11.6 (20.8)
				(Approach)		(Approach)	